HYALURONIC ACID BASED THERAPEUTIC BANDAGE CONTACT LENSES FOR CORNEAL WOUND HEALING

HYALURONIC ACID BASED THERAPEUTIC BANDAGE CONTACT LENSES FOR CORNEAL WOUND HEALING

By

JENNIFER (JING YUAN) TIAN, BSc

A Thesis Submitted to the School of Graduate Studies In the Partial Fulfillment of the Requirements For the Degree Master of Applied Science

MASTER OF APPLIED SCIENCE (2021) McMaster University

Department of Chemical Engineering Hamilton, Ontario, Canada

TITLE: Hyaluronic Acid Based Therapeutic Bandage Contact Lenses For Corneal Wound Healing

AUTHOR: Jennifer (Jing Yuan) Tian, B.Sc (McMaster University)

SUPERVISOR: Dr. Heather Sheardown

NUMBER OF PAGES: xiv, 90

Abstract

The cornea is an avascular transparent tissue exposed to the environment and therefore highly susceptible to damage. With an increase in corneal refractive surgeries, corneal transplants, and corneal injuries, understanding and improving corneal healing mechanisms are extremely important. Impaired healing of corneal wounds can lead to decreased visual acuity and extreme pain. Serum eye drops, amniotic membranes, pharmaceutical agents, biopolymers, and cell transplants are just a few approaches that have been employed to improve wound healing. Bandage contact lenses (BCLs) have been proposed as a simple method to facilitate wound healing while reducing pain. The synthesis of a silicone hydrogel contact lens capable of surface binding hyaluronic acid (HA) for corneal wound healing was explored in the current work. HA was used as both a wetting agent and a therapeutic.

The work presented describes the synthesis, characterization, and cell testing of the HA binding model silicone hydrogels, composed of the hydrophilic monomer, 2-hydroxyethyl methacrylate (HEMA) and a hydrophobic silicone monomer, methacryloxypropyltris (trimethylsiloxy) silane (TRIS). Three different methods were evaluated for increasing HA binding and improving surface wettability.

"Caged lenses" utilized the same base polymer with the incorporation of methacrylated N-Hydroxysuccinimide (NHS). Hydrophilic polyethylene glycol (PEG) chains were then tethered from the NHS, forming a "cage" with the potential to physically entrap HA. Although surface wettability was improved, less HA was entrapped in the caged

lenses compared to model silicone hydrogels, presumably due to the increased hinderance resulting from the PEG chains.

"Tethered HA" lenses utilized PEG as a spacer to conjugate HA to the lens surface in order to improve surface hydrophilicity. Methacrylated HA conjugation resulted in a significant decrease in contact angle (p <0.01) compared to model pHEMA-co-TRIS whereas tethered thiolated HA did not lead to a significant decrease (p >0.05) in contact angle. It was clear that neither of these methods would lead to sufficient HA binding.

Ionic interaction lenses utilize monomers and small molecules that contain a positive charge to bind to the negatively charged HA under physiological conditions. The monomer diethylaminoethyl methacrylate (DEAEM) was polymerized directly into the polymer backbone, but resulted in no significant decrease (p >0.05) in contact angle. In comparison, surface functionalization using thiolene "click" chemistry allowed conjugation of the small molecule, dimethylamino ethanethiol (DMAET) and diethylamino ethanethiol (DEAET). DMAET and DEAET modified lenses showed significantly higher (p <0.001) HA binding compared to model pHEMA-co-TRIS controls at all time points. The modified lenses improved release kinetics preventing an initial burst release and showed consistent release when unloaded and reloaded with HA. The contact angle was significantly decreased (p <0.05) for the modified lenses with HA without affecting the equilibrium water content. Optical transparency was reduced following lens modifications although the thickness of the disks prepared was higher than a typical contact lens. Finally, the modified lenses did not exhibit any cytotoxicity *in vitro* with human corneal epithelial cells (HCECs).

The synthesis of silicone hydrogels capable of surface binding HA have potential to be used as a bandage contact lens while improving surface wettability and enhancing comfort.

ACKNOWLEDGEMENTS

There are many people I would like to thank who have helped me along the way throughout my thesis. First and foremost, thank you to my supervisor, Dr. Heather Sheardown for giving me this incredible experience and being an incredible mentor. For giving me so many opportunities to work with companies, conduct my own research, and present it at many conferences. Thank you for your incredible mentorship, continuous support, and guidance.

Thank you to all the members of the Sheardown lab past and present who made the lab an incredible place to work at. To Taylor and Nicole, thanks for being amazing lab and office mates but also amazing friends. To Eva, for all the adventures we had and will continue to have and for teaching me the correct way to apply skincare. To Lina, who has guided me to become the scientist I am today. Thank you for your continuous guidance throughout my thesis and always helping me troubleshoot. To Ben, thank you for teaching me all the *in vivo* techniques and for the countless laughs along the way. To Aftab, who helped me immensely along the way with cell work and for the many laughs in the CAF. To Talena, who taught me a lot about chemistry, lab safety, and NMRs. To Fran, thank you for your guidance throughout my thesis. To Dr. Lyndon Jones and Dr. Boyang Zhang for taking time to meet with me and offer suggestions to improve my project.

To Emily Anne, thank you for being my best friend through it all. Walking through Stanley park and Korean food sparked such an incredible friendship. From puzzles to puppy

quizzes to getting our nails done, thank you for making these 2 years amazing. You are going to be an incredible mom.

To my friends back home, I cannot thank you guys enough for being here for me through it all. From our annual cottage trips, karaoke, and game nights on zoom I am so grateful to have you guys in my life. To Bonnie, who I started my masters with and the many laughs we shared throughout our thesis. To Nate, thank you for being an amazing roommate, making me coffee, and not getting mad at me when I am a sore loser in Catan.

To Mitch, thank you for putting up with me, encouraging me, and supporting me and through it all. Thank you for always making me laugh, helping me when I need it, and being my best friend. Finally, a huge thank you to my parents who have continuously supported me, sent me back with a ton of food, and always voiced their love and how proud they are of me.

Table of Contents

LIST OF FIGURES

LIST OF TABLES

LIST OF ABBREVATIONS

BCL	Bandage Contact Lens
HA	Hyaluronic Acid
HEMA	2-hydroxyethyl methacrylate
TRIS	methacryloxypropyltris (trimethylsiloxy) silane
RHAMM	Hylauronan mediated motility receptor
GPI	Glycosylphosphatidylinositol
TGF	Transforming growth factor
bFGF	basic Fibroblast Growth Factor
HGF	Hepatocyte Growth Factor
KGF	Keratocyte Growth Factor
SiHys	Silicone hydrogels
IPA	Isopropyl Alcohol
NHS	N-Hydroxysuccinimide
PEG	Polyethylene glycol
DMAEM	Dimethylamino ethyl methacrylate
DEAEM	Diethylamino ethyl methacrylate
DMAET	Dimethylamino ethane thiol
DEAET	Diethylamino ethane thiol
HCECs	Human corneal epithelial cells
TACs	Transient amplifying cells
MTT	Thiazolyl blue tetrazolium bromide
EGDMA	Ethylene glycol dimethacrylate
MEHQ	Methoxyphenol hydroquinone
DMF	Dimethylformamide
TEA	Triethylamine
PBS	Phosphate buffered saline
D_2O	Deuterium oxide
NMR	Nuclear Magnetic Resonance
TCEP	Tris (2-carboxyethyl) phosphine
FTIR	Fourier transform infrared spectroscopy
AIBN	Azobisisobutyronitrile
DIPEA	N,N-Diisopropylethylamine
ATR	Attenuated total Reflection
EWC	Equilibrium water content
FITC	luorescein isothiocyanate
MES	2-(N-morpholino)ethanesulfonic acid
DAMP	4-(Dimethylamino) pyridine
ICL	Iodine monochloride
KSFM	Keratinocyte serum free medium
EGF	Epithelial growth factor
UV	Ultraviolet
ANOVA	Analysis of variance

1. Introduction

The physiology and anatomy of the cornea make it highly susceptible to injuries. It is a transparent avascular tissue composed of three cellular layers, the epithelium, stroma and endothelium, separated by two basement membranes (Bowman's membrane and Descemet's membrane). Approximately 3% of all emergency department visits are the result of eye trauma with 80% of them being corneal injuries.[1] The blink response is often not fast enough to react to events that cause corneal injuries.[2] The extent of injuries can range from small corneal abrasions to injuries that can compromise vision. Corneal abrasions typically heal on their own but may last for several days and are extremely painful.[3] The cornea is highly innervated and any defect results in an immense amount of pain, although this can vary depending on the level of disruption to the epithelium.[2,4] Along with corneal surface injuries, corneal defects are also becoming more frequent due to the rise of corneal refractive surgeries.[5] Therefore, better mechanisms need to be explored to improve corneal wound healing.

Eye patches have been a common treatment option for corneal abrasions as they have been thought to reduce blinking and eye-lid induced pain.[6] However, they lead to increased pain, a decreased amount of oxygen to the wound, an increased chance of infection, impeded vision, and overall an increased in the time the healing.[4,6] Current methods of treating corneal wound involve amniotic membrane bandages, serum eye drops, collagen shields, and BCLs. BCLs were first approved in the 1970s and have been used to treat a variety of corneal and ocular surface disorders. They have been shown to provide

pain relief, enhance corneal wound healing, provide corneal protection, drug delivery, and most importantly maintain vision.[7] BCLs have been shown to be a safe and effective way to treat corneal wounds while alleviating pain and promoting corneal epithelial regeneration.[8] BCLs help promote epithelial cell migration and regeneration of the basement membrane while protecting the eye against the shearing effects of the eyelid on the denuded area which can further inhibit re-epithelialization and cause pain to the patient.[9,10]

HA is a naturally occurring glycosaminoglycan which makes up a large component of the extracellular matrix. Due HA's low immunogenicity, high water retention, and viscoelastic properties, it is ideal for ophthalmic purposes. HA has been shown to improve corneal re-epithelization, improve tear stability, and provide hydration to the cornea optimizing the conditions for wound healing.[11,12]

The aim of this thesis is to design a HA binding bandage contact lens that may be useful in treating corneal wounds. In order to develop a lens to improve wound healing, different materials and HA incorporation methods were synthesized and tested. The material needs to have adequate oxygen permeability to avoid hypoxia as to promote corneal healing, the lens needs to be worn for extended periods of time. It is hypothesized that by binding HA, the lens can double as a therapeutic for improving corneal wound healing as well as enhance the hydrophilicity and therefore comfort of the lens. This comfort is necessary to ensure user compliance. Important parameters for a contact lens material including equilibrium water content (EWC), dehydration profiles, contact angle, and transparency were all tested. Through this work, it is hoped that a lens which is capable

of binding more HA compared to conventional hydrogels, improve corneal wound healing, and enhance comfort for extended wear can be designed.

2. Literature Review

2.1 Anatomy of the Anterior Segment of the Eye

The human eye, shown in Figure 1, is a complex organ that is protected solely by the eyelids, making it susceptible to damage. The eye is divided into two segments: the anterior segment and posterior segment. The anterior segment consists of the sclera, pupil, iris, lens, aqueous humor, and the cornea. The posterior segment consists of the retina, choroid, vitreous humor and the optic nerve.

2.2 Cornea: Anatomy and Physiology

The cornea (Figure 1), is a transparent avascular structure that contributes two thirds of the refractive power of the eye, provides a structural barrier, and protects the eye from infections while also filtering out ultraviolet rays.[13,14] The cornea is composed of 5 sections including the epithelium, Bowman's layer, the stroma, Descemet's membrane, and the corneal endothelium and consists of three major cell types: endothelial, stromal, and epithelial cells.[15-17]

2.2.1 Corneal Epithelium

The corneal epithelium is the outermost superficial layer of the cornea. The epithelium, along with the tear film, provides the smooth refractive surface of the cornea. It protects the stroma and prevents pathogens and tears from entering.[18] These cells have

an average 7-10 day turnover as they shed (become desquamated) and continue to get replenished.

The epithelium is divided into three layers: the superficial cells, wing cells, and basal cells. Superficial cells form two to three layers of flat cells which are covered by apical microvilli and microplicae.[19] These projections increase surface area and are covered by charged glycocalyx to allow interaction with the mucin layer of the tear film. Adjacent to the superficial cells are tight junctions which form a permeability barrier for the cornea. Beneath the superficial cells are wing cells which are less flat in shape and possess the same tight junctions. The final layer are basal cells which are a single layer of columnar epithelium which are about 20 μm tall.[19] Basal cells are the only corneal epithelial cells capable of mitosis. Daughter cells formed are pushed anteriorly and change morphology to become wing and superficial cells. Basal cells are adherent to the basement membrane through a hemi-desmosomal system.[19] Bowman's membrane rests between the stroma and the corneal epithelial layers and contains a specialized layer of collagen which cannot be regenerated after injury. It has been suggested that the primary role of Bowman's layer is to protect the subepithelial nerve plexus.[18]

2.2.2 Stroma

The corneal stroma comprises 90% of the corneal thickness and is key for structural integrity.[19,20] The stroma is composed of mainly water and stacked lamellae of collagen fibrils which are aligned in a fashion to reduce light scatter while providing mechanical strength to the cornea.[19] Each lamellae is formed from collagen fibres that lie parallel to each other and each alternating layer lays parallel forming an interwoven network which

maintains the corneal transparency and structural integrity.[19,20] Keratocytes are the main cell type in the stroma which comprise 10% of the stroma by volume, and are responsible for maintaining the ECM and collagen fibrils.[19,20]

2.2.3 Endothelium

The endothelium is a monolayer consisting of polygonal cells located on the posterior surface of the cornea.[21] They maintain their clarity by being in a deturgescence state.[21,22] The corneal endothelium also helps to maintain the hydration and nutrition of the cornea by pumping solutes and nutrients from the cornea to the rest of the anterior chamber.[21] Endothelial cells have a well-defined nucleus and are packed with mitochondria to keep up with the energy requirement of the cells as a fluid pump.[19,21] Endothelial cells are also responsible for the continuous synthesis of a collagenous product known as Descemet's membrane.[19,21]

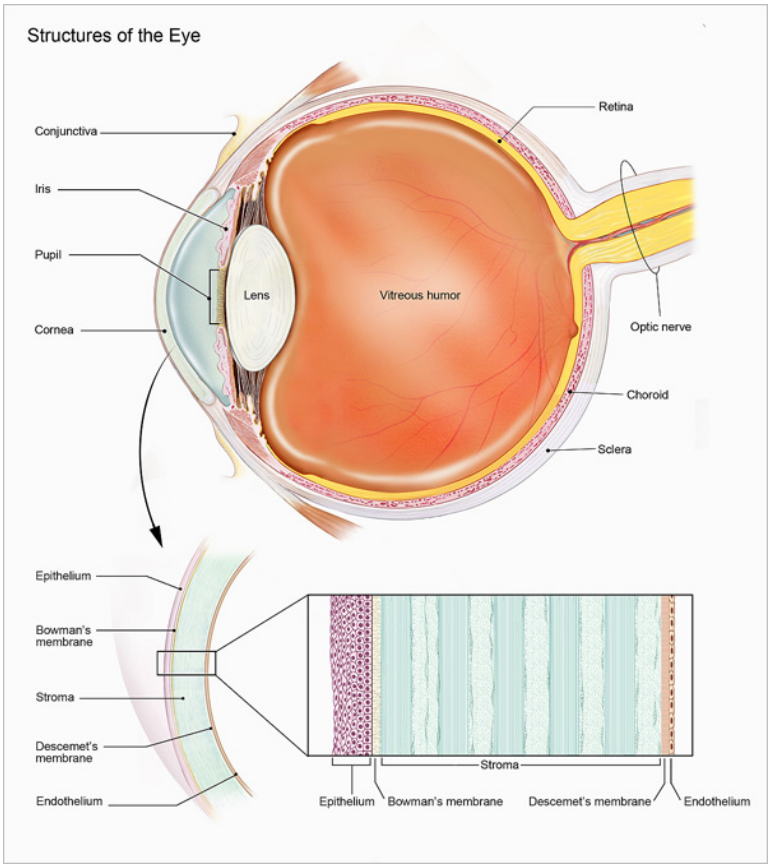

Figure 1: Cornea taken from[23]

2.3 Sclera, Conjunctiva, and Limbus

The sclera, the white robust part of the eye that provides support, is composed of primarily collagen fibrils within hydrated proteoglycans.[24] The conjunctiva, is the clear translucent mucous membrane that covers the sclera to provide ocular mechanical strength and immune defence. [24]

The limbus is located at the transition zone between the cornea and sclera.[25] Limbal stem cells reside in the limbal niche which contain cellular and chemical characteristics allowing them to remain stem cells or to promote growth and differentiation.[26,27] When

stem cells leave this niche they become transient amplifying cells (TACs) which allow them to rapidly proliferate and expand. TACs will migrate out the of the limbal stem cell niche and differentiate into corneal epithelial cells. Other cells within the niche include melanocytes, stromal (mesenchymal) cells, immune cell, vascular, and nerve cells.[28] Melanocytes protect the niche from UV irradiation and stromal mesenchymal cells helps maintain the stem cells as limbal stem cells.

2.4 Tear Film

The tear film shown in Figure 2, is a thin fluid layer that helps lubricate the eye, and smooths out the irregular microplicae on corneal epithelial cells.[29] The tear film is approximately 3 μm thick and 3 μl in volume with three distinct layers.[30,31] This includes an oil layer, aqueous layer, and a mucin layer.

The oil layer is approximately 50 to 100 nm thick and its main function is to prevent evaporation and reduce surface tension.[30,32] Tears lost through evaporation and drainage is replenished at a rate of 1-3 μL/min.[30] The oil layer is composed of many oily substances derived from the meibomian gland and contributes to the low evaporation rate of tears at 0.085 μL/min.[31] The superficial oil layer also plays a significant role in protecting the eye from small dust particles.[31]. The aqueous layer contains water, proteins, electrolytes, vitamins, immunoglobulins, peptides, and growth factors.[30-34] This layer is important for ocular lubrication, removing foreign bodies, antimicrobial activity, and nourishing the cornea.[33] Approximately 500 different proteins have been found in the tear film including lactoferrin, lysozyme, immunoglobulin G, albumin, and transferrin.[33] The final layer is a 2.5-5.0 μm thick mucin layer produced by both the corneal and conjunctival epithelium,

lacrimal gland, and goblet cells.[33] There are both secreted and transmembrane bound mucins. The aqueous layer contains soluble mucins which decrease surface tension, impact coherence, and decrease surface tension; while the surface bound mucin layer is anchored to the epithelium and composes predominantly of sugar rich glycosylated proteins.[32,33] The surface associated mucins form a thick cell surface glycocalyx which acts as a pathogen barrier.[34]

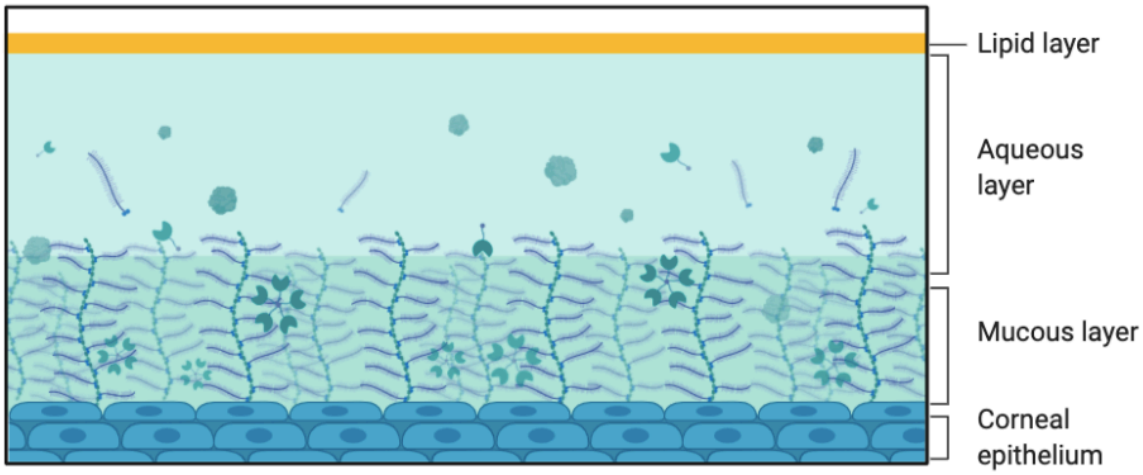

Figure 2: Schematic of the tear film. Created with Biorender.com

2.5 Corneal Epithelial Wound Healing

Due to the exposed nature of the cornea, it is highly susceptible to injury. The healing mechanism depends on the severity of damage and the corneal cell type impacted. Corneal epithelial wounds are the most common eye injury as they can be caused by day to day activities.[15] The epithelium will heal through cell migration and frequent replenishment from limbal stem cells.[5] Corneal epithelial wound healing can be described in three different phases but occurs continuously. This includes the latent phase, the migration and adhesion phase and the proliferation phase.[35]

The Latent Phase

The latent phase occurs from onset of injury to when cell migration occurs.[35,36] Cells undergo cleanup of the wound site as well as begin the process to start cell migration.[15] In this phase, there is cellular reorganization, protein synthesis, and change in tear film composition to prepare for wound healing as well as the synthesis of cell surface receptors such as CD44, glycoproteins, and glycolipids. [35,36] The production of enzymes is enhanced leading to degradation of cellular adhesion molecules as well as the damaged epithelial membrane.[37] Epithelial cells that are damaged undergo apoptosis and are cleared into the tear film.[35] Following this, the adherens and gap junctions are broken down.[35] Basal cells will flatten, separate, and then form cellular extensions to prepare for migration.[35] The epithelial cells will get covered with fibronectin which aid in the migration of neighbouring cells.[35]

Cell Migration

The migration phase occurs when epithelial cells migrate across the wound before mitosis occurs.[35] The movement is mediated by the contraction and formation of actin filaments.[35] Cellular extensions formed during the lag phase serve as temporary anchors. Contractile mechanisms draw the cell forward as the anchor points are cleaved and the process starts over.[35] Fibronectin is an important glycoprotein in providing a subepithelial matrix for the migrating cells to adhere to and appears within hours at the site after injury.[35] Once the migration of a monolayer of cells is complete, the cells become more firmly anchored. The attachment of cells require hemidesmosomes which are electron dense adhesion structures along the basal cell membrane that joins the cell to it.[35] Until the cells

are firmly anchored, the epithelial cell layer is relatively weakly bound and can easily be rubbed off.[35]

Proliferation

After migration of the monolayer is complete and is covering the wound, proliferation of epithelial cells occurs. Stem cells and transient amplifying cells (TACs) are located in the basal layer of the limbus and peripheral corneal epithelium.[17,35] These TACs begin to rapidly divide via mitosis, to what are called post mitotic cells, where they will move inward to fill the wound and upwards to restore thickness as shown in Figure 3.[17,35] The corneal epithelial cells divide and produce terminally differentiated corneal epithelial cells.[35] The cells ultimately change from basal to wing cells to then squamous cells as they move upwards.[38] Finally, hemidesmosomes anchor the epithelial to the stroma and desmosomes and tight junctions reform between the cells.[35]

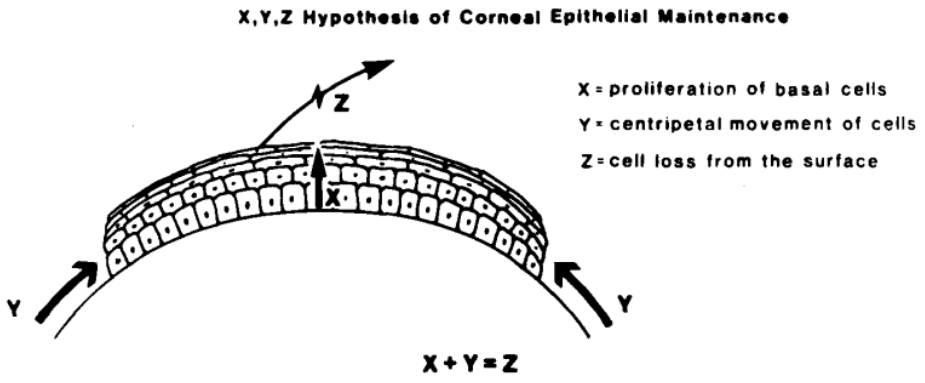

Figure 3: Mechanism of corneal wound healing taken from [39]

2.6 Hyaluronic Acid

Hyaluronic acid (HA) is a naturally occurring glycosaminoglycan conserved throughout all mammals. It is present in high concentrations in the skin, synovial fluid, soft connective tissue, and even in the brain, lungs, and kidneys. HA is naturally synthesized by a class of integral membrane proteins called hyaluronan synthases and found in the extracellular matrix of tissues.[40] The HA molecule, shown in Figure 4, consists of repeating units of N-acetylglucosamine and guluronic acid.[40] The first pharmaceutical grade HA was produced by Balazs *et al.* who extracted and purified HA from umbilical cord and rooster combs. HA has since been implemented for many uses in medicine.[41]

HA performs its biological function by either acting as a passive structural molecule or a signalling molecule.[41] Passively, HA in the body helps with lubrication, elasticity, and hydration of joints and muscles.[40] HA traps water between the coiled chains, acting like a sponge, allowing it to be excellent at retaining water.[42] As a signalling molecule, HA is able to interact with proteins and cause pro or anti-inflammatory activity, promotion or inhibition of cell migration, and activation or deactivation of mitosis.[41] Although the mechanisms of action for HA have not been fully elucidated, studies have shown the benefits of using exogenous HA for wound healing include pain reduction, reduction in activity of pro-inflammatory cytokines, and tissue hydration.[38,41] Since the first discovery of HA in the vitreous humor in 1934, it has been well studied and documented to be safe and efficacious for use for many applications including ophthalmology.[43]

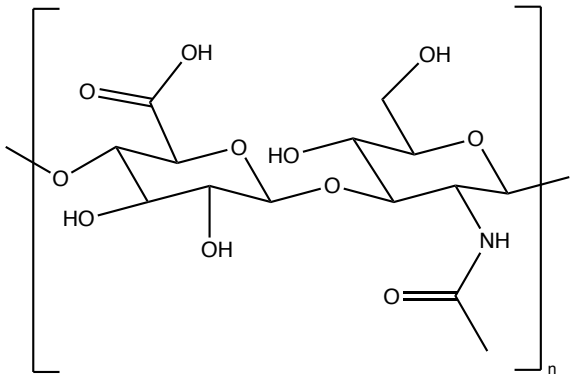

Figure 4: Structure of Hyaluronic Acid

2.6.1 Hyaluronic Acid in Ophthalmology

There are many uses for HA in ophthalmology; it reduces irritation, moisturizes the eye, and replenishes the naturally occurring HA in the tear film.[44] HA is found in many tissues in the eye including the aqueous humor, trabecular meshwork, and vitreous humor. In ophthalmology, it has been used for in ophthalmic surgeries, treatment of dry eye, and as a wetting agent in contact lenses.

The physiochemical properties of high molecular weight HA allow for its use in ophthalmic surgeries.[45] The first viscoelastic device was approved by the FDA in 1980 under the name Healon®. The elasticity of HA increases with an increase in molecular weight which helps protect cells from damage during surgery.[45] It has been shown that 1-3% HA significantly reduces endothelial damage and improves corneal endothelial wound healing.[45] 1% HA has been shown to provide good ocular manipulation, maintain the anterior chamber, and protect against endothelium damage when used for cataract surgeries.[46] HA has also been used to promote healing after corneal transplantation by enhancing wound healing and re-epithelization.[42,46] The exact mechanism by which HA

enhances cell proliferation and migration is not fully understood. However, HA has been shown to not only promote healing, but provide better quality of healing, resulting in a well layered and developed epithelium.[47] Mechanically, it enhances tear film stability, reduces friction caused by blinking, and reduces foreign substances from binding to the eye.[44] This provides optimal and comfortable post-surgery healing conditions.

The most common use for HA in ophthalmology is for the treatment of dry eye disease. HA has been shown to stabilize the tear film, lubricate, and increase conjunctival goblet cells.[11] Its elasticity, viscosity, and rheological properties allow it to act as an ocular lubricant in the treatment of dry eye, administered as eye drops or a gel.[45] A mixture of high and low molecular weight HA protects against dehydration and helps promote wound healing.[11] HA has been added to artificial tears to enhance moisture and duration of retention. HA eye drops have been used as a replacement for serum eye drops for the treatment of dry eye and wound healing.[48] Many eye drops on the market including SystaneULTRA®, HYLO®, and HydraSense® contain HA.

HA has also been added to supplement gels to prolong ocular residence time, improve biocompatibility, and prolong drug release.[11] The high biocompatibility, and capacity for HA to prolong drug release have made HA an excellent material of choice as artificial vitreous or for use with intravitreal injections.[11] HA was also investigated since the early 1980s for use as a raw material to develop intraocular lenses.[41]

2.6.2 Hyaluronic Acid Use in Contact Lenses

HA has been used in the contact lens field for over 20 years, enhancing comfort, wettability, and improving drug release. HA has been incorporated into contact lenses in

many ways including but not limited to direct entrapment, surface modification, and molecular imprinting.[11] The incorporation of HA onto contact lenses enhance biocompatibility, reduces protein adsorption, and slows tear removal.[11] Some multi-purpose solutions contain HA to decrease surface roughness of the lens and enhance water retention ultimately improving comfort of the contact lens.[49] Prolonged periods of wearing contact lenses causes them to dry out, which can be mitigated through the incorporation of HA. HA modified hydrogels are commonly used for improving wettability of both HEMA and silicone hydrogels. Korogiannaki *et al.* coated the surface of pHEMA lenses by grafting thiolated HA onto acrylated pHEMA hydrogels through the use of TCEP- mediated Michael addition thiolene based click chemistry. These lenses showed improved wettability, resistance to protein, and water retention properties.[49] Weeks *et al.* explored the incorporation of photo-crosslinkable methacrylated HA into the polymer as well as a dendrimer based method, with both methods showing an increase in surface hydrophilicity and decreased lysozyme absorption.[50,51] Lenses modified with HABpep allowed for the non-covalent binding of HA, which resulted in enhanced water retention and decreased evaporation.[52] More synthetic modifications to HA led to a decrease in the mobility as the molecule was shown to have a lower range of motion and decreased hydrophilicity.[51] All HA modified lenses show trends of increased wettability, decreased protein adsorption, and increased water retention making, it an excellent candidate as a wetting agent for hydrogels.

HA has been used synergistically as a comfort molecule for contact lens drug delivery.[53] HA has been used in conjunction with drugs delivered from contact lenses to enhance comfort. In the treatment of dry eye, HA can be used to improve lens wettability,

comfort, and to treat dry eye. By releasing HA from contact lenses instead of as an eye drop, the crosslinked nature of the lenses makes it harder for HA to diffuse out of the matrix, prolonging HA release and increasing residence time. Release from HA laden contact lenses has been shown to occur within the first 6 h and then slows but continues to release for 48 h.[11] Molecular imprinting strategies have been shown to further improve release rates and tailor release duration of HA at a therapeutic level for the treatment of dry eye.[54]

2.6.3 Hyaluronic Acid Receptors

HA, along with its degradation products generated during corneal epithelial wound repair, is capable of initiating many intracellular responses.[55] HA is able to regulate both micro and macro environments by binding to ECM molecules and cell receptors.[56] Cellular actions of HA are mediated by surface receptors with the main ones being CD44 and RHAMM (receptor for hyaluronate mediated motility) signalling.[55]

CD44 is the main HA binding receptor.[57] It is a cell surface adhesion molecule expressed on many different cells including corneal epithelial and endothelial cells.[57,58] CD44 has an amino terminal HA- binding region but binding is not always guaranteed.[59] Binding of HA is cell specific and depends on the activation state of CD44.[59] The ligands for CD44 are commonly ECM molecules such as HA, fibronectin, and collagen I and IV.[58] CD44 has an extracellular binding domain for HA and an intracellular binding domain to allow for interaction with cytoskeletal proteins, regular cell signalling, cell migration, cell adhesion HA degradation, and proliferation. [60-62] HA levels are elevated in wounds after injury along with an increase in CD44.[63]

RHAMM, a hyaluronan mediated motility receptor, is a large helical hydrophilic protein present intracellularly in the cytoplasm, in the nucleus, and on cell surfaces of conjunctival, corneal, and limbal epithelial cells.[57,59,64] RHAMM binds to HA through the positively charged amino acids in the carboxyl terminus.[64] RHAMM expression is significantly increased in response to injury and has been shown to be essential for tissue repair processes including cell migration, invasion, and ECM remodeling.[64] RHAMM is GPI anchored to the cell membrane where it can interact with CD44 and participate in many cellular functions including cell motility and wound healing.

2.7 Current Methods for Enhancing Corneal Wound Healing

Corneal epithelial wound healing has been a well-studied topic and the high percentage of corneal surface diseases, and an increase in refractive surgery, have led to many treatment options including topical steroids, autologous serum eye drops, amniotic membrane patching or grafting.

The utilization of blood derived products for ocular surface treatments was proposed decades ago. It was first adopted for Sjögrens syndrome and has since been an emerging way of treating a wide variety of ocular surface diseases.[65] These eye drops can be prepared with the patient's own blood serum (autologous) or from a donor (homologous).[65,66] Serum contains many biological substances which are contained in tears including growth factors, vitamins, and immunoglobulins which have therapeutic effects in the healing of ocular surface disorders.[66,67] Conventional eye drops on the market focus on alleviating symptoms of dry eye but do not contain factors that aid in healing whereas serum eyedrops provide both lubrication and components that speed up the healing process.

Serum eyedrops have been shown to support viability, proliferation, and migration of corneal epithelial cells.[67] Currently, there is no standardized international protocol for the production of serum eye drops, which leads to high variability. Serum can be affected by clotting time, centrifugation, dilution, and storing conditions.[67] Another issue that arises from this method is the potential spread of infectious diseases. Proper screening methods, sterilization protocols, and quality control will need to be implemented as the field develops.

Amniotic membranes (AM) are often used as a graft for corneal epithelial wound healing. The first use of AM for acute ocular burn was conducted by Sorsby and Symons in 1946[68] followed by Kim and Tseng in 1995.[69] where the successful reconstruction of rabbit corneas was observed. AM has been shown to have anti-inflammatory, anti-angiogenic, and anti-scarring properties.[67] AM acts as a supporting matrix for the adhesion of cells and promotion of wound healing by promoting inflammatory cell apoptosis, suppression of myofibroblast differentiation, inhibition of proteases and TGF- β signalling pathways.[70] It is composed of HA, collagen, and growth factors. AM grafting have been shown to provide both mechanical and biochemical effects on improving corneal epithelial wounds. Mechanically, the AM provides a basement like substrate for the healing of the corneal epithelium while providing hydration and protection from the shearing forces of the eyelid.[71] Biochemical factors involved in the reepithelization are derived from the AM epithelium including EGF (epithelial growth factor), keratinocyte growth factor (KGF), hepatocyte growth factor (HGF), and basic fibroblast growth factor (bFGF). AM therapy is reserved for use when measures such as ocular lubricants, therapeutic bandage contact

lenses, and/or serum eyedrops have failed or when there has been a loss of Bowman's layer.[67] The issue with using AM is the extensive serological screening, critical handling, storage requirements, poor mechanical strength, variation in quality, and is extremely expensive.[70] Current AM bandages on the market include Prokera®, AmbioDisc™, BioDOptix®, Aril™, and Petil™

Biomaterials are another common way of treating corneal wounds. Artificial tears and lubricants have been used to reduce mechanical stress and inhibit the inflammatory response. Chitosan, silk fibrin, and polyarginine, and hyaluronic acid are the most commonly studied biopolymers for corneal wound healing.[72] Several types of hydrogels have been employed for wound healing. Hydrogels made of collagen, gelatin, fibrin, and alginate have all been utilized. Collagen has been extensively studied as it is the most abundant protein in the human cornea.[73] Collagen shields, made of porcine or bovine collagen, are commonly employed for use as a bandage lens to treat corneal epithelial and stromal healing.[74] Polyethylene glycol (PEG) and cellulose derivatives are other common biomaterials used for corneal wound healing.[15] Alginate and chitosan based hydrogels have been shown to promote wound healing while facilitating cell delivery.[73] Chitosan is a de-acetylated form for chitin that is positively charged allowing interaction with the negatively charged mucin to allow for stronger attachment. Hydrogels used for corneal wound healing can be also employed as a cell carrier. Fibrin gels have been used as a limbal stem cell carrier as it increases the survival rate.

Proteins and growth factors are commonly used to accelerate wound healing. Growth factors are important for the maintenance of corneal epithelial cells. The most

common growth factors include EGF, transforming growth factor (TGF), and heparin binding EGF like (HBEGF) growth factor.[15] The ECM plays a vital role in proliferation, differentiation, and migration of corneal epithelial cells.[75] Extracellular matrix components have also been shown to facilitate wound healing. ECM components such as fibronectin, lumican, vitronectin, and hyaluronic acid are commonly used for wound healing.[15] Various other molecules including polysaccharides, and small molecules such as adenosin, timolol have also been employed to speed healing.

Methods of improving corneal wound healing continue to be developed with the ultimate purpose of expediting recovery time and reducing amount of pain.

2.8 Components of Contact Lens Materials

Contact lenses can be divided into two main categories: hard and soft. All polymer lenses are made using free radical polymerization of various co-monomers and a crosslinker. Hard contact lenses are rigid gas permeable (RGP) lenses whereas soft lenses are hydrogels made of flexible and high water content materials.[76] However, these lenses are not widely used, due to their relative discomfort. The discovery of the hydrophilic monomer, hydroxyethyl methyl methacrylate (HEMA), opened the field for the development of various soft hydrogel lenses.

The first soft contact lens made of pHEMA was FDA approved and introduced into the market in 1971.[77] Hydrogels made of just HEMA have a water content of approximately 38% which can be altered to 20-80% depending on the incorporation of various comonomers.[76,78] Soft hydrogel lens oxygen permeability is directly proportional to the amount of water within the lens and inversely proportional to lens thickness.[77] Most soft

contact lenses are co-polymers because different monomers allow different physical and chemical properties to be obtained. HEMA is often co-polymerized with monomers like methacrylic acid (MAA), and n-vinyl pyrrolidone (NVP) which increase water content to 55-75% but can lead to increased protein deposition.[76,79] MAA is an extremely hydrophilic monomer due to the presence of the free carboxylic acid which can bind water.[79] Poly vinyl alcohol (PVA) is another common biocompatible hydrophilic monomer that has excellent deposit resistance and can be added to improve water retention.[79] Methyl methacrylate is often used to lower water content and increase modulus.[79] With numerous available monomers, formulations and ratios need to be optimized to achieve desired lens attributes. Ethylene glycol dimethacrylate (EGDMA) is often used as the crosslinker as it contains two functional groups that allow the formation of networks between polymer chains.[76] An increased amount of crosslinker can affect properties like modulus and swelling ratios. The need for extended wear lenses caused various hydrogels to be introduced but posed high risks. Ultimately, HEMA hydrogels lacked sufficient oxygen permeability for extended wear which led to the evolution of silicone hydrogels (SiHys).[76]

Early lenses made of entirely silicone possessed exceptional oxygen permeability but were extremely uncomfortable and prone to deposition.[79] The silicone-oxygen bonds are more mobile compared to carbon-carbon bonds, less angled, and require much less energy to move which allows higher oxygen permeability.[80] Silicone, despite its excellent oxygen permeability, is quite hydrophobic, making it very uncomfortable to wear. This has led to the co-polymerization of silicone monomers with hydrophilic monomers. The introduction of SiHys which possessed the benefits of both high water content and

enhanced comfort with high oxygen permeability for extended wear, was a significant step in lens development. However, due to the enhanced mobility, the silicone oxygen bonds have a tendency to make their way to the surface which poses an issue with SiHys.[80] Early SiHys used surface treatments to mask the hydrophobic portions of silicone.[79] Alcon and Bausch+Lomb both used a gas plasma technique to improve hydrophilicty of the lenses. These lenses are referred to as first generation SiHys as these were the first attempts to combat hydrophobicity. Second generation SiHys utilize the incorporation of internal wetting agents including PVP, HA, and PEG.[79] The third generation lenses utilize specialized silicone based macromers that, when incorporated into the material, provide a naturally wetting lens.[79] Lens development continues to create new materials, with the ultimate goal of improving lens comfort. Since the introduction of SiHys, these lenses have not only been used for vision correction but have also been researched as drug delivery vehicles and bandage contact lenses.

2.9 Bandage Contact Lenses

Bandage contact lenses (BCLs) are lenses worn after an injury to protect the cornea and help facilitate its ability to heal. Since their approval in the 1970s, they have been used to treat a wide array of ocular diseases including dry eye, allergies, ulcers, and persistent epithelial defects to list a few.[81-83] A survey conducted showed that 72% of ophthalmic practitioners in North America prescribed BCLs for corneal wound healing and post-operative complications.[82] BCLs can provide mechanical protection, structural support, maintenance of corneal hydration, and drug delivery.[83] BCLs offer a protective barrier against the shearing forces of the eyelids, protecting the denuded area, and acting as a

scaffold for re-epithelialization.[7,84] They can also act as a splint, seal perforations, and apply pressure to stabilize loose adherent epithelium.[84] Cosmetic lenses are currently prescribed as BCLs as there are no specifically designed BCLs.

BCLs need to be worn for extended periods of time and therefore need to be made of high oxygen permeability materials, such as silicones, to avoid hypoxia.[83] However, silicone hydrogels are inherently more hydrophobic, decreasing wettability and comfort. Any disruption in the cornea, such as corneal abrasions, may affect tear distribution and production, therefore, adequate hydration is an important parameter for BCLs to improve comfort and enhance healing.[83] Clinicians have three different types of hydrogels to choose from when prescribing lenses as a therapeutic: high water content (70-80%) thick lenses (0.15-0.20 mm), intermediate water content (50-60%) and intermediate thickness lenses, and low water content (38-40%) ultra-thin lenses (0.01-0.06 mm).[84] High water content thick lenses are shown to be better used for corneal or limbal surface irregularity and disorders that cause high inflammation, whereas ultra-thin lenses have been shown to be better for diseases with minimal inflammation.[84] A properly fitted lens is important as the lens should provide adequate but not excessive movement to minimize shearing forces which create pain and cause further disruption on to the denuded area.[82-84] The coverage of the lens should be sufficient to cover the limbus and the wound while allowing some movement to promote healing.[83] Contact lenses with a flatter base curve results in greater BCL movement which results in increase tear exchange and greater oxygen permeability.[84] A decrease in lens movement is observed for steeper base curve contact lenses which is important for irregular corneal topography but may lead to a decrease in vision.[84] Irregular

corneas might lead to bubble formation under the lens and deformation of the lens apex upon blinking, causing decreased visual acuity.[84] Larger diameter lenses behave similar to steeper base curve lenses which is caused by the flattening at the corneal periphery.[84] Finally, the modulus of lens needs to be considered as higher moduli lenses may enhance the trauma to the epithelium but also enhance the lenses visual performance.[83] Therefore, based on the patient's disease, clinicians need to prescribe the correct lens as the treatment.

Bandage lenses pose two main problems: dehydration and infection. Contact lenses can alter the surface of the eye significantly. The hydrogel can cause dehydration of the tear film and the lens.[81] Although, new generations of silicone lenses show good wettability, the placement of a contact lens disrupts the tear film and increases evaporation rates by 2-fold.[30] During contact lens wear, the tear film is split into pre and post lens tear film. This results in decreased tear film stability and an impaired lipid layer, ultimately resulting in less lubrication and greater friction.[85] As a result, many contact lenses incorporate wetting agents such as PVP, HA, or HPMC to improve wettability. Silicone BCLs are prone to bacterial adhesion especially when there is lack of proper care.[82] Microbial keratitis is an infection that causes corneal inflammation which is often the cause of hypoxia or contact lens contamination.[86] Biofilm formation, consisting of lipids and proteins deposited on the lens, increases the risk of infection.[8,82] Ophthalmologists often supplement BCLs with antimicrobial eye drops but non-compliance results in higher rates of infection.[8]

3. Rationale/ Scope of Thesis

Wound closure is complex and requires rapid and proper healing to maintain corneal integrity. Bandage contact lenses have been shown to be an effective method of improving corneal wound healing. However, due to the extended wear time, silicone hydrogel contact lenses are necessary to ensure adequate oxygen permeability. However the high hydrophobicity of the lenses can lead to decreased comfort and secondary mechanical complications. HA is a common wetting agent that has been shown to improve corneal wound healing through improving tear film stability, cell migration, and cell proliferation. It has also been shown to enhance wound healing in some studies. Therefore, the hypothesis of this thesis is that by creating an HA binding silicone contact lens, wetting of the lens is improved, increasing comfort and improving corneal wound healing. The lens should have good EWC, transparency, and low water contact angle. The lens should be non-cytotoxic and capable of improving corneal wound closure.

Caged lenses, tethered HA lenses, and ionic interaction lenses were the three different methods used to create the HA containing lens material with a goal of improving surface wettability to enhance comfort and promote corneal wound healing.

In the cage lenses (Figure 5A), a PEG cage is formed on the surface of the lens that physically entraps HA. By incorporating PEG side chains, hydrophilicity and HA binding was predicted, with release kinetics that can provide a good material for therapeutic bandage contact lenses.

Although HA conjugated lenses have been previously reported in literature, a novel method of tethering HA to the lens with a PEG spacer was used (Figure 5B). The hypothesis

with these materials was that the PEG adds additional hydrophilicity, further improving comfort and corneal wound healing.

The rationale for ionic binding lenses was based on the work of Ali *et al.* who synthesized molecularly imprinted lenses and incorporated multiple monomers that have similar residues to CD44. DEAEM is a cationic acrylate that bears a positive charge similar to the residues, lysine and arginine, which were deemed crucial for binding. From their study, it was found that DEAEM out of the monomers used, allowed for the most immobilization of HA. In this work, DEAEM was incorporated into the backbone of the polymer or surface polymerized. DEAEM can be replaced with DEAET to allow more specific surface binding and mitigate DEAEM self-polymerization. HA under physiological conditions will ionize and bear a negative charge due to the carboxyl group (pKa= 3-4).[87] It was thought that this would in turn allow for the formation of an ionic bond on the surface between the positive charge of DEAEM and the negative charge on the HA, ideally create a reloadable system (Figure 5C).

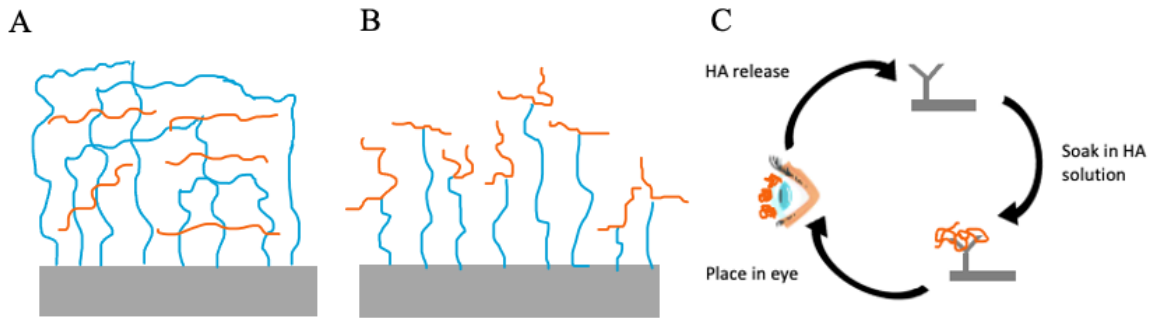

Figure 5: Schematic drawing of (A) Caged Lenses, (B) Tethered HA with PEG spacer, (C) Ionic Interaction lenses. Blue showing PEG spacers and Orange showing HA

4. Materials and Methods

Chemical and Materials. All chemicals and reagents were purchased from Sigma Aldrich (Oakville, ON, Canada) and used as obtained unless otherwise specified. Purified water with a resistivity of 17.9 MΩ cm was prepared using a Milli-pore Barnstead water purification system (Graham, NC, USA). Phosphate buffered saline (PBS 10X, pH 7.4) was purchased from BioShop (Burlington, ON) and diluted to 1x with MilliQ water prior to use. Regenerated cellulose 3.5 kDA dialysis bags were purchased from Spectrum Laboratories Inc (Rancho Dominguez, CA, USA). Slide-A-Lyzer 3.5 MWCO 3 mL were purchased from ThermoFischer scientific (Massachusetts, USA). Cellulose extraction thimble filters (30mm x80mm) were purchased from GE Healthcare Life Sciences (Chicago, IL, USA). Sodium hydroxide 1.0 M was purchased from LabChem INC (Pennsylvania, USA). Sodium hyaluronate (HA) with a molecular weight of 20 kDA was obtained from LifeCore Biomedical (Chaska, MN, USA), UV photoinitiator 1-hydroxy-cyclohexyl-phenyl-ketone and 2-Hydroxy-4′-(2-hydroxyethoxy)-2-methylpropiophenone (Irgacure® 184 and Irgacure® 2959) were donated from BASF Chemical Company (Vanalia, IL, USA). Bifunctionalized PEGs with a molecular weight of 10k were purchased from BiochemPEG (Waterdown, MA, USA). LIVE/DEAD™ Cell stain kit was purchased from ThermoFischer Scientific. Thiazolyl blue tetrazolium bromide (MTT) was purchased from Millipore Sigma (MA, USA) and diluted 10x using 0.1M autoclaved PBS.

4.1 Synthesis of Model pHEMA-co-TRIS Lenses

The monomers (HEMA and TRIS) as well as the crosslinker EGDMA were purified using a column packed with inhibitor remover to remove methoxyphenol hydroquinone (MEHQ). The initiator was prepared by dissolving Irgacure® 184 (500 mg/ml) in anhydrous ethanol; the mixture was placed on a shaker to ensure homogeneity. The model lenses were prepared using the concentrations of monomer, crosslinker, and initiator (weight %) shown in Table 1 The monomers were added into a vial and then placed on a shaking incubator for 10 minutes.

Table 1:Concentration in wt% of silicone hydrogel components in formulations

Lens Type	**HEMA (wt%)**	**TRIS (wt%)**	**EGDMA (wt%)**	**Irgacure ®184 (500mg/mL in EtOH)**
pHEMA-co-TRIS	90%	10%	3%	1%
pHEMA-co-TRIS with double initiator and double crosslinker	90%	10%	6%	2%

Due to the light sensitivity of the monomer solution, the vial was covered with aluminium foil. The monomer mixture was injected into a mould with 2 acrylic plates surrounding a 0.5 mm thick sheet spacer, as shown in Figure 6. The molds were placed into a 400 W UV chamber (ƛ=365 nm) (Cure Zone 2 Con-trol-cure, Chicago, IL) cured for 7.5 mins on one side and flipped and cured for 7.5 minutes on the other side to prevent the sheet from sticking. The polymer sheets were left overnight at room temperature. The sheet was removed from the mold the following day and placed in MilliQ water for 3 days to allow for swelling and the removal of any unreacted monomer. Model lenses were punched into discs (15mm in diameter), dried in the vacuum oven and stored at room temperature.

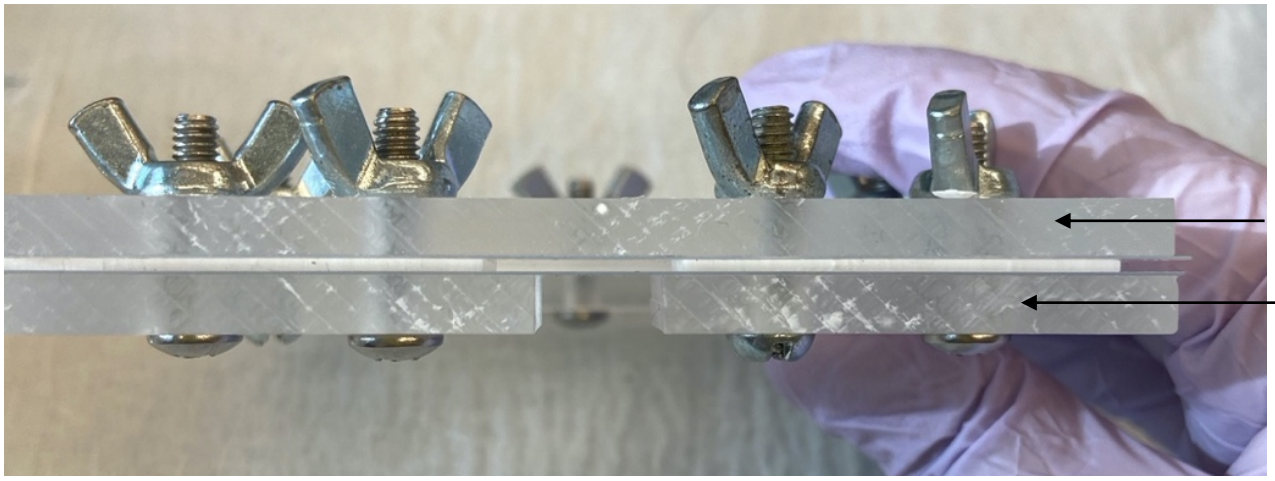

Figure 6: Custom made UV transparent acrylic mould with spacer. (A) acrylic plates (B) spacer.

4.2 Modified Lens Synthesis

4.2.1 Caged Lenses

Table 2:Concentration in wt% of silicone caged hydrogel components.

Monomer	**HEMA (wt%)**	**TRIS (wt%)**	**EGDMA (wt%)**	**Irgacure®184 (500mg/mL)**	**Methacrylated NHS**
Concentrations	90%	10%	3%	1%	2.5% (0.1 g in 200 µL of DCM)

The base material for the caged lenses were made following the same protocol as the conventional pHEMA-co-TRIS hydrogels but with the addition of 2.5% methacrylated NHS shown in Table 2. The monomer was dissolved in 200 µL of DCM followed by the addition of the subsequent monomers and initiator. The mixture was wrapped with foil to avoid light and stirred vigorously for 10 mins. The lenses were injected into the molds and then polymerized in the UV oven for 7.5 minutes on each side. 0.1 g of NH_2-PEG-maleimide was dissolved into 10 mL of PBS and the lens sheet was directly soaked into the solution. An optimal pH of 7 was monitored using a pH meter and maintained using 0.1 M NaOH. The lenses were reacted at 4 ^oC. Once the lenses had reacted and were hydrated,

they were punched into discs and Soxhlet extracted for 24 hours and dried until further use. The HA was dissolved in PBS at a concentration of 10 mg/mL and the lenses soaked for 20 minutes before the "top" of the cage was added. 0.1 g of bifunctionalized thiol terminated PEG was added to close the cage. The reaction was completed in the presence of a TCEP catalyst with a 0.7:1 molar ratio of TCEP to thiol. The reaction was left on the shaker for 3 days.

4.2.2 Tethered Lenses

Thiolated HA

The protocol for the preparation of thiolated HA was adapted from Korogiannaki *et al*.[49] Thiolated HA was prepared with degrees of thiolation of 10%, 50%, and 100% degree using the concentrations shown in Table 3. The amount of EDC and cysteamine dihydrochloride added was based on degree of thiolation as shown. 0.5 g of HA was added to a round bottom flask with 50 mL of MES buffer. EDC was added into the solution and stirred for 1.5 hours. Cysteamine dihydrochloride was added after 1.5 hours and the solution was left to mix for an additional 24 hours. The solution was then dialyzed using a 3.5 kDa cellulose dialysis membrane against MilliQ water for 3 days prior to freeze drying.

Table 3:Degree of HA thiolation (%) and corresponding components.

Batch percentage thiolation (theoretical)	**Hyaluronic Acid**	**EDC**	**Cystamine dihydrochloride**
10%	0.5 g	0.17 g	0.014 g
50%	0.5 g	0.84 g	0.071 g
100%	0.5 g	0.76 g	0.43 g

The conjugation was confirmed by NMR on a Bruker AVANCE 600 mHxz spectrometer with D_2O as the solvent (D, 99.96%, Cambridge Isotope Laboratories, Inc.).

Methacrylated HA

The methacrylation protocol was adapted from Sigen *et al.*[88] Briefly, 0.25 g of HA was dissolved using 30 mL of PBS, 0.936 g (0.87 mL) of glycidyl methacrylate, 10 mL of DMF, and a 5x excess of TEA (0.46 mL) was added to a 100 mL round bottom flask and the reaction was left stirring at room temperature and 350 rpm for a week. The product was precipitated into a 20x excess volume of cold acetone. The HA was then dialyzed against MilliQ water for 3 days. The conjugation was confirmed through NMR on a Bruker AVANCE 600 mHxz spectrometer with D_2O as the solvent (D, 99.96%, Cambridge Isotope Laboratories, Inc.).

The base material for the thiolated and methacrylated tethered HA contact lenses was prepared using a method similar to the cage lenses. For thiolated HA tethered lenses, after the addition of the NH_2 PEG maleimide, the lenses were put into a round bottom flask with 0.1 g of thiolated HA and 15 mL of PBS. 0.36 g of TCEP (3 molar excess) was added and pH was adjusted to 8. The solution was then degassed and left on the stirrer for 3 days. The finished lenses were extracted using MilliQ water. For methacrylated lenses, the same steps as the cage lenses were followed until the thiol PEG thiol closing step. At this point, 60 mg of TCEP was added along with 0.5 g methacrylated HA at room temperature for 3 days. The model lenses in this case were extracted using MilliQ water.

4.2.3 Ionic Interaction Lenses

4.2.3.1 Bulk Polymerization of Monomer

Post polymerization HA incorporation

2 g batches of lenses with DEAEM incorporated into the gel matrix at different concentrations were prepared using the weight percentages shown in Table 4.

Table 4:Concentration in wt% of silicone hydrogel components with the incorporation of DEAEM monomer

Lens Type	**DEAEM (wt%)**	**HEMA (wt%)**	**TRIS (wt%)**	**EGDMA (wt%)**	**Irgacure (500mg/mL in EtOH)**
More DEAEM	45%	45%	10%	3%	1%
Less DEAEM	5%	90%	5%	3%	1%

After the monomers are added, the mixture was placed on a shaking incubator for 10 mins to allow homogenous mixing. The lens fabrication steps followed the same protocol as the model pHEMA-co-TRIS lenses. The successful incorporation of the monomer was verified using an extraction with IPA and confirmed using NMR. A solution of 10 mg/mL HA solution in PBS of different molecular weights were used for the soaking of the lenses. The lenses were soaked in HA for 24 hours prior to testing using contact angle.

Pre- Polymerization HA Incorporation

In contrast to post-polymerization modification, batches of lenses were made with the incorporation of HA directly in the monomer mixture shown in Table 5. For a 2 g batch, the following concentrations were used. HA (6.5 mg for every g of polymer) was first

dissolved in 300 µL of water prior to the addition of the other monomers. The mixture was then placed on the shaking incubator and once the mixture was homogenous, the monomer solution was injected into the mould and cured in the UV oven.

Table 5:Concentrations in wt% of DEAEM monomer with HA incorporation into the bulk matrix of silicone hydrogels

Lens Type	**DEAEM (wt%)**	**HEMA (wt%)**	**TRIS (wt%)**	**EGDMA (wt%)**	**Irgacure (500mg/mL in EtOH)**	**HA (wt%)**
More DEAEM	25%	70%	5%	3%	1%	0.5%
Less DEAEM	5%	90%	5%	3%	1%	0.5%
Control (No DEAEM)	0%	90%	10%	3%	1%	0.5%

4.2.3.2 Surface modification of Lenses

Surface Methacrylation of pHEMA-co-TRIS Lenses

For surface methacrylation of pHEMA-co-TRIS model lenses (MethAcrpHEMA-co-TRIS), discs and glassware were dried overnight in a 70 ºC vacuum oven. 20 model lenses were placed into a 50 mL Erlenmeyer flask with a stir bar. The dried lenses were placed in a 1:1 v/v anyhydrous dicholormethane: toluene solution with 4 mL of triethylamine. The flask was sealed with a rubber stopper and covered with parafilm. The reaction was stirred at 350 rpm and 0.8 mL of methacrylol chloride was added dropwise. The by-products and unreacted chemicals were removed by thorough rinsing using fresh DCM: toluene 3 times followed by 3 rinses with MilliQ. The lenses were then blotted dry with a Kimwipe® and dried under vacuum and stored at room temperature until further use. The successful methacrylation of lenses was then confirmed with FTIR.

Polymerizing Monomer from MethAcrpHEMA-co-TRIS

The dried methacrylated model lenses were then placed into an Erlenmeyer flask with 20 mL of anhydrous toluene, 483 µL (451 mg) of DEAEM monomer, and 960 µL of 6.7 mg/mL AIBN (initiator). The flask was sealed, covered with parafilm and allowed to degas for 25 mins. The flask was then placed into an oil bath for 3.5 hours at 70 ^{o}C and 350 rpm. Once the reaction was completed, the flask was opened and exposed to oxygen to terminate the reaction. The discs were rinsed 3x in toluene and 3x in water to remove unreacted molecules. Finally, they were blotted dry with a Kimwipe® and dried overnight at 35^{o}C in a vacuum oven. The confirmation of the reaction was conducted using FTIR.

Surface Acrylation of pHEMA- co-TRIS Lenses

The surface acrylation of pHEMA-co-TRIS (AcrpHEMA-co-TRIS) model lenses followed the same protocol as the surface methacrylation of lenses except for the replacement of TEA with DIPEA (1.42mM per disc) as a catalyst. Methacrylol chloride was replaced with acryloyl chloride, (0.428 mM per disc).

Surface Grafting of Small Molecules on AcrpHEMA-co-TRIS

In a 20 mL glass vial containing fully hydrated surface acrylated model lenses in PBS, (0.642 mM per lens, 1:1.5 mol acrylate:thiol) either DMAET or DEAET was added. 1:1 molar ratio of Irgacure® 2959:acrylates was dissolved in 200 µL of anhydrous ethanol and added to the solution. The vial was placed on the shaking incubator for 10 minutes to allow homogenous mixing before the pH was adjusted to 7.15 using 1.0 M NaOH. The vial was placed into a 400 W UV chamber (ƛ=365 nm) for 20 minutes. Following the catalyzed thiol-ene ‘click’ reaction, the lenses were Soxhlet extracted with MilliQ water for 2 days to

remove any unreacted chemicals. The purified lenses were then dried and the surface modification was confirmed with FTIR.

4.3 Material Characterization

4.3.1 Contact Angle using Sessile Drop

Surface wettability of hydrogel surfaces was measured using contact angles by the sessile drop technique (Krüss Drop Shape Analysis System-DSA 10, Matthews, NC, USA). Water contact angles were measured on fully hydrated discs. The lenses were soaked in MilliQ or 10 mg/mL HA dissolved in PBS overnight. The lenses were blotted with a Kimwipe® to remove excess water before a 5 µl drop of water was placed on the surface. The angle between the drop and the hydrogel surface was measured and calculated using a video software (Drop shape Analyzer). All measurements were completed at ambient temperature and humidity.

4.3.2 Fourier Transform Infrared Spectroscopy

To determine surface lens chemistry, ATR Fourier Transform Infrared Spectroscopy (FTIR) was used. The lenses were dried in the vacuum oven for at least 12 hours prior to checking the lens. A Nicolet 6700 Fourier Transform Infrared Spectrometer (Thermoscientific, Waltham, Massachusetts USA) was used. The absorption spectra used for characterization were in the range of 600- 4000cm^{-1} (64 scans, 4 cm^{-1} resolution).

4.3.3 Water Content and Dehydration Study

To assess the dehydration profile of the model contact lenses, the lenses were swollen in MilliQ water ($W_{swollen}$) for 48 hours before being weighed individually. The lenses were carefully blotted with a Kim Wipe to remove excess water. The lenses were

then weighed at various time points over the span of 24 hours to determine mass change (n=4). The dehydration rate was calculated using the following equation;

Equation 1

$$water\ loss(\%) = \frac{W_{Swollen} - W_t}{W_{swollen} - W_{Dry}} \times\ 100\%$$

Equilibrium water content was calculated using the same swollen lenses and lenses dried in the vacuum oven for at least 48 hours. The equilibrium water content was calculated using the following equation;

Equation 2

$$Eqilibrium\ Water\ Content(\%) = \frac{W_{Swollen} - W_t}{W_{dry}} \times\ 100\%$$

4.3.4 Transparency

Optical transparency of the model lenses was determined using light transmittance (%) of fully hydrated lenses. The model lenses (n=6) were placed in a UV-Star® UV transparent 96 well microplate with 200 µl of MilliQ water to measure transmittance using UV-VIS spectrometer (Molecular Devices SpectraMax® ABS PLUS, San Jose, USA) over the 400-750 nm range.

4.3.5 Quantitative HA Binding using Radiolabelled HA

Phenolated HA

100 mg of HA was dissolved into either MilliQ or MES buffer. A 2 mg/ml solution of DAMP was added into the flask and the mixture allowed to react for 2 hours. The pH was measured at the beginning of the reaction. After 2 hours, 6.15 mg of 3-phenolamino

was added to the flask and the pH was adjusted to 7.5. The reaction was left stirring at 350 rpm for 24 hours. Once the reaction was completed, the solution was transferred to a 3.5 kDa dialysis bag and dialyzed for 3 days against MilliQ water and subsequently freeze dried. The conjugation was confirmed through NMR on using D_2O as the solvent (D, 99.96%, Cambridge Isotope Laboratories, Inc.).

Radiolabelled HA

For quantification of bound and released HA from modified HA surfaces, phenolated HA was radiolabelled with I^{125} using the iodine monochloride (ICL) method.[89,90] HA was radiolabelled using two different methods, glycine and PBS method. In the glycine method, 0.5 mL of 10 mg/mL phenolated HA was added to 200 μL of glycine buffer. In another vial, 280 μL of ICL 0.0033M and 1000 μL of glycine were added. 10 μL of I^{125} was added to the second vial for 5 mins and then the 2 vials were mixed for 10 mins. In the PBS method, the first vial contained 0.5 mL of 10 mg/mL phenolated HA in PBS. In the second vial, 280 μL of ICL (0.0033 M) and 560 μL of PBS was added. Similar to the glycine buffer method, 10 μL of I^{125} was mixed with the second vial for 10 mins.

Following iodination, the radiolabelled HA solution was placed in a Slide-A-Lyzer with a MWCO of 3.5 kDA to remove unreacted I^{125}. The solution was dialyzed against PBS for 4 days. The solutions were then mixed with non-radioactive HA to create a working solution that had a HA concentration of 1 mg/mL (10% radiolabelled). The radioactivity of the solution was measured using a Gamma Counter (Perkin Elmer, Wallac Wizard 1470 Automatic Gamma Counter, Wellesley MA). The radioactivity was converted to amount of HA using a calibration curve.

To determine the quantitative binding of the HA to the model lenses, the lenses (n=6) were placed in 48 well plate with 1.1 mL of the HA working solution (1 mg/mL) . At specified time points, the lenses were removed and the radioactivity determined by Gamma Counting. To test the release of HA, the lenses were soaked in the working solution for 8 and 24 hours and then released into fresh PBS. The PBS release solution as well as the lenses were read on the gamma counter at each time point.

4.4 Cell Interactions with HA Modified Materials

Human corneal epithelial cells (provided by Dr. May Griffith, University of Montreal) were cultured in Gibco™ Defined Keratinocyte Serum Free Medium (KSFM), containing 25 mg of bovine pituitary extract and 2.5 µg human recombinant epidermal growth factor, at 37°C, 5% CO_2. Cells were counted using a hemocytometer.

4.4.1 Cell Viability

Human corneal epithelial cells (HCECs) were seeded at a 30,000 cell per well density into a 96 well plate. The cells were allowed to adhere overnight before replacing the media and adding the respective treatments. The treatment groups included: positive control with no treatment, negative control, pHEMA-co-TRIS, DMAET modified lenses, DEAET modified lenses. To produce negative controls, untreated cells were exposed to 100 µL of 0.25% Triton and incubated for 3 mins. Following incubation, the wells were washed 3x with 200 µL of sterile PBS. Model lenses (n=4) were placed vertically for 24 and 48 hrs. The discs were removed at the respective time points and the remaining media in each well was removed. A 5 mg/mL MTT solution was made and diluted 10x using

KSFM before adding 100 µL to each well. The plate was returned to the incubator for 3 hours. The MTT mixture was then carefully removed to not disrupt formazan crystals and 200 µL of sterile filtered DMSO was added to each well and mixed. The plate was then covered with aluminium foil and allowed to sit at room temperature for 15 mins.

Absorbance measurements were taken on a SpectraMax® ABS Plus UV-vis micro-plate reader (Molecular Devices, San Jose, California, USA) at the wavelength of 570 nm. The cell viability was then calculated using the following equation.

Equation 3

$$Cell\ Viability\ (\%) = \frac{Abs_{sample}}{Abs_{control}} \times 100$$

4.4.2 LIVE/DEAD

Cell cytotoxicity was also visualized through LIVE/DEAD staining. Cell seeding, culture, and treatment followed the same protocol as MTT cell viability study. Following treatments, the cells were treated with 100 µL of the Invitrogen LIVE/DEAD™ working solution made from 10 µL of 2 mM ethidium homodimer-1 stock solution and 2.5 µL of the 4 mM calcein AM stock solution diluted in 5 mL of sterile PBS and vortexed. The working solution was added to each well and allowed to incubate for 45 mins at room temperature prior to imaging.

Cells were imaged using an Olympus IX51 inverted bright field and fluorescent microscope. Images were taken at 10x magnification with an n of 4 using the FITC and Texas red filters. Monochromatic grayscale imaging Retiga 2000R cameras were used to

capture the images and Olympus cellSensDimension™ software was used to process the images (Shinjuku, Tokyo, Japan).

4.4.3 Scratch Model

Cells were seeded in a 24 clear bottom well plate at 100,000 cells per well and allowed to adhere and become 100% confluent prior to creating a scratch. KSFM changes were conducted every other day until confluency. A P10 pipette tip was used to create a scratch in the well. The wells were washed 3 times with sterilized PBS prior to the treatment. Four markings were placed on the underside of the wells to locate the scratch. Treatment groups were as follows: control, EGF (as a positive control), and 20k and 100k HA (n=4). EGF was diluted to 50 ng/mL using KSFM and HA was prepared at a concentration of 10 mg/mL and UV sterilized for 12 hours. Images of the scratch were taken at 0 and 24 hours using a Zeiss Axiovert200 inverted microscope with the AxioVision software. The area of the cells was calculated using the open-source software ImageJ (NIH).

4.4.4 Boyden Chamber

Cells were seeded at a density of 50,000 cells/well into 8 μM and 12 μM cell inserts and covered with 0.5 mL of KSFM. The chemoattract treatment groups: EGF (50 ng/mL) and UV sterilized HA (10mg/mL) were diluted with KSFM and placed into the well plate. The cells were incubated for 24 hours. A sterilized Q-tip was used to scrape away the cells from the top of the insert. The cell insert was then washed 3x with PBS prior to staining. The inserts are then place into a 5 μg/mL solution of Hoescht stain and incubated for 10 minutes prior to 3 rinses with PBS. The cells were then imaged at 10x magnification using

the Zeiss Axiovert 200 Inverted microscope with fluorescence using the AxioVision software.

4.5 Statistical Analysis

Statistical analysis was carried out using student t-test, single- factor analysis of variance (ANOVA), and post-hoc Tukey test in IBM® SPSS statistical tool and Microsoft excel as appropriate. The p value was set to $p < 0.05$ for significance and $p < 0.001$ for high significance. All data are shown as mean ± standard deviation (SD).

5 Results and Discussion

5.1 Synthesis and Characterization of "Caged" Lenses

For the synthesis of caged lenses, the base material was similar to model pHEMA-co-TRIS with the addition of methacrylated NHS shown in Figure 7. NHS esters react with primary amines at slightly alkaline conditions to form stable amide bonds releasing an NHS leaving group.[91] This reaction competes with hydrolysis and amine reactivity which both increase with pH.[91]

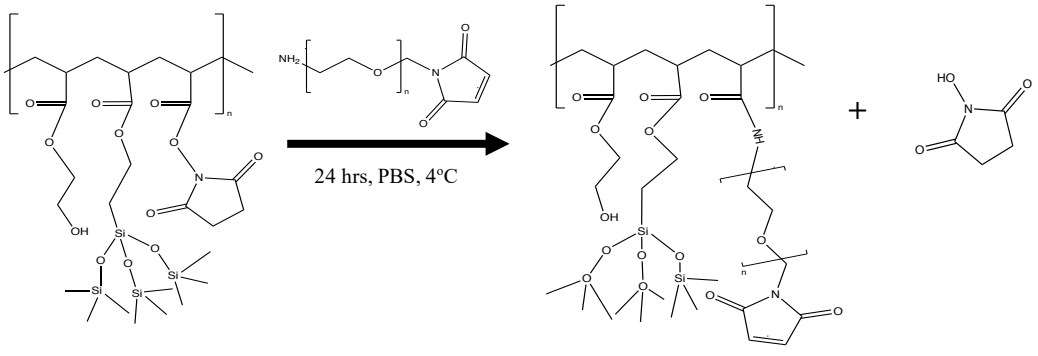

Figure 7: Schematic scheme of NMS incorporated into the backbone of the lens, followed by the incorporation of NH_2 PEG maleimide displacement.

The lens sheets, after polymerization, were directly soaked into the bi-functionalized amine maleimide terminated PEG shown in Figure 8, to mitigate hydrolysis. Hydrolysis was monitored through frequent pH measurements. The successful incorporation of PEG was quantified through mass recovery. The residual PEG was dialyzed to remove NHS in order to determine amount of PEG reacted. The final percentage of reacted NH_2-PEG-Maleimide was 18.9 % (0.02 mg). ATR-FTIR was run on the NMS materials shown in Figure A1, but due to the lack of distinct functional group peaks and relatively low surface specificity of this method, characterization was not successful. The sheets were cut into disc shapes prior to the addition of HA. The HA was premixed for 10 mins to allow entanglement; this was followed by the addition of the bi-functional thiol PEG. The pH was set to 7-7.3 as maleimides react specifically with thiols at a pH range of 6.5-7.5.[91] pH was monitored closely as an increase in pH also increases the potential for the maleimides to undergo hydrolysis and become unreactive to sulfhydryls.[91]

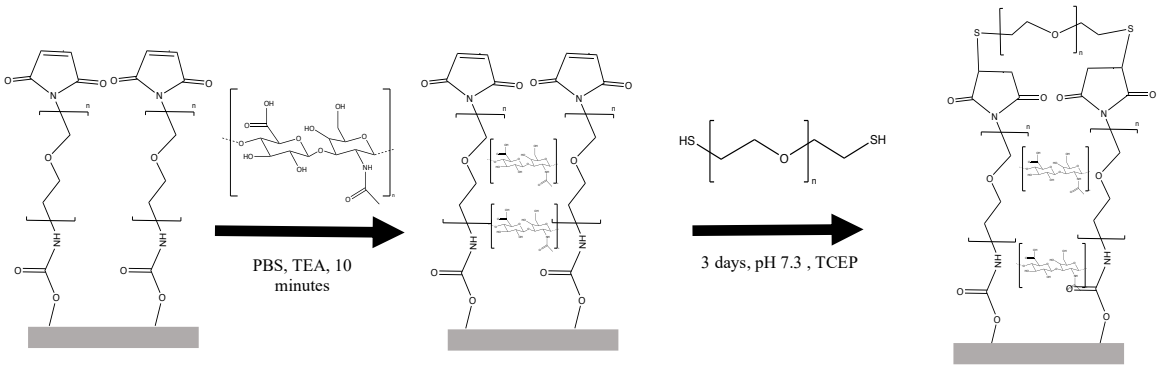

Figure 8: Schematic scheme showing synthesis of caged lenses

As shown in Figure 9, lenses with HA incorporated exhibited a lower contact angle which was to be expected as the highly hydrophilic HA should increase the wettability of

the lens. The final HA modified materials showed a highly significant decrease (p <0.005) in contact angle.

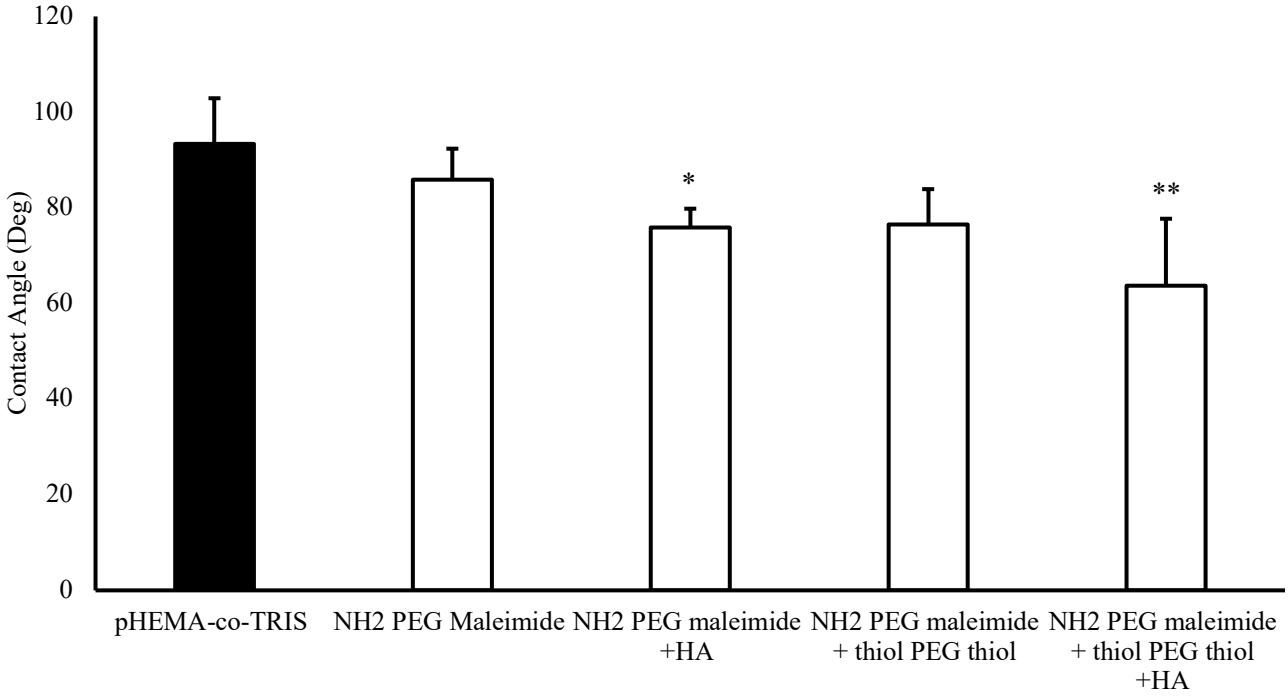

*Figure 9: Water contact angle (±SD) of unmodified model pHEMA-co-TRIS lenses, NH2 PEG Maleimide modified lenses with and without HA, and closed cage lenses with and without HA. Significant decrease in contact angle shown for lenses incorporated with HA (*p<0.05 and **p<0.005) (n=3).*

To further quantify the amount of HA associated with the lens materials, radiolabelled HA was used. Despite the decrease in contact angle, the amount of HA incorporated into the cage lenses was significantly less (p <0.02) than observed with the model pHEMA-co-TRIS controls (Figure 10). This could be attributed to the fact that the PEG chains on the caged lenses blocked the HA from penetrating deeper into the matrix whereas the model pHEMA-co-TRIS lenses did not contain this hinderance. Furthermore, since the contact angle measures surface properties which show a positive trend, it is likely

that the absolute amount of HA associated with the materials is not an indication of wetting or ultimately lens performance.

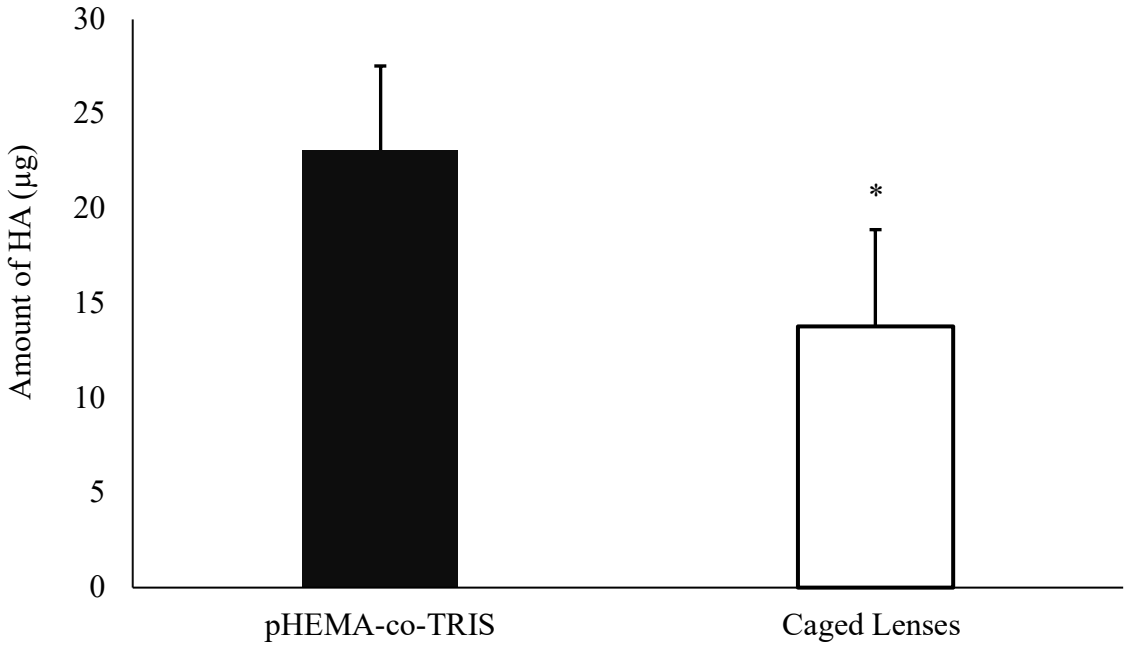

*Figure 10: The amount of HA (µg) (±SD) bound and/or incorporated into the lenses. Caged lenses show a lower amount of HA bound/incorporated into the lens compared to model pHEMA-co-TRIS (n=6) (*p <0.02)*

5.2 Synthesis and Characterization of Tethered Lenses

5.2.1 Methacrylated HA

Using a method adapted from Sigen *et al.,* methacrylated HA was synthesized as shown in Figure 11.[88] In this reaction, methacrylate groups conjugate to HA through the competition of two reactions. The epoxy group on the glycidyl methacrylate can undergo a ring-opening or a reversible transesterification through the hydroxyl group of HA. The reaction was left for 7 days to favour the irreversible epoxide opening step.

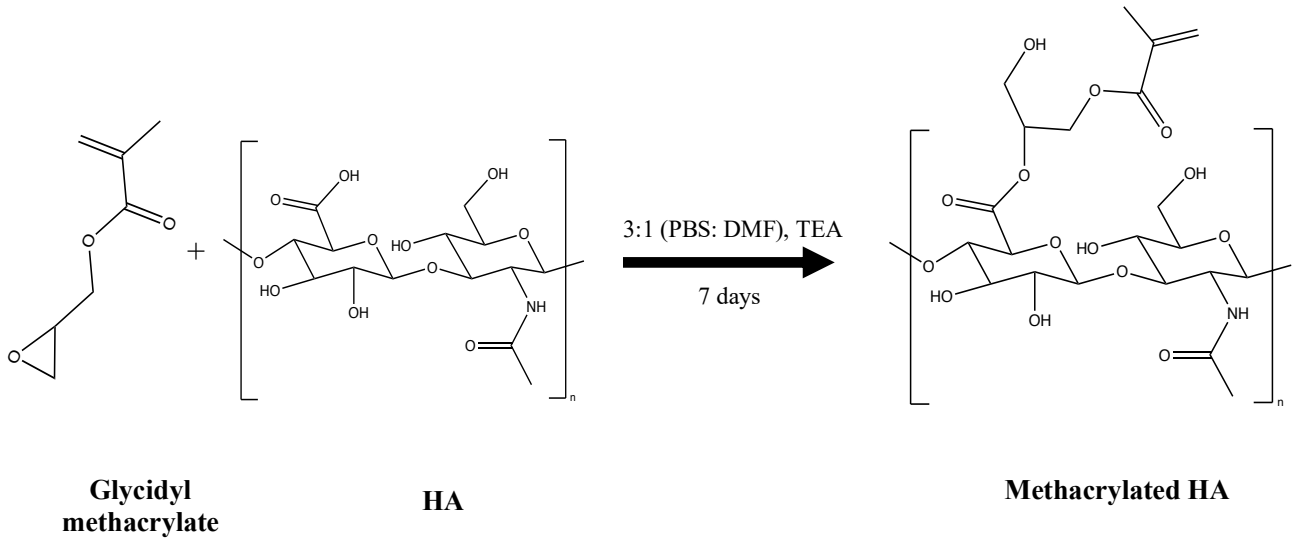

Figure 11: Reaction scheme of the synthesis of methacrylated HA.

The confirmation of the successful methacrylation of HA was obtained using NMR (Figure 12). Peaks at 3.4 to 3.9 ppm correspond to the six methine groups of the 6 membered rings of the HA backbone. Peaks at 3.8 and 4.6 ppm are indicative of the double bond of the methacrylate which is absent in the unmodified HA. Integration indicates that the degree of functionalization was approximately 4%.

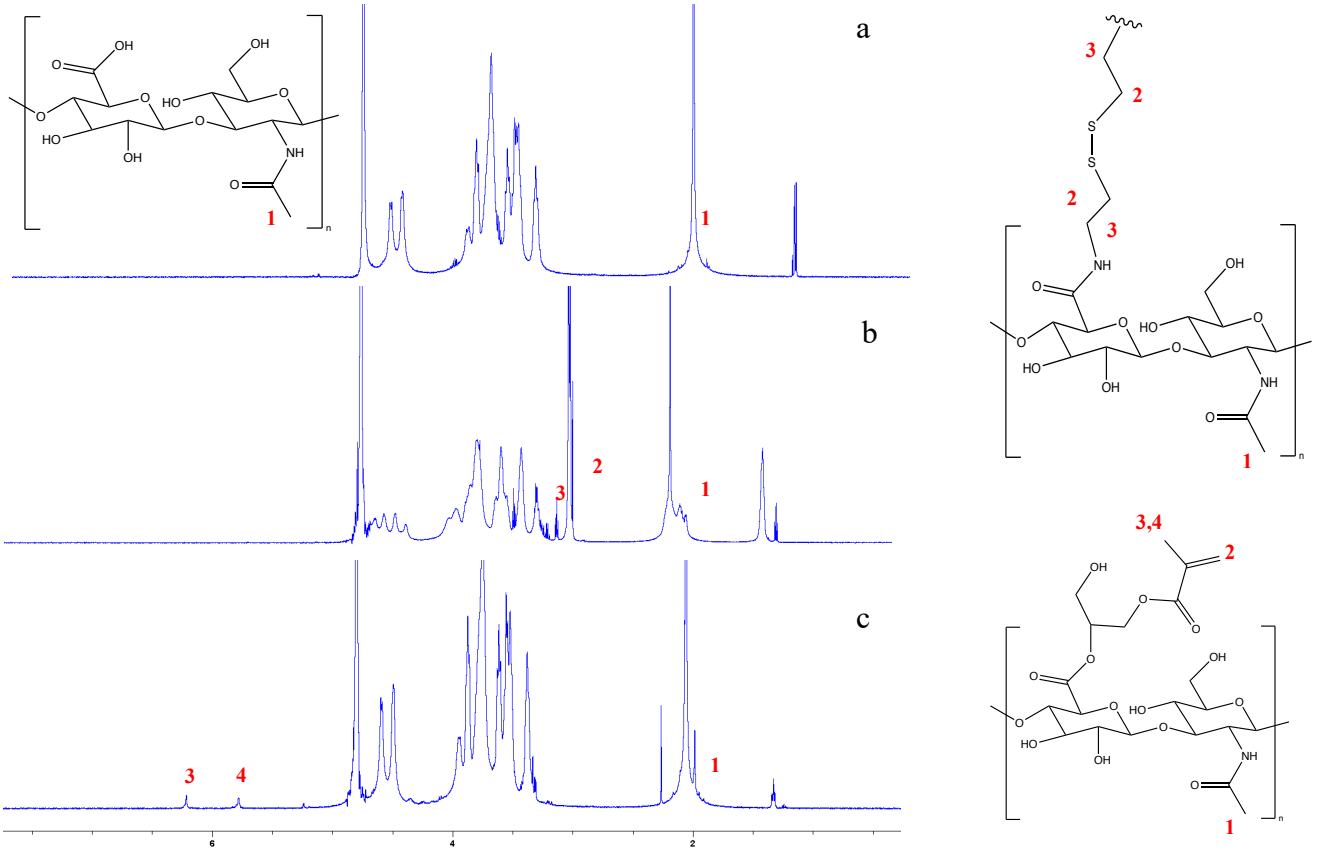

Figure 12: [1]H NMR spectra of (a) unmodified HA Modified HA (b) Thiolated HA (c) Methacrylated HA

The methacrylated HA was tethered onto the lens following the addition of bi-functionalized thiol PEG to complete a thiol maleimide "click" reaction (Figure 13). By incorporating long chain thiolated PEG from the polymer backbone, a simultaneous increase in the HA binding would be expected in addition to increased hydrophilicity.

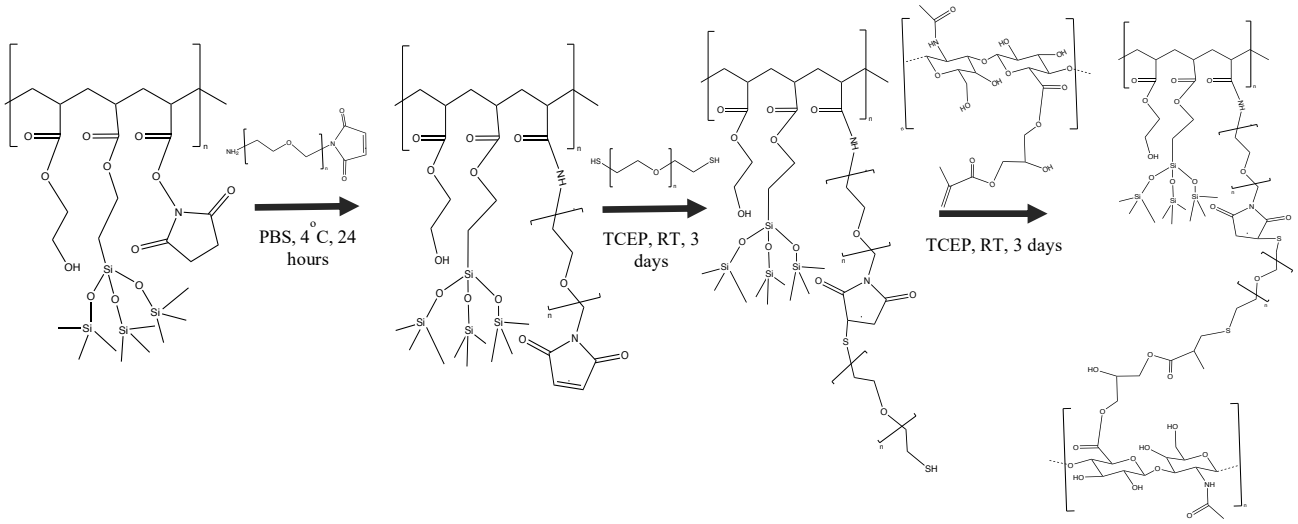

Figure 13: Schematic scheme of the synthesis of tethered methacrylated HA onto model pHEMA-co-TRIS lenses.

Following attachment of the methacrylated HA, contact angle was used to assess tethering. Although the results shown in Figure 14 demonstrate a significant decrease in contact angle, chemical analysis of the surfaces will be necessary to confirm covalent surface modification.

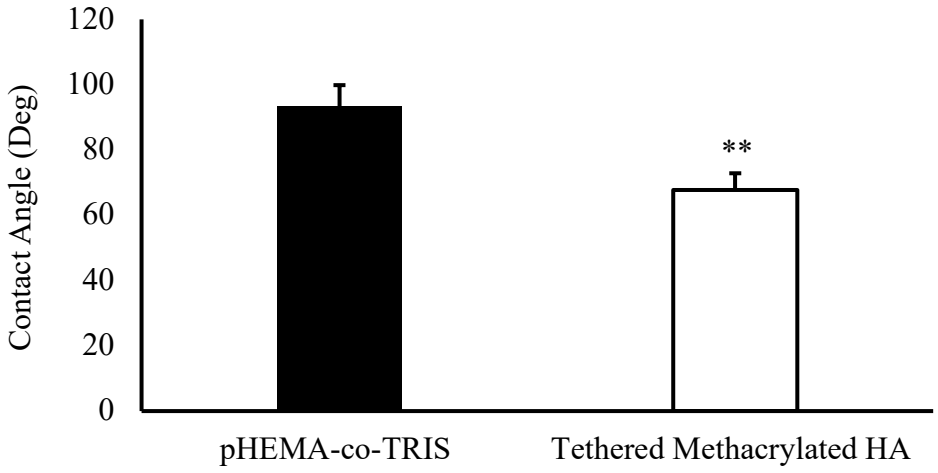

*Figure 14: Contact angle comparing model pHEMA-co-TRIS lenses to tethered methacrylated HA lenses. Tethered methacrylated lenses shows a significant decrease in contact angle. (n=3) (**p<0.007)*

5.2.2 Thiolated HA

Thiolated HA was synthesized using EDC chemistry, in which EDC reacts with the carboxylic acid of HA to form an active o-acylisourea intermediate as shown in Figure 15.[91] This intermediate can then be easily displaced through a nucleophilic attack by primary amines.[91] Successful conjugation was confirmed using NMR (Figure 12,C). The peaks around 2.7-2.9 ppm are indicative of hydrogens near the disulfide. The degree of thiolation can be altered by adjusting EDC and cysteamine dihydrochloride concentrations. Lower thiol content allows tethered HA to be more mobile and exhibit less toxicity; therefore HA with 10% thiolation was chosen for further testing.[49]

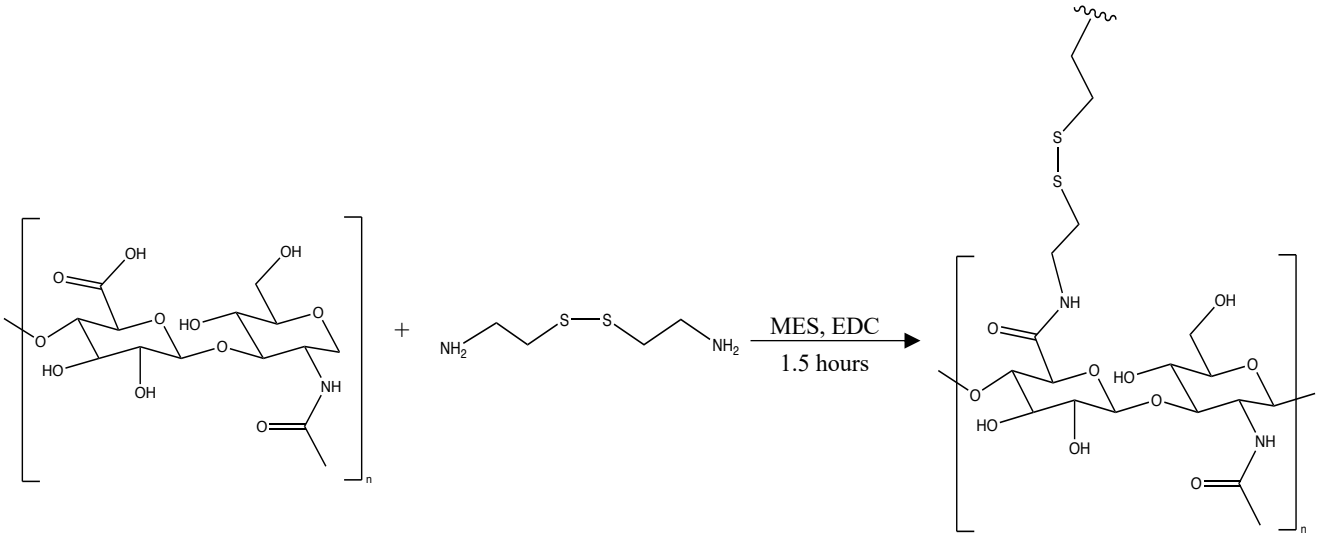

HA **Cysteamine dihydrochloride** **Thiolated HA**

Figure 15: Reaction scheme for the synthesis of thiolated HA.

The method used for tethering of thiolated HA lenses was similar to the tethering of methacrylated HA except there was no need for the thiol PEG thiol intermediate step shown in Figure 16. Once the NH_2-PEG-Maleimide had been conjugated, the thiolated HA

could be tethered directly through a maleimide thiol click reaction. The TCEP acted as a catalyst, cleaving the disulfide bond in the thiolated HA.

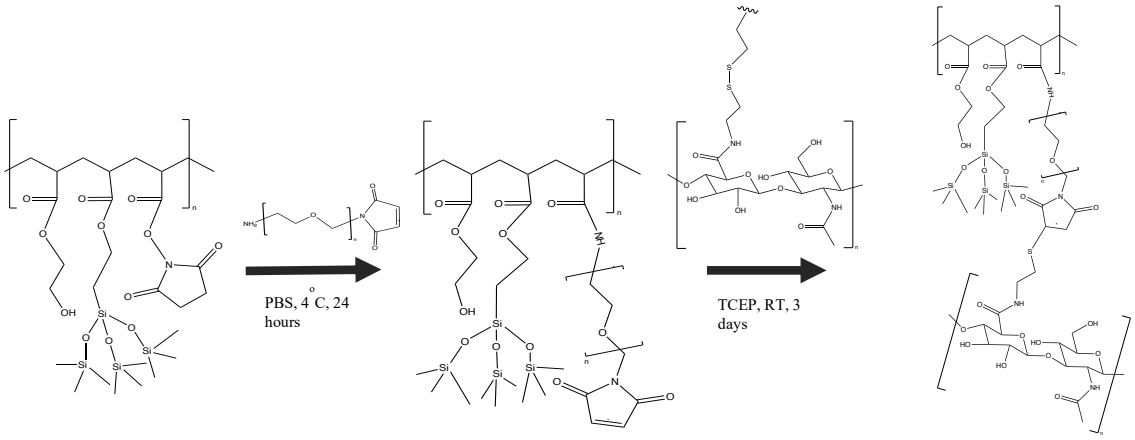

Figure 16: Thiolated HA tethered lenses reaction scheme.

Following attachment of 10% thiolated HA, contact angle measurements were performed (Figure 17). Surprisingly, there was no significant reduction in contact angle relative to pHEMA-co-TRIS. These results can be attributed to two different things. Similar to the bulk polymerization, it is thought that the HA might reside within the lens matrix, making it difficult to observe a decrease in contact angle. Secondly, there might not be enough thiolated HA incorporated into the lens. Overall, contact angle is generally not an optimal tool to determine the successful incorporation of thiolated HA and should be followed by a more rigorous chemical tool for surface analysis such as XPS.

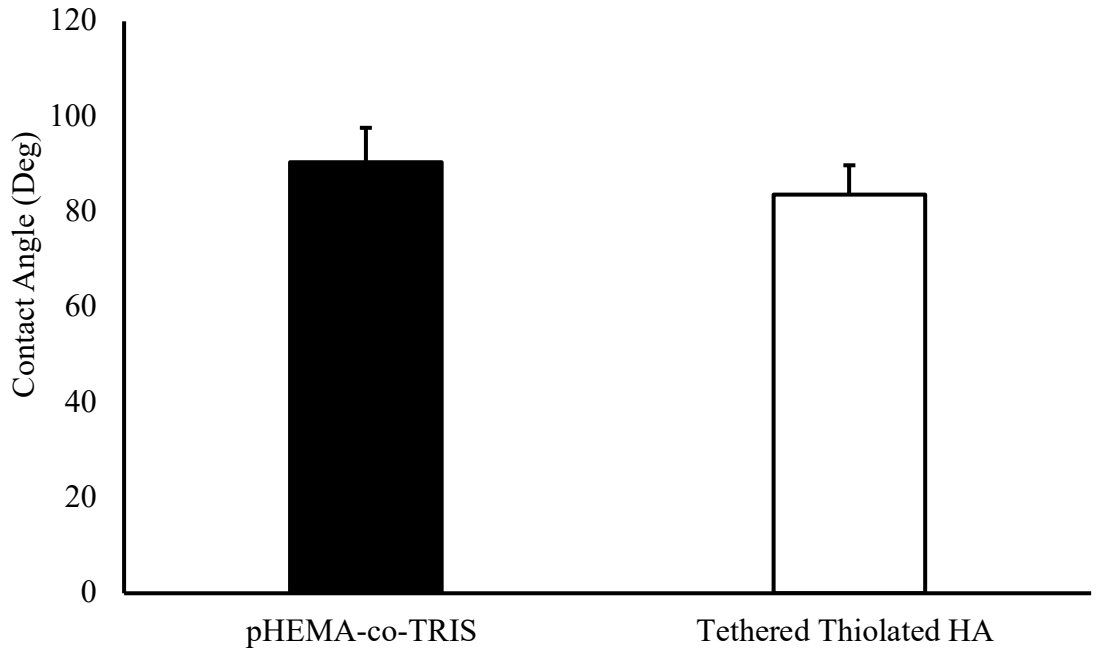

Figure 17:Contact angle between pHEMA-co-TRIS and tethered thiolated HA. No significant difference between the tethered thiolated HA and model pHEMA-co-TRIS control group. (n=4) ($p>0.05$)

Both methacrylated and thiolated HA lenses were characterized using ATR-FTIR, but the results were not conclusive due to the presence of a number of functional groups which caused overlapping peaks. Despite the methacrylated lenses showing significant decrease in contact angle, these methods were not explored further as the ionic lenses, described below, showed better binding.

5.3 Synthesis and Characterization of Ionic Interaction Lenses

5.3.1 Bulk Polymerization

5.3.1.1 Pre Polymerization of HA into the Matrix

Entrapment of HA within the matrix of the lens is a common way of providing sustained release due to the cross-linked nature of the hydrogel. By incorporating the monomer DEAEM (Figure 18A) and HA into the matrix pre-polymerization, HA binding should be enhanced and HA release prolonged. High amounts of HA (13 mg) led to the formation of clumps which floated within the monomer solution despite vigorous shaking (Figure 18B). Similarly, when HA was dissolved in MilliQ water prior to the addition of the monomers, phase separation was observed and large aggregates of HA were formed. Maulvi *et al.* showed incorporation of up to 200 µg of HA without changes to optical transparency. Therefore, future directions for this project should focus on optimal HA loading without impacting transparency.

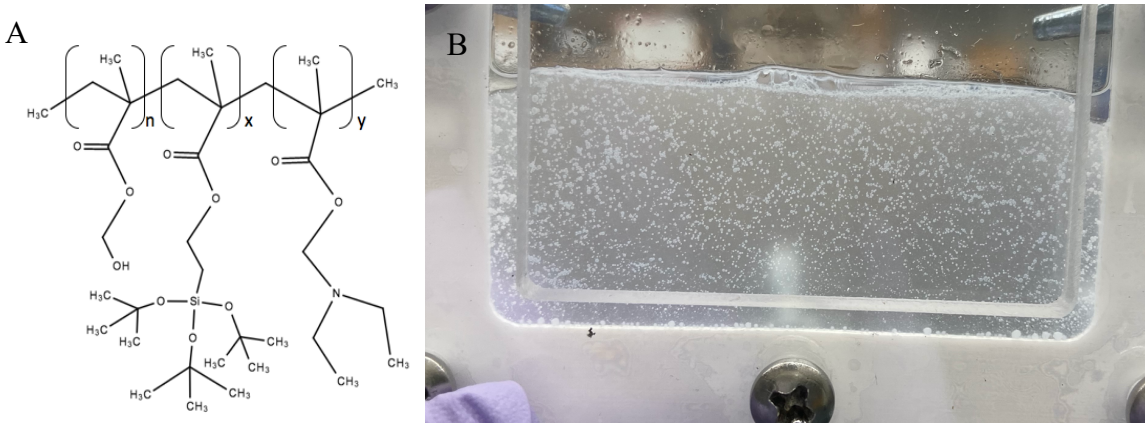

Figure 18: (A) Polymer backbone of DEAEM incorporated lenses (B) Incorporation of HA pre polymerization showing HA aggregates.

5.3.1.2 Post Polymerization of HA into the matrix

Following extraction, the successful incorporation of the monomers into the lenses was tested by NMR as shown in Figure 19. The absence of the double bond from the acrylates around 5.6 and 6.1 ppm and a DEAEM distinct peak around 2.6 ppm indicate that the monomer was successfully polymerized within the lens.

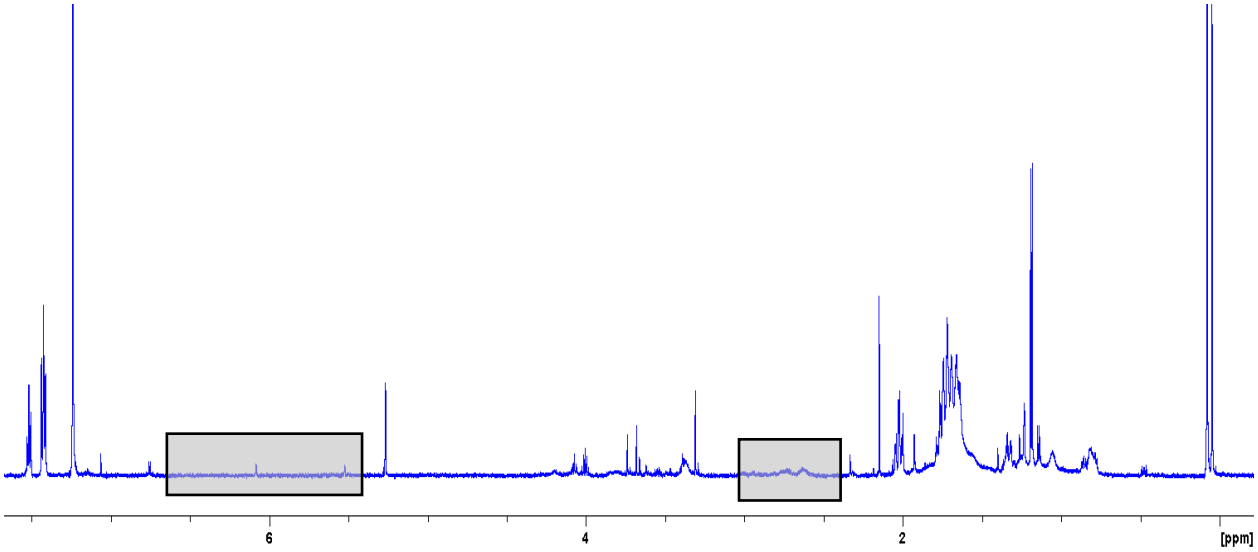

Figure 19: ^{1}H NMR of IPA extracted DEAEM incorporated lenses. The absence of the acrylate peak around 5.6, 6.1, and 2.6 shows successful incorporation of DEAEM.

The lenses post polymerization were soaked in HA and characterized via contact angle measurements, with no significant differences (p >0.05) between the DEAEM modified lenses, DMAEM modified lenses, and pHEMA-co-TRIS (Figure 20). It is thought that the highly crosslinked nature of the lens might block binding sites, preventing interactions from occurring. Contact angle only measures surface hydrophilicity, and does not provide any information about the interactions within the matrix of the lens. Therefore,

radiolabelled HA was used as it provides quantitative results. Surface functionalization of the monomer might also provide better properties for a bandage contact lens.

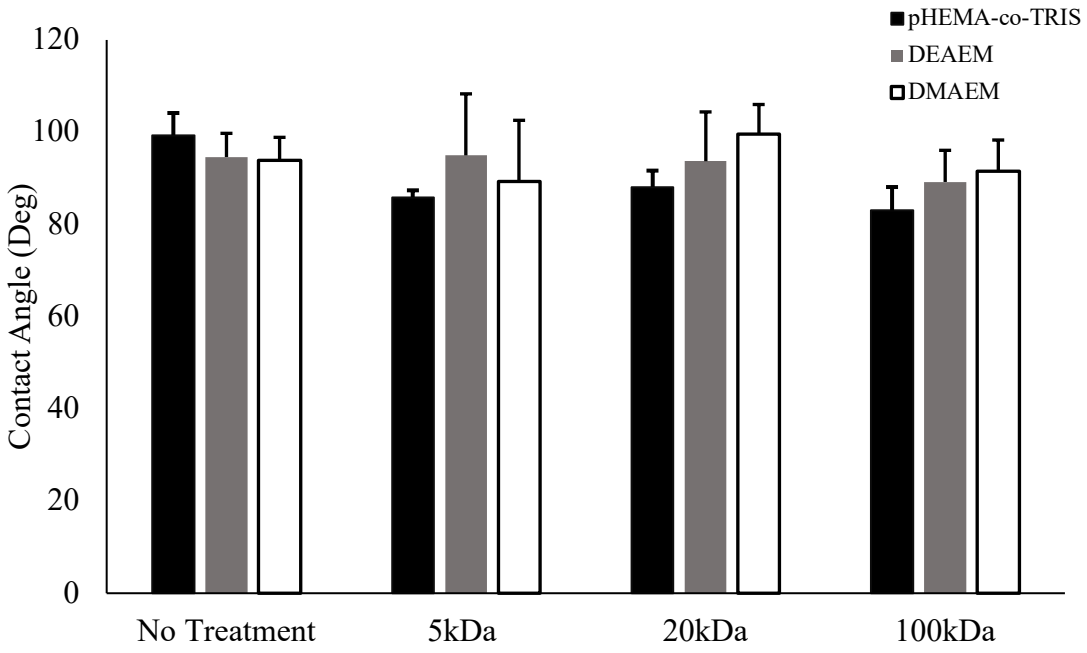

Figure 20:Contact angle results between pHEMA-co-TRIS model lenses, DEAEM, and DMAEM incorporated lenses using different molecular weight HA. No significant difference is observed between lenses and between different molecular weight HAs. ($p > 0.05$) (n=3)

5.3.2 Surface Polymerization

Ionic interactions were explored as a method to incorporate HA and create a reloadable system. By tethering cationic acrylates onto the surface of the lens, negatively charged HA could reversibly bind with these sites, creating a system that can be used as an HA releasing bandage contact lens. The initial step was to introduce a methacrylate group onto the lens through an esterification of the hydroxyl group of pHEMA-co-TRIS lenses (Figure 21). Anhydrous DCM was used as the solvent for methacrylation of the lenses as it does not swell the lenses, building on previous studies to optimize reaction conditions.[92]

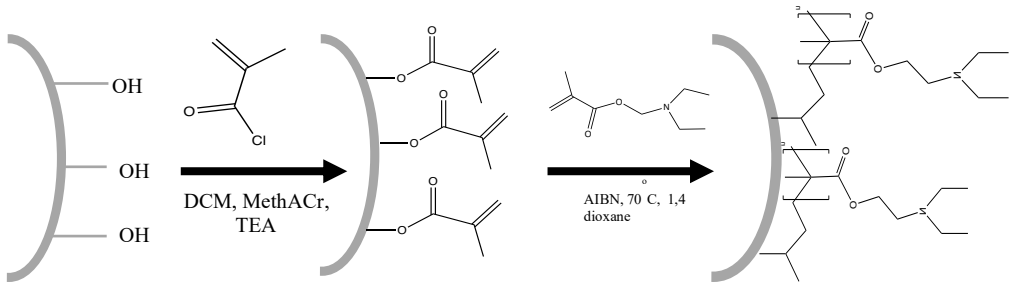

Figure 21: Synthetic scheme for surface polymerization of DEAEM.

Successful lens methacrylation was confirmed with ATR- FTIR (Figure 22 i-ii). Specifically, methacrylation was confirmed by the presence of the alkene peak around 1600 cm^{-1} and the decrease around 3000 cm^{-1} to 3600 cm^{-1}. TEA was chosen as the nucleophilic catalyst to help neutralize the HCl liberated from the reaction. Although the lenses showed successful methacrylation, the lenses were very prone to cracking (Figure 23).

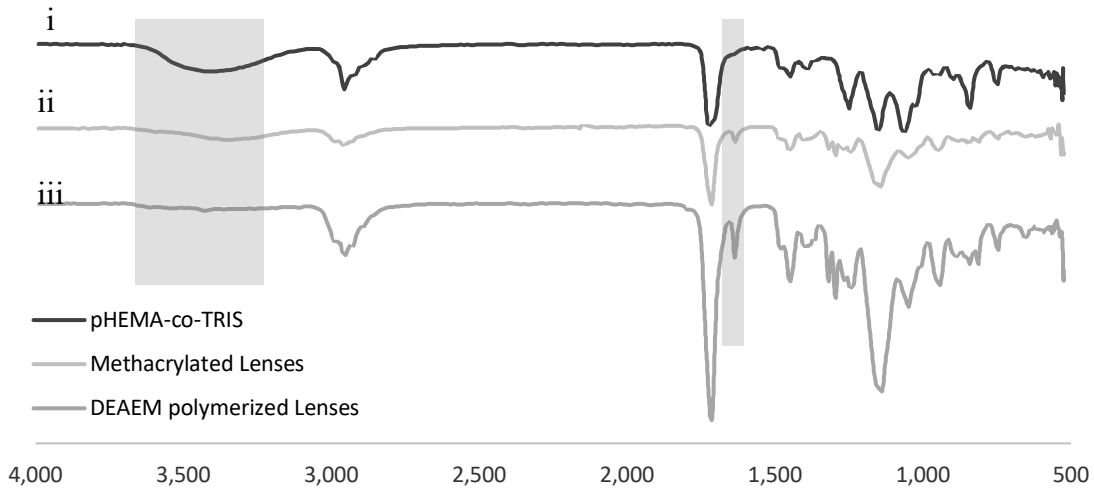

Figure 22: ATR- FTIR spectra of methacrylated lenses compared to model pHEMA-co-TRIS lenses compared to DEAEM polymerized. The presence of the alkene peak around 1600 cm^{-1} and a decrease in the hydroxyl peak around 3000- 3600 cm^{-1} confirms successful methacrylation.

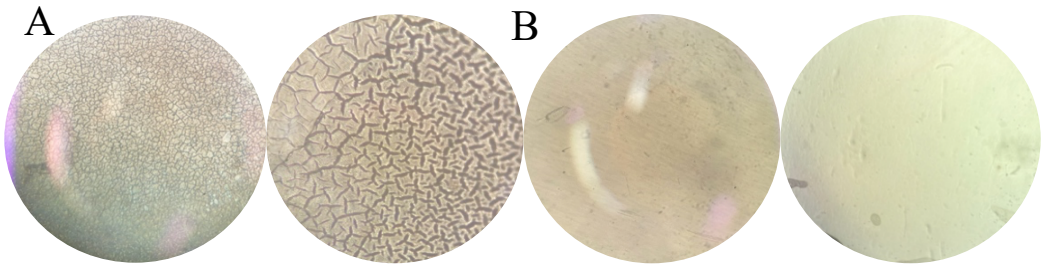

Figure 23:Microscope images at 10 x magnification of (A) TEA catalyzed lenses (B) DIPEA catalyzed lenses.

The polymerization of the monomer was conducted using free radical polymerization using the thermal initiator, AIBN. ATR-FTIR was used to confirm successful polymerization. The presence of the double bond remained on the spectra indicating unsuccessful polymerization off the methacrylate shown in Figure 22 iii. The reaction solution was rotary evaporated and the formation of a thick viscous gel indicated that self-polymerization occurred. The high ratio of monomer to methacrylate groups increases the probability of DEAEM self-polymerization. Therefore, a thiolene click reaction was tested for its high specificity.

5.3.3 Thiolene Click

To modify the grafted lenses with HA-binding small molecules, the surface needed to be acrylated to allow for the thiol-ene "click" reaction to occur.[49] Acrylates were chosen for their superior reaction rates compared to other esters.[49] The surface acrylation was based on the esterification of the hydroxyl groups of HEMA shown in Figure 24. Dicholoromethane and toluene were the chosen solvents for the acrylation step as they did not swell the lenses and have been shown to yield the optimal reaction properties. DIPEA was chosen as the nucleophilic catalyst instead of TEA based on previous experience.[49]

DIPEA is more hindered which allows for a more controlled reaction, producing less salts and resulting in less cracks in the lenses (Figure 23B). Base- and radical-mediated thiolene click chemistry were both tested with results showing higher HA binding and faster reaction rates with the radical-mediated reactions.[93] The proposed mechanism of the radical-mediated thiol-ene "click" reaction is the addition of a thiol across an alkene to form a thioether.[93] The initiator begins by making a thiyl radical which then adds across an alkene to generate a carbocation intermediate.[93] From this step, one of two reactions can occur: step growth or chain growth. In the step growth, the radical intermediate abstracts a hydrogen atom from another thiol and creates another thiyl radical. In a chain growth reaction, where the radical reacts with another alkene and forms a carbocation intermediate to continue the reaction.

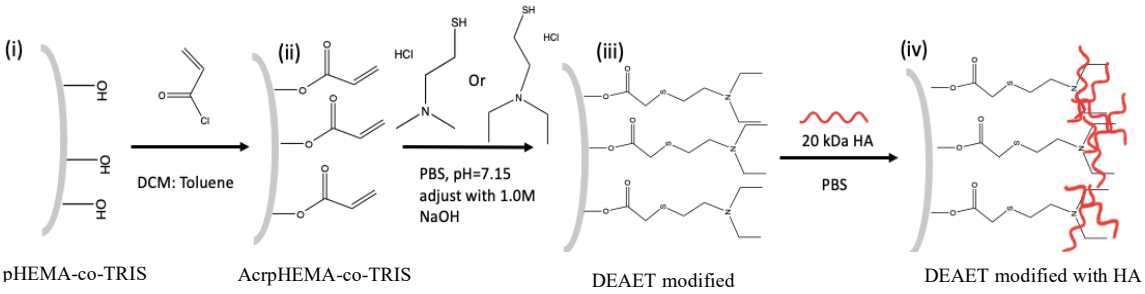

Figure 24: Synthetic scheme of surface modification. (i) Unmodified pHEMA-co-TRIS lenses (ii) pHEMA-co-TRIS lenses modified with acryloyl chloride (AcrpHEMA-co-TRIS) with equal parts DCM and toluene as the solvent (iii) AcrpHEMA-co-TRIS thiol-ene click reaction with either small molecule DEAET and DMAET with pH adjusted using 1.0 M NaOH (iv) lenses soaked with 20kDA HA in PBS.

Lens surface chemistry was analyzed before and after modification by ATR-FTIR (Figure 25). All lenses were dried in a vacuum oven prior to analysis to avoid the presence of water peaks in the spectra. The acrylation of pHEMA-co-TRIS caused a decrease in the broad hydroxyl peak between 3000 cm^{-1} to 3600 cm^{-1} (i-ii), indicating the esterification of

hydroxyl groups on HEMA. The successful incorporation of the acrylates is further supported by the increase in the C=C stretch vibrations around 1635 cm^{-1} (ii-iii). The incorporation of the small molecules DMAET and DEAET on the surface of the lens was confirmed using ATR-FTIR through the decrease of the C=C stretch vibration. (Figure 25 iii, iv).

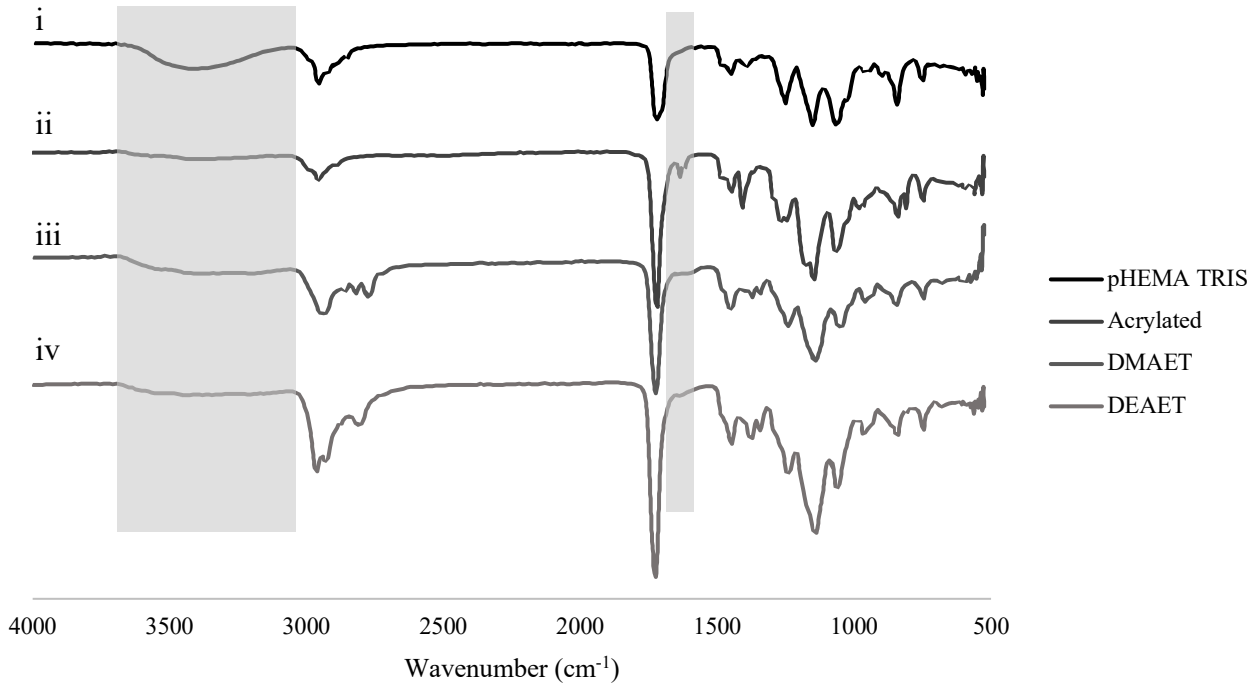

Figure 25: ATR-FTIR transmittance spectra of (i) pHEMA-co-TRIS, (ii) AcrpHEMA-co-TRIS ,(iii) DMAET modified lens, (iv) DEAET modified (n=10)

To further confirm the grafting of the monomer, XPS was used to determine elemental composition (%) on the surface of the hydrogels (Table 6). As expected, nitrogen and sulfur peaks were present in the DMAET-modified lenses but not in the pHEMA-co-TRIS controls, indicating that DMAET was successfully tethered to the lenses. Siloxanes tend to be mobile and move to the surface of the lens.[46] Since XPS measures the top 1-10 nm of

the surface, DMAET and DEAET surface modifications could affect the surface chemistry resulting in the decrease in silicon seen in Table 6.[94]

Table 6: XPS showing elemental composition (%) of the surface of pHEMA-co-TRIS, DMAET modified lenses, and HA bound DMAET modified lenses (n=1)

Sample	C	O	Si	S	N
pHEMA-co-TRIS	63	21.7	15.4	0	0
DMAET modified	67.6	24.1	4.5	1.8	2.1
DMAET modified with HA	70.6	21.4	5.2	0.8	1.9

HA binding of the Lenses

Finally, to quantify the amount of HA bound to the surface of the lens, radiolabelled HA was used. Radiolabelling quantification have been shown to provide 50 to 100 times more sensitivity compared to UV or fluorescence methods.[89,90] Phenolated HA needs to be synthesized prior to the binding of I^{125}. Similar to thiolated HA, phenolated HA was prepared using EDC chemistry (Figure 26).

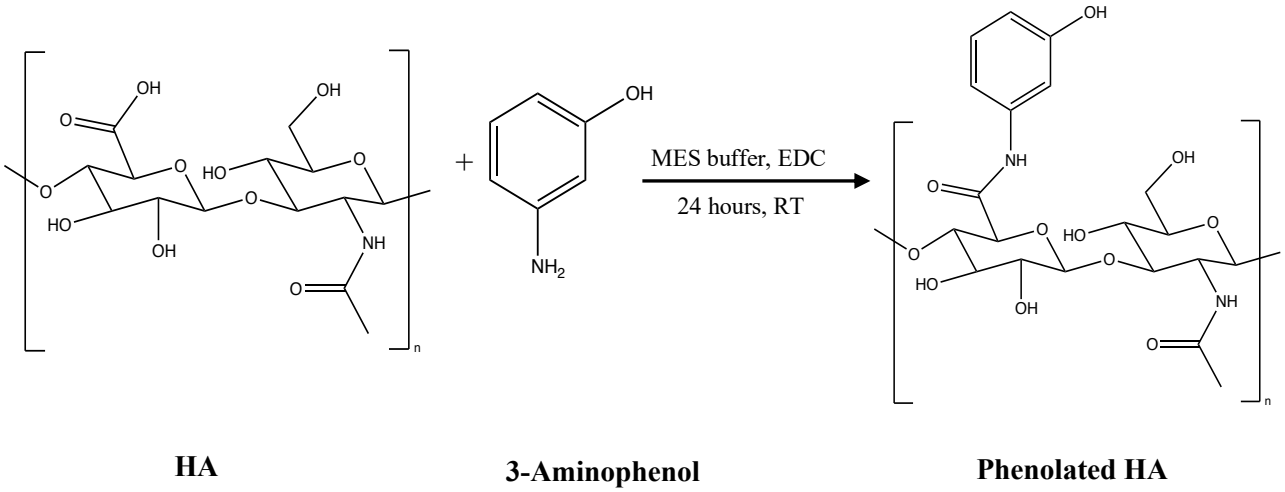

Figure 26: Reaction scheme for phenolated HA.

The primary amine on 3-aminophenol forms a stable amide bond with the carboxylic acid group on the HA. The conjugation was then confirmed using NMR (Figure 27). The peaks shown on the NMR at 7.4, 6.9, and 6.7 are peaks from the phenol group indicating successful conjugation. The integration showed approximately 3-4% functionalization.

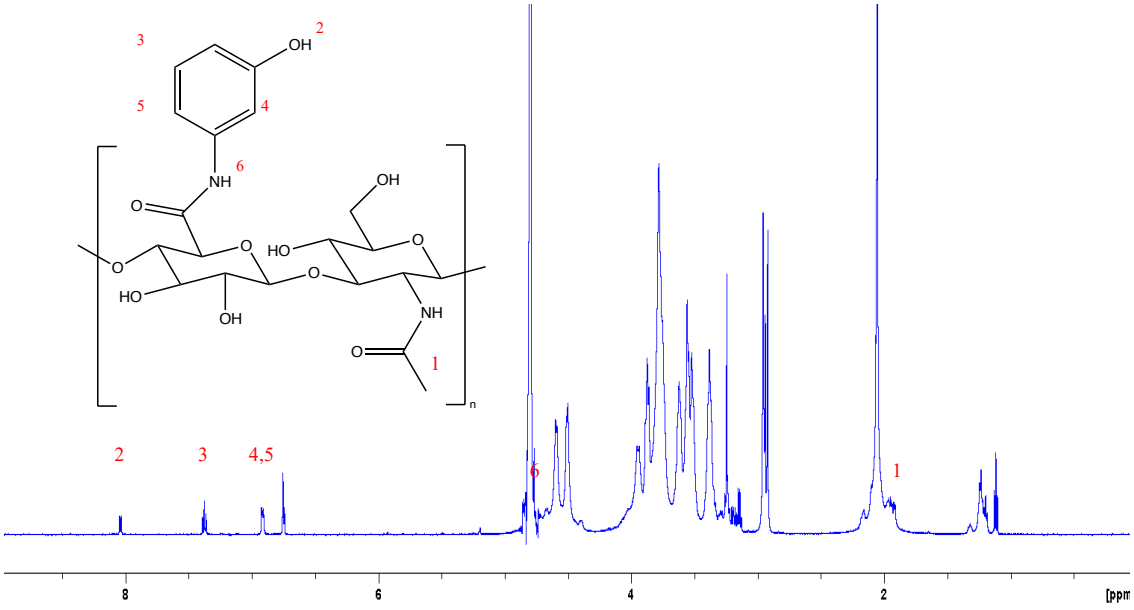

Figure 27: ^{1}H NMR showing successful phenylation of HA.

Contact lenses have been shown to act as a reservoir for HA, contingent on factors such as thickness, water content, concentration of drug in the solution, molecular weight of the drug, and solubility of HA within the gel matrix.[95] The amount of radiolabelled HA bound to the lens was determined using gamma counting (Figure 28). For the first 2 hours of soaking, pHEMA-co-TRIS showed significantly less (p <0.001) HA bound 3.88± 0.5 µg compared to DMAET and DEAET modified lenses, which showed approximately 20 times greater binding at 62.0± 2.3 µg and 71.9± 8.0 µg HA, respectively. Shorter soak times are more representative of surface binding compared to longer soak times which have more time to allow HA to penetrate deeper into the matrix. This suggests that modified surfaces have a high affinity for HA and are being surface bound rather than penetrating into the matrix. The difference in the amounts of HA bound between 5 and 8 hours can be attributed to the use of different lenses. As the soaking time increases, the difference in bound HA

between the control and the modified lenses decreases. This is due to the fact that pHEMA-co-TRIS model lenses incorporated HA into the matrix. The DEAET and DMAET modified lenses had surface bound HA which presumably increased hinderance, making it harder for HA to penetrate into the matrix. Overall, the modified lenses consistently showed more bound HA compared to the model pHEMA-co-TRIS lenses as expected.

Maulvi *et al.* showed that soaking a conventional hydrogel lens in a 5 mg/mL HA solution resulted in the entrapment of 35.9±2.3 µg of HA after 24 hours.[95] Here, we show that our modified lenses soaked in a 1 mg/mL solution for 24 hours bound 4-5 times more HA despite having a 5 times lower concentration. It is also important to note that our control lenses at 24 hours entrapped 39.70± 2.3 µg of HA, which is comparable to their lenses. The similar extent of HA binding despite a much lower initial HA concentration may be attributed to the molecular weight of HA used. Higher molecular weight HA would be expected to lead to adsorption rather than penetration into the gel.[96]

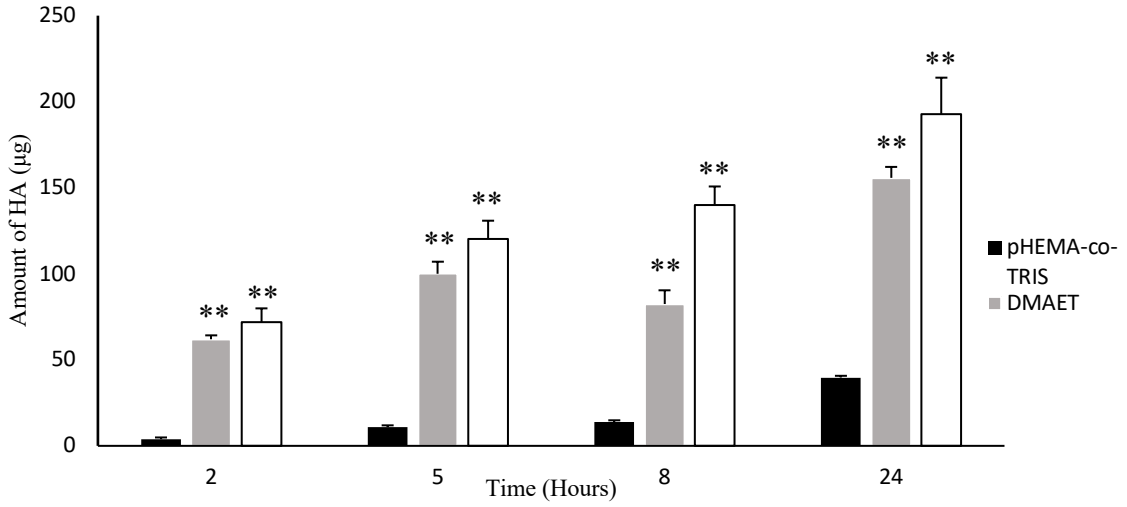

*Figure 28: Amount of HA in µg bound to pHEMA-co-TRIS, DMAET, and DEAET modified lenses at 2,5, 8, 24 hour time points. Modified lenses show statistically significantly (**p <0.001) higher amounts of HA bound to the lens at all time points. (n=5)*

HA release from hydrogels

To compare the release profiles, the pHEMA-co-TRIS model lenses and the modified lenses were soaked in HA solution (1 mg/mL) for 24 hours prior to the release. The cumulative release (%) and amount released are shown in Figure 29. The concentration of HA incorporated after 24 hours was found to be 39.7± 4.6 μg, 155.7± 6.4 μg and 192.7± 21.3 μg for pHEMA-co-TRIS, DMAET modified, and DEAET modified, respectively. As shown in Figure 29B, the pHEMA-co-TRIS model lenses experienced a burst release, releasing approximately 33.4 ± 10.9% upon initial release and 51.4± 11.9% within the first 3 hours. Upon initial release, 8.8 ± 4.7% and 7.2± 1.0% were released for DMAET and DEAET, respectively, and 22.4 ± 4.3 % and 19.6 ± 2.4 % within the first 3 hours. This indicates that the modified lenses have a stronger affinity for HA compared to model pHEMA-co-TRIS. The HA associated with the pHEMA-co-TRIS model lenses is thought to be mainly surface adhered, whereas the modified lenses exhibit primarily surface binding. Surface adherence of HA will show a burst release as there is nothing binding the HA to the lens so it will be released as soon as it is placed into fresh PBS; whereas modified lenses will exhibit HA binding, anchoring HA to the lens to prevent the burst release. The lenses display similar release kinetic curves after the initial burst but with modified lenses releasing more HA at each time point. This is to be expected, as not only will the active sites on the surface of the lens bind HA, but some HA will also slowly penetrate into the lens matrix and release out with the same pattern. The modified lenses released up to 3 times more HA at the two-week mark compared to the pHEMA-co-TRIS model lenses.

In a study conducted by Maulvi *et al.*, implant modification technology was able to release 50.56 ± 5.96 µg (63.23 ± 7.45 %), of HA with 23.18 ± 6.78 µg (28.94 ± 8.47 %) still entrapped in the implant over the span of 2 weeks.[97] Our modified DMAET and DEAET lenses show double the amount of HA released 95.5± 8.8 µg (61.7 ± 4.1%) and 101.0 ±7.3 µg (52.9 ± 2.3%), respectively and 2-3x more HA still entrapped within DMAET and DEAET lenses 44.9 ±5.2 µg (29.5± 3.6%) and 75.1 ±10.2 µg (39.4 ± 2.6%), respectively (Figure 29B).

In a study conducted by Ali *et al.*, it was found that increasing pH disrupts the interaction between DEAEM and HA as it deprotonates the monomer resulting in a reduction in the electrostatic interaction. It was determined that at pH of 8, the monomer should immobilize HA.[54] Therefore, it is expected that DMAET and DEAET should immobilize HA, making it harder for HA within the lens to release while providing a coating of HA on the surface for added comfort.

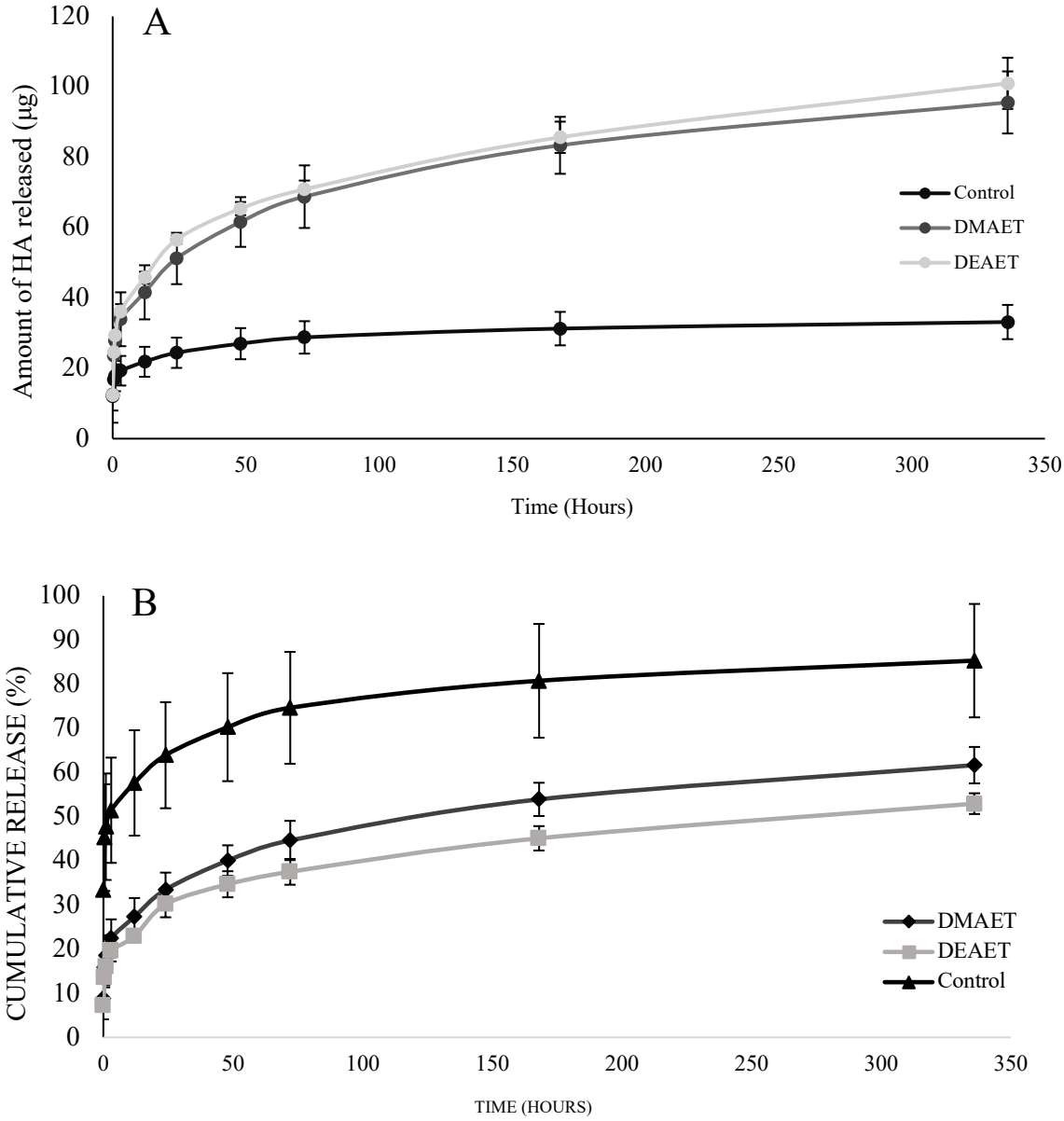

Figure 29: Release profiles of pHEMA-co-TRIS, DMAET, DEAET modified lenses soaked in HA for 24 hours and released over a 2 week period in PBS at room temperature (25°C) . (A) HA (µg) mass release profile (B) Cumulative release of HA (%) over a 2 week period ±SD. (n=5)

Reloading and Loading Study

Results shown in Figure 30 show the binding and release capabilities of control pHEMA-co-TRIS lenses compared to modified DEAET lenses. DEAET modified lenses

bind 4-5x more HA compared to control lenses and release up to 6x more HA. It is interesting to note that the first release cycle for pHEMA-co-TRIS releases up to 67% of the loaded HA, whereas each release from the modified lenses remains consistent throughout. DEAET modified lenses show no statistically significant difference ($p > 0.05$) in the amount of HA released between each soak. For the control pHEMA-co-TRIS lenses, the first release showed a statistically significant ($p < 0.03$) decrease in the amount of HA released with every soak, reaching equilibrium by the fourth release. This is because the high molecular weight HA will take some time to penetrate deep within the lens. Therefore, the first burst release is a result of superficially entangled and surface adhered HA. As the lenses continue to soak, the HA penetrates more deeply and cannot leach out as easily. The DEAET modified lenses show consistent release rates and lack the initial burst release, further suggesting there is an interaction on the surface of the lens. The consistent release and binding rates of the DEAET modified lenses show promise for a good reloadable lens system.

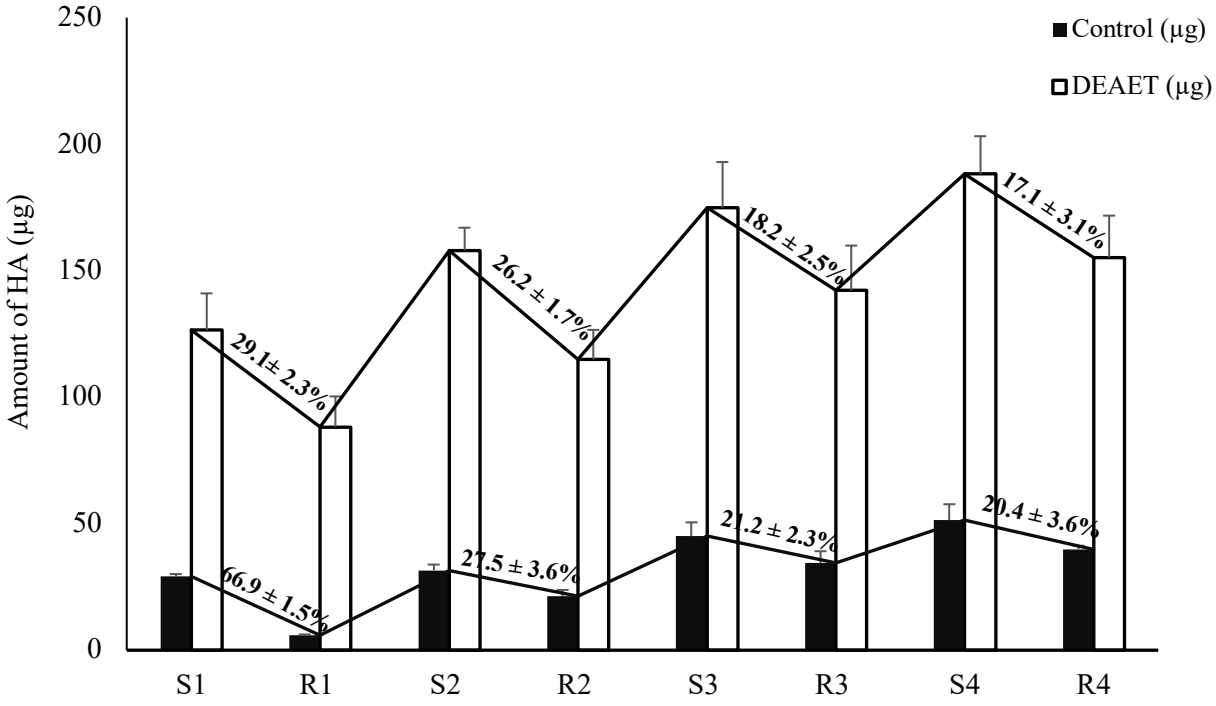

Figure 30: Loading and release of HA in µg comparing control and DEAET modified lenses ±SD. (n=4)

Optical Transparency

Optical transparency is an important parameter for contact lens applications. Contact lenses should have a transparency ideally above 90% at 400-750 nm.[98] Hydrophilic and hydrophobic domains can result in decreased optical transparency. As shown in Figure 31A, the lenses decrease in transparency after acylation and further decrease after thiolene click modifications but still remain above 80%. The decrease in transparency is ranked pHEMA-co-TRIS > Acrylated > DMAET > DEAET with 2-3% difference between each group. The acrylation of the lens causes the smooth surface to develop small etches which results in a slight decrease in transparency as shown in Figure 32B. The radical-initiated thiolene reaction causes a unique pattern to develop on the surface of the lens which further

decreases optical transparency. Although the exact reason for the appearance of this pattern is unknown, it is consistent and only appears with this specific thiolene "click" reaction. This pattern appears throughout the lens and is different from the cracking which appeared with the TEA initiated lens shown in Figure 23A. It is important to note that these lenses have double the crosslinker and are 0.5 mm thick, five times the thickness of commercially available lenses. Further optimization needs to be performed to create a clinically relevant and transparent lens.

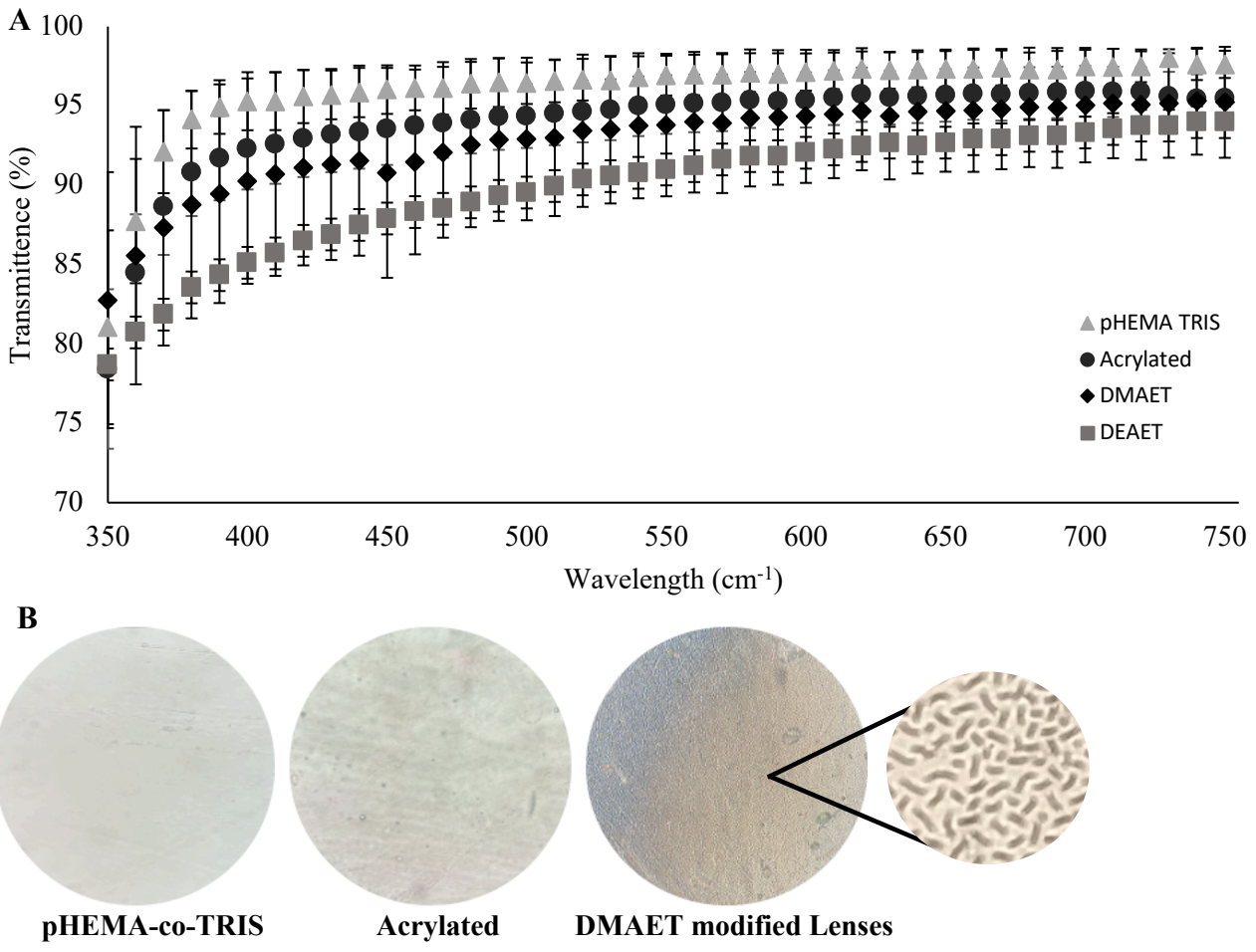

Figure 31:(A) Optical transparency of pHEMA-co-TRIS, AcrpHEMA-co-TRIS, DMAET modified and DEAET modified lenses over a range of 350 to 700nm ±SD (n=6) (B) Enlarged 10x microscopy images of lens surfaces.

Equilibrium Water Content and Dehydration Rate

Ocular dryness is a major issue often associated with contact lens wear. All hydrogels will dehydrate during wear, with an associate decrease in comfort. Contact lens dryness often occurs due to environmental changes and an increase in the amount of friction, leading to decreased comfort which is highly unfavourable in wound healing.[99] Therefore, water content and dehydration rates of contact lenses are important parameters. Dehydration rates are based on properties such as water content, thickness, and water binding. It has been suggested that evaporation is closely related to EWC.[100] Dehydration rate has a large impact on conventional hydrogels as it plays a significant role in oxygen permeability. Although oxygen permeability is less affected by water content in silicone hydrogels, dehydration rate is a key determinant in contact lens performance and has an impact on the ocular comfort.

EWC was measured using the gravimetric method and calculated using Equation 2. EWC can be affected by a variety of parameters including pH, temperature, and thickness of the lens.[49,96] The results in Table 7 show that there are no significant differences (p >0.05) between the control and the modified lenses and between HA and no HA lens groups. The results were not as expected as it was thought that the HA would increase EWC due to its hygroscopic nature. It is commonly accepted that higher modulus lenses exhibit lower water content. [101] Since the lenses were made with double the crosslinker, this increase in modulus might explain why there is no significant change in EWC. Alternatively, the surface bound HA may not have impacted the bulk properties of the lenses.

Table 7: Equilibrium water content for pHEMA-co-TRIS, DMAET Modified, and DEAET modified lenses ±SD (n=4). No significant difference ($p > 0.05$) was observed between modified and control lenses as well as with and without HA lenses.

	EWC (%) Without HA	**EWC (%) With HA**
pHEMA-co-TRIS	31.27 ± 1.15	30.57 ± 0.42
DMAET	31.25 ± 1.15	32.88 ± 1.47
DEAET	31.02 ± 0.57	32.05 ± 1.88

The water loss (%) of the lens was calculated using Equation 1 and depicted in Figure 32. Control lenses and modified lenses showed similar trends in dehydration where the first 30 mins followed a linear trend followed by a plateau. There is no significant difference between model pHEMA-co-TRIS, DMAET, and DEAET ($p > 0.05$) with and without HA. This is to be expected because they are made of the same base material they should follow similar dehydration trends. The hygroscopic nature of HA allows for greater water sorption and retention, which was expected to yield a slower dehydration rate. HA-soaked materials show a significant difference ($p < 0.01$) compared with non HA soaked materials at 20 mins with differences only becoming apparent with increasing time. However, within the HA soaked group, model pHEMA-co-TRIS compared to DMAET and DEAET modified lenses show no significant difference ($p > 0.05$) at all time points. This might be attributed to the fact that in DMAET and DEAET modified lenses, HA is bound to the surface of the lens where it is more exposed and therefore any water bound is more easily evaporated. In pHEMA-co-TRIS lenses, HA is more likely entangled in the matrix

allowing more water to penetrate into the matrix resulting in slower evaporation. Therefore, the dehydration study may not be an accurate indication of surface dehydration and comfort.

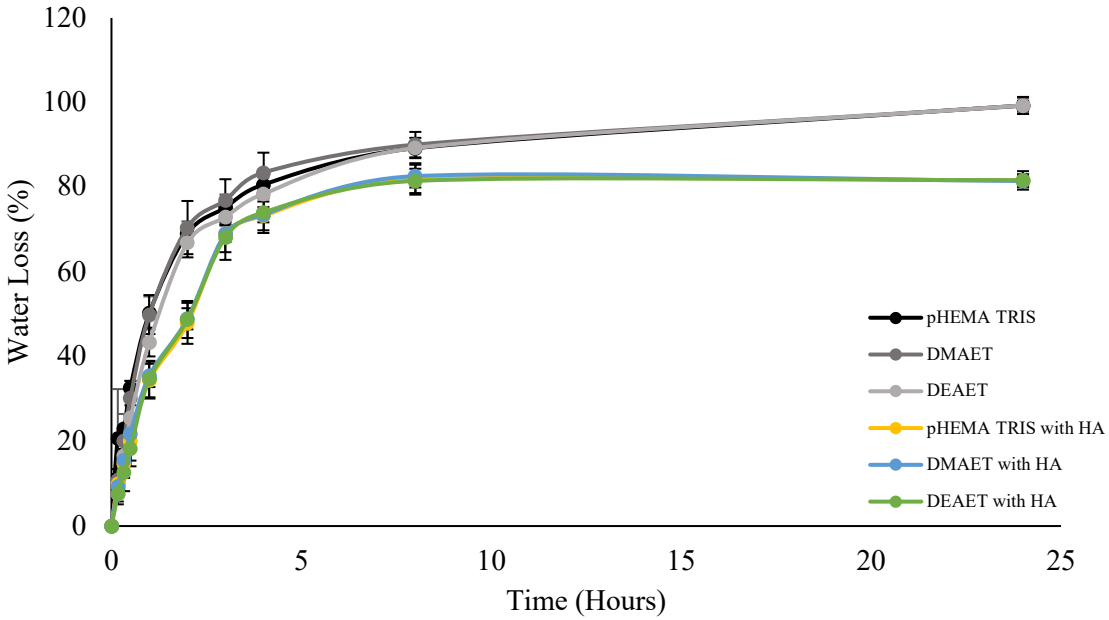

Figure 32:Dehydration profile of fully hydrated pHEMA-co-TRIS, DMAET, DEAET discs with and without HA over 24 hours ±SD (n=4). No significant difference (p >0.05) was observed between control and modified lenses.

To evaluate surface hydrophilicity of modified lenses, contact angle measurements were used. All contact angle results shown in Figure 33 displayed a decrease with the incorporation of HA (p <0.05). This was expected, as HA improves the hydrophilicity of the lens surface. DEAET modified lenses exhibited the largest decrease in contact angle, which is in accordance with radiolabelled data, showing that DEAET modified lenses had the highest binding affinity for HA.

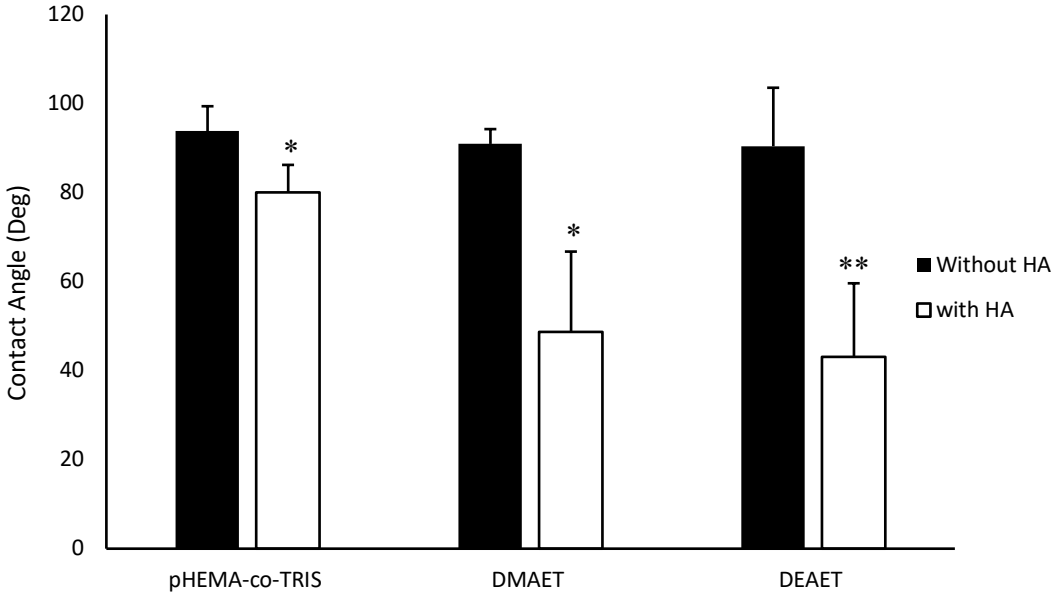

Figure 33: Contact angle comparing control and modified lenses with and without HA. (n=4) (p<0.02, **p<0.005)*

5.3.4 Cell Studies

MTT Cytotoxicity

Cytotoxicity of materials were assessed using MTT assay with human corneal epithelial cells. The MTT results show no statistically significant difference (p >0.05) in viability, calculated using Equation 3, with exposure to pHEMA-co-TRIS, DMAET modified, and DEAET modified for 24 or 48 hours. Therefore, this indicates that these materials exhibit compatibility to HCECs and are non-toxic.

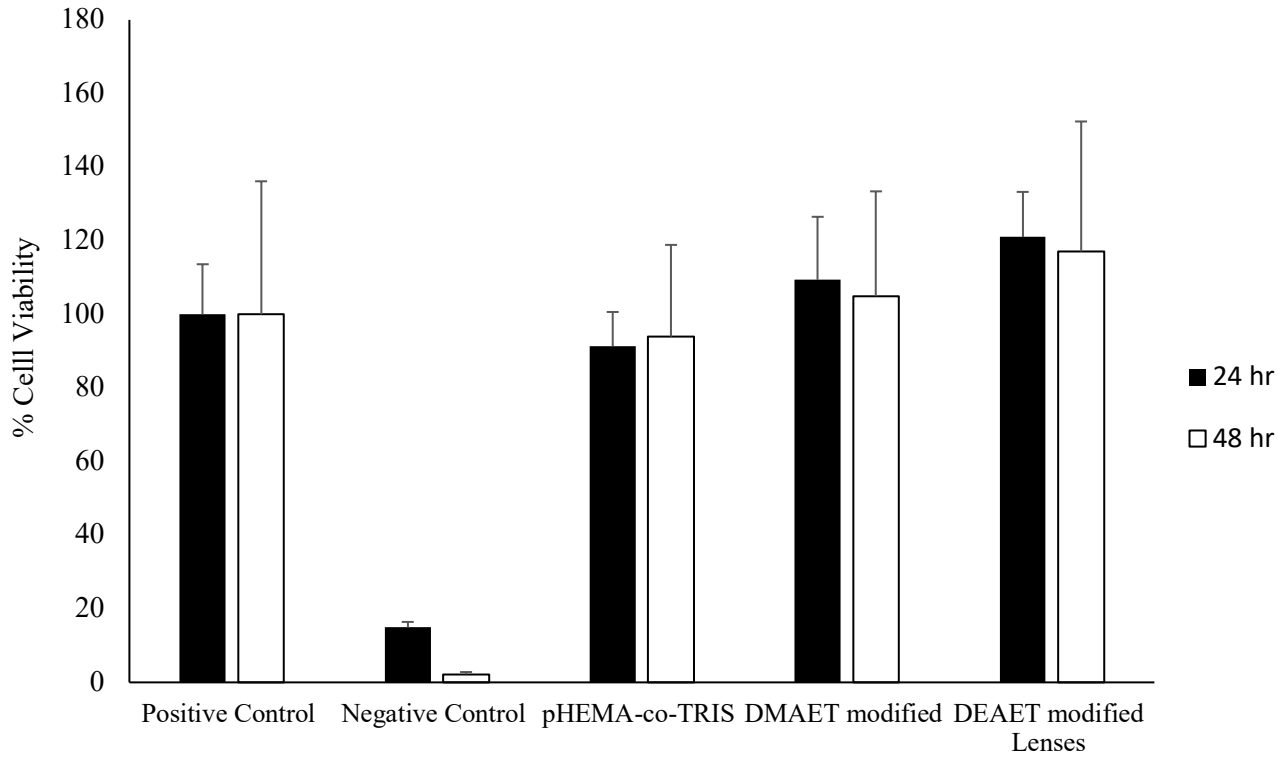

Figure 34: MTT results at 24 and 48 hr for positive control (just cells), negative control, pHEMA-co-TRIS controls, and modified lenses. No significant difference ($p > 0.05$) between positive controls, pHEMA-co-TRIS model, and modified lenses for both time points. (n=3)

Cell viability was further confirmed with LIVE/DEAD assay. As shown in Figure 34, modified lenses did not have an effect on cell viability. The % dead cells are summarized in Table 8. There is no significant difference ($p > 0.05$) between positive control lenses compared to pHEMA-co-TRIS model, DMAET, and DEAET modified lenses. This further confirms that the modified lenses are not cytotoxic.

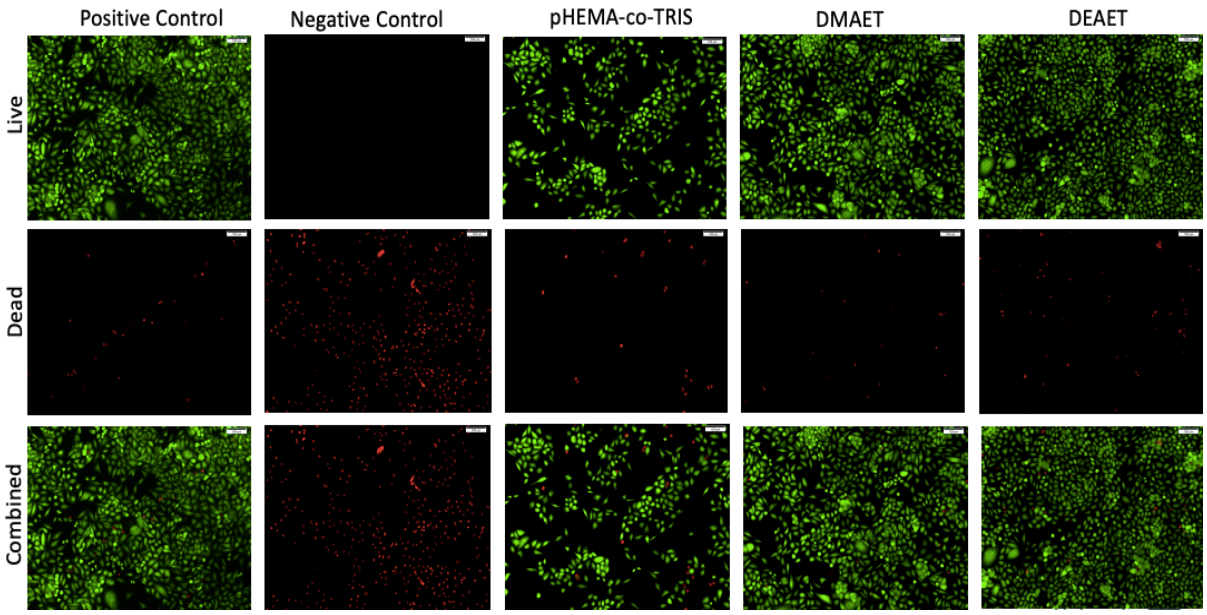

Figure 35: LIVE/DEAD assay of corneal epithelial cells at 48 hrs of incubation. Live cells (green) and dead cells (red). Scale bar= 100 µm

Table 8: % dead cells of positive control (just cells), negative control, pHEMA-co-TRIS, DMAET, and DEAET modified lenses at 48 hr ±SD (n=4)

	% Dead
Positive Control	4.67 ± 1.99 %
Negative Control	100 ± 0 %
pHEMA-co- TRIS	9.47 ± 7.29 %
DMAET modified	5.31 ± 2.17 %
DEAET modified	5.84 ± 1.07 %

Boyden Chamber

Boyden chamber cell inserts are frequently used to observe cell migration. The Boyden chamber results, shown in Figure 36 , were not as expected. EGF used as a positive control should have displayed the highest number of cells migrating through the pores based on literature. Surprisingly, there was no statistically significant difference between non treated and EGF or HA treatment groups (p >0.05). 50ng/mL of EGF was used as the chemoattractant because it showed the greatest wound closure in rabbit models but lower concentrations of EGF (10ng/mL) may be necessary to avoid oversaturation of receptors.[102] The study was also repeated with 8 μm inserts instead of 12 μm; the results are shown in Figure B3. Interestingly, the 3 μm inserts showed an opposite trend to the 12 μm insert results where 100k and 20k HA showed a statistically significant difference (p <0.05) in migration compared to non-treated controls.

One disadvantage of this technique is the reproducibility. As shown in Figure 37, Figure B4, and Figure B6 there is high standard deviation among groups and inconsistent results between studies. Consistency between groups may vary depending on how hard the swab was and how well the inserts were washed.

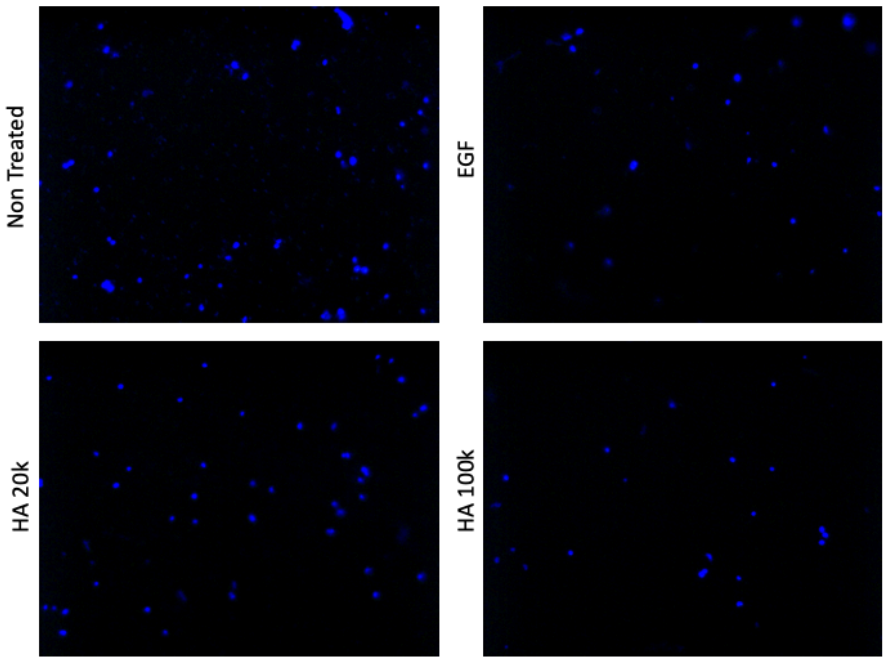

Figure 36: Boyden chamber images of HCECs (x10 magnification) stained with Hoesct stain through a 12 µm membrane filter. Images taken at 24 hours with cells in the top chamber removed using a cotton swab.

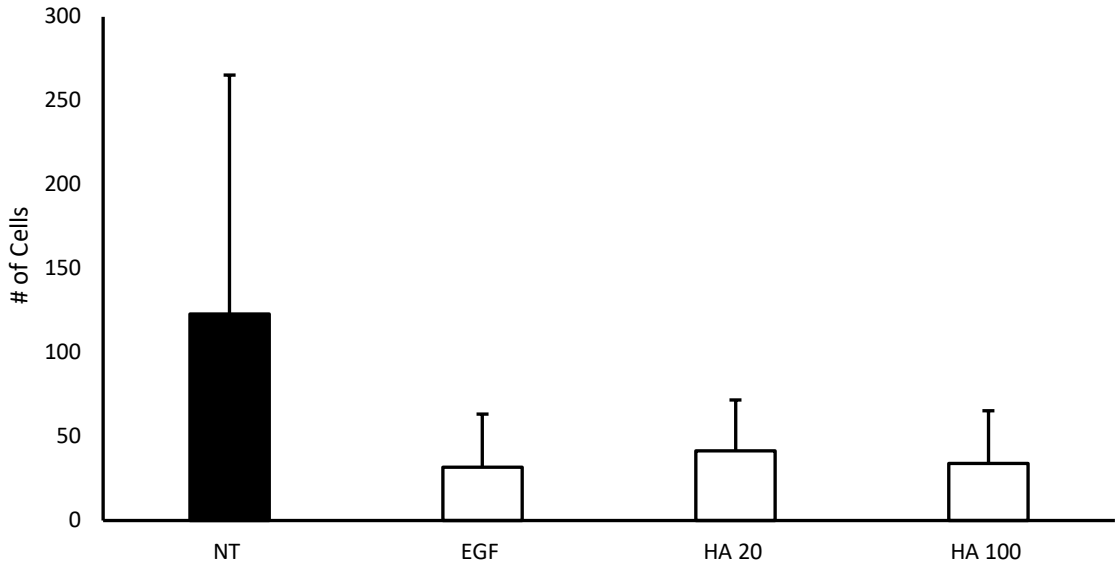

Figure 37: Number of HCEC cells counted at the bottom of the chamber through 12 µm pores. Results reported in standard deviation with no statistically significant difference amongst groups ($p > 0.05$). (n=4)

Scratch Assay

An *in vitro* scratch assay was used to determine wound closure effects based on different chemoattractant treatments. The results of wound closure, shown in Figure 38 and Figure 39, shows no significant difference (p >0.05) between the non-treatment group compared to the treatment groups. The results were repeated numerous times with high variability between trials. Similar to the Boyden chamber assay, the results are hard to replicate as shown Figure B2 which was another repeat of this study. Consistency depends on how well the scratch can be replicated. Smaller scratches show faster healing, as there is less area to close. This study can be improved with an incubating microscope to record cell migration over the full duration of the study.

Based on preliminary cell culture data, there are no significant difference between the treatment groups; an *in vivo* model would provide more depth in efficacy.

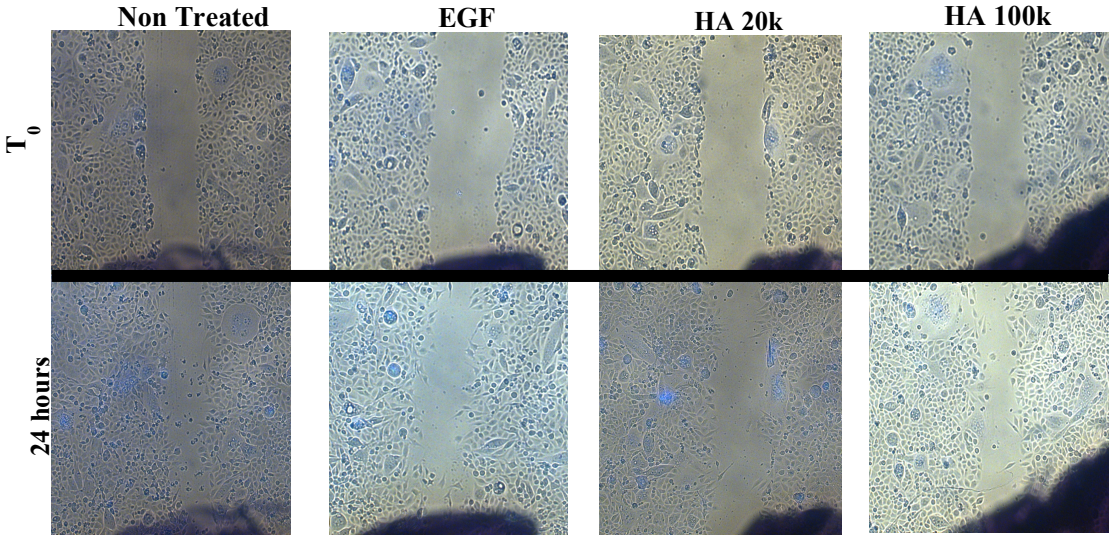

Figure 38: Wound closure model using HCECs measured at 0 and 24 hours. Cells are scraped using a p10 pipette and incubated for 24 hours. Images are taken at 10x magnification.

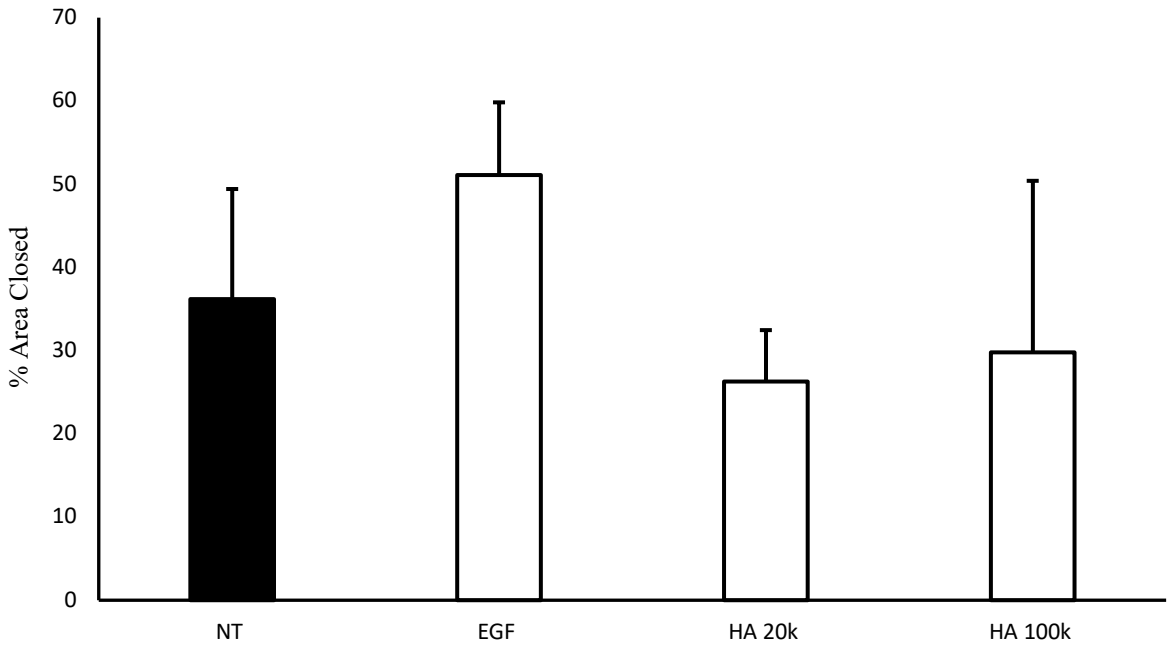

Figure 39: Wound Closure % calculated based on area from 0 -4 hours. No statistically significant difference between treatment groups(p >0.05). (n=4)

6 Conclusion

In this work, three different materials were used to synthesize a lens capable of binding HA and potentially releasing HA, for application as a therapeutic bandage contact lens. The caged lenses focused on creating a structure that physically entraps HA onto the lens surface. Despite promising contact angle results, radiolabelled HA quantification proved it to be an ineffective method of incorporating HA. Furthermore, the lenses were difficult to synthesize and were difficult to characterize. Tethered HA lenses with PEG side chains only displayed a decrease in contact angle with tethered methacrylated HA. Since the lenses followed the same initial mechanism as the cage lenses, quantification was also difficult. Overall, the tethered HA lenses were expensive to synthesize and difficult to characterize.

DMAET and DEAET modified thiolene "click" lenses were explored as the HA binding therapeutic bandage contact lens and showed simple characterization, high binding efficiency of HA, and ease of synthesis. Successful acrylation and subsequent radical mediated thiolene "click" of the DMAET and DEAET were confirmed through FTIR. Acrylation and addition of the small molecule did not alter the EWC but did result in decreased transparency. The binding of HA was quantified by radiolabelling and subsequent gamma counting. Modified lenses showed up to twenty times more HA binding and the prevention of an initial burst release. The loading, unloading, and reloading of the modified lenses further confirmed the lack of an initial burst release, which was observed in the model pHEMA-co-TRIS lenses. The modified lenses consistently bound and released more HA than controls. Contact angle measurements showed a highly significant decrease for modified lenses, especially DEAET lenses, confirming improved wettability after ionic incorporation of HA. *In vitro* compatibility was observed with HCECs and no cytotoxicity was observed by MTT and LIVE/DEAD assays. Based on the results, the DEAET surfaced modified lenses were found to have the greatest potential for future bandage lens applications.

Future work should begin with optimization to yield a more optically transparent lens. By making the lens thinner, at 0.25 mm instead of 0.50 mm, might be useful to improve transparency. Base mediated thiolene "click" reactions seem to yield a more transparent lens compared to radical mediated thiolene "click" reaction. Therefore, it might be worth conducting comparative studies between the two types of lenses. Protein deposition onto contact lens studies should also be explored. Following optimization, *in vivo* models should

be conducted between model pHEMA-co-TRIS compared to DEAET modified lenses. An *in vivo* corneal scratch model or more difficult to heal anterior keratectomy would be beneficial to understanding how well the lenses would work in the desired application.

7 References

1 Willmann, D., Fu, L. Scott W.Melanson Corneal Injury*. StatsPeals Publishing (*2021).

2 Lubeck, D. & Greene, J. S. Corneal Injuries. *Seminars in Ophthalmology* **5**, 61-73, doi:10.3109/08820539009060156 (1990).

3 Acheson, J. F., Joseph, J. & Spalton, D. J. Use of soft contact lenses in an eye casualty department for the primary treatment of traumatic corneal abrasions. *Br J Ophthalmol* **71**, 285-289, doi:10.1136/bjo.71.4.285 (1987).

4 Kaiser, P. K. A comparison of pressure patching versus no patching for corneal abrasions due to trauma or foreign body removal. Corneal Abrasion Patching Study Group. *Ophthalmology* **102**, 1936-1942, doi:10.1016/s0161-6420(95)30772-5 (1995).

5 Ljubimov, A. V. & Saghizadeh, M. Progress in corneal wound healing. *Prog Retin Eye Res* **49**, 17-45, doi:10.1016/j.preteyeres.2015.07.002 (2015).

6 Wilson, S. F. & Last, A. R. Management of corneal abrasions. *American family physician* **70**, 123-128 (2004).

7 Lim, L. & Lim, E. W. L. Therapeutic Contact Lenses in the Treatment of Corneal and Ocular Surface Diseases—A Review. *The Asia-Pacific Journal of Ophthalmology* **9** (2020).

8 Zhu, B. *et al.* Characteristics of Infectious Keratitis in Bandage Contact Lens Wear Patients. *Eye Contact Lens* **45**, 356-359, doi:10.1097/ICL.0000000000000593 (2019).

9 Kanpolat, A. & Uçakhan, Ö.O. Therapeutic Use of Focus® Night & Day™ Contact Lenses. *Cornea* **22** (2003).

10 Solomon, A. in *Ocular Surface Disease: Cornea, Conjunctiva and Tear Film* (eds Edward J. Holland, Mark J. Mannis, & W. Barry Lee) 195-203 (W.B. Saunders, 2013).

11 Chang, W.-H. *et al.* Applications of Hyaluronic Acid in Ophthalmology and Contact Lenses. *Molecules* **26**, 2485, doi:10.3390/molecules26092485 (2021).

12 Chaidaroon, W., Satayawut, N. & Tananuvat, N. Effect of 2% Hyaluronic Acid on the Rate of Healing of Corneal Epithelial Defect After Pterygium Surgery: A Randomized Controlled Trial. *Drug Des Devel Ther* **15**, 4435-4443, doi:10.2147/dddt.S336372 (2021).

13 Sridhar, M. S. Anatomy of cornea and ocular surface. *Indian J Ophthalmol* **66**, 190-194, doi:10.4103/ijo.IJO_646_17 (2018).

14 Zhu, J., Zhang, E. & Rio-Tsonis, K. Eye Anatomy.*eLS, John Wiley & Sons, Ltd (Ed.), d*oi: 10.1002/9780470015902.a0000108.pub2 (2012).

15 Son, Y. J. *et al.* Biomaterials and controlled release strategy for epithelial wound healing. *Biomater Sci* **7**, 4444-4471, doi:10.1039/c9bm00456d (2019).

16 Ljubimov, A. V. & Saghizadeh, M. Progress in corneal wound healing. *Prog Retin Eye Res* **49**, 17-45, doi:10.1016/j.preteyeres.2015.07.002 (2015).
17 Ebrahimi, M., Taghi-Abadi, E. & Baharvand, H. Limbal stem cells in review. *J Ophthalmic Vis Res* **4**, 40-58 (2009).
18 Gandhi, S. & Jain, S. in *Keratoprostheses and Artificial Corneas: Fundamentals and Surgical Applications* (eds M. Soledad Cortina & Jose de la Cruz) 19-25 (Springer Berlin Heidelberg, 2015).
19 Farjo, A. A., Brumm, M. V., Soong, H. K. & Hood, C. T. Corneal anatomy, physiology, and wound healing. *Ophthalmology E-Book* **155** (2018).
20 Sheardown, H. & Cheng, Y.-L. Mechanisms of corneal epithelial wound healing. *Chemical Engineering Science* **51**, 4517-4529 (1996).
21 Whikehart, D. R. in *Encyclopedia of the Eye* (ed Darlene A. Dartt) 424-434 (Academic Press, 2010).
22 DelMonte, D. W. & Kim, T. Anatomy and physiology of the cornea. *J Cataract Refract Surg* **37**, 588-598, doi:10.1016/j.jcrs.2010.12.037 (2011).
23 Cornea and Corneal Disease, *EyeWorks Louisville* (2015).
24 Read, S. A. *et al.* Anterior eye tissue morphology: Scleral and conjunctival thickness in children and young adults. *Scientific Reports* **6**, 33796, doi:10.1038/srep33796 (2016).
25 Van Buskirk, E. M. The anatomy of the limbus. *Eye* **3**, 101-108, doi:10.1038/eye.1989.16 (1989).
26 Amin, S. *et al.* The Limbal Niche and Regenerative Strategies. *Vision* **5**, 43, doi:10.3390/vision5040043 (2021).
27 Dua, H. S., Shanmuganathan, V., Powell-Richards, A., Tighe, P. & Joseph, A. Limbal epithelial crypts: a novel anatomical structure and a putative limbal stem cell niche. *British Journal of Ophthalmology* **89**, 529-532 doi:10.1136/bjo.2004.049742 (2005).
28 Yazdanpanah, G., Jabbehdari, S. & Djalilian, A. R. Limbal and corneal epithelial homeostasis. *Curr Opin Ophthalmol* **28**, 348-354, doi:10.1097/ICU.0000000000000378 (2017).
29 Pflugfelder, S. C. Tear dysfunction and the cornea: LXVIII Edward Jackson Memorial Lecture. *Am J Ophthalmol* **152**, 900-909 e901, doi:10.1016/j.ajo.2011.08.023 (2011).
30 Dartt, D. A. & Willcox, M. D. P. Complexity of the tear film: importance in homeostasis and dysfunction during disease. *Exp Eye Res* **117**, 1-3, doi:10.1016/j.exer.2013.10.008 (2013).
31 Dilly, P. N. Structure and function of the tear film. *Adv Exp Med Biol* **350**, 239-247, doi:10.1007/978-1-4615-2417-5_41 (1994).
32 Cwiklik, L. Tear film lipid layer: A molecular level view. *Biochimica et Biophysica Acta (BBA) - Biomembranes* **1858**, 2421-2430, doi:10.1016/j.bbamem.2016.02.020 (2016).

33 Kopacz, D., Niezgoda, Ł., Fudalej, E., Nowak, A. & Maciejewicz, P. Tear Film–Physiology and Disturbances in Various Diseases and Disorders. *Ocular Surface Diseases: Some Current Date on Tear Film Problem and Keratoconic Diagnosis* Doi:10.5772/intechopen.94142 (2020).

34 Peters, E. & Colby, K. A. Chapter 3 The Tear Film (2009).

35 Steele, C. Corneal wound healing: a review. *Optometry today*, 28-32 (1999).

36 Agrawal, V. & Tsai, R. Corneal epithelial wound healing. *Indian J Ophthalmol* **51**, 5-15 (2003).

37 Lu, L., Reinach, P. S. & Kao, W. W. Y. Corneal Epithelial Wound Healing. *Experimental Biology and Medicine* **226**, 653-664, doi:10.1177/153537020222600711 (2001).

38 Lee, J. S., Lee, S. U., Che, C.-Y. & Lee, J.-E. Comparison of cytotoxicity and wound healing effect of carboxymethylcellulose and hyaluronic acid on human corneal epithelial cells. *International journal of ophthalmology* **8**, 215 (2015).

39 Thoft, R. A. The role of the limbus in ocular surface maintenance and repair. *Acta Ophthalmol Suppl* **192**, 91-94, doi:10.1111/j.1755-3768.1989.tb07099.x (1989).

40 Necas, J., Bartosikova, L., Brauner, P. & Kolar, J. Hyaluronic acid (hyaluronan): a review. *Veterinarni medicina* **53**, 397-411 (2008).

41 Fallacara, A., Baldini, E., Manfredini, S. & Vertuani, S. Hyaluronic Acid in the Third Millennium. *Polymers (Basel)* **10**, 701, doi:10.3390/polym10070701 (2018).

42 Rah, M. J. A review of hyaluronan and its ophthalmic applications. *Optometry* **82**, 38-43, doi:10.1016/j.optm.2010.08.003 (2011).

43 Price, R. D., Myers, S., Leigh, I. M. & Navsaria, H. A. The Role of Hyaluronic Acid in Wound Healing. *American Journal of Clinical Dermatology* **6**, 393-402, doi:10.2165/00128071-200506060-00006 (2005).

44 Salwowska, N. M., Bebenek, K. A., Żądło, D. A. & Wcisło-Dziadecka, D. L. Physiochemical properties and application of hyaluronic acid: a systematic review. *J Cosmet Dermatol* **15**, 520-526, doi:10.1111/jocd.12237 (2016).

45 Goa, K. L. & Benfield, P. Hyaluronic acid. A review of its pharmacology and use as a surgical aid in ophthalmology, and its therapeutic potential in joint disease and wound healing. *Drugs* **47**, 536-566, doi:10.2165/00003495-199447030-00009 (1994).

46 Chirila, T.V., Harkin, D. *Biomaterials and Regenerative Medicine in Ophthalmology.*263-279 (Woodhead Publishing, 2010).

47 Stiebel-Kalish, H. *et al.* A comparison of the effect of hyaluronic acid versus gentamicin on corneal epithelial healing. *Eye (Lond)* **12**, 829-833, doi:10.1038/eye.1998.213 (1998).

48 Beck, R. *et al.* Hyaluronic Acid as an Alternative to Autologous Human Serum Eye Drops: Initial Clinical Results with High-Molecular-Weight Hyaluronic Acid Eye Drops. *Case Reports in Ophthalmology* **10**, 244-255, doi:10.1159/000501712 (2019).

49 Korogiannaki, M., Zhang, J. & Sheardown, H. Surface modification of model hydrogel contact lenses with hyaluronic acid via thiol-ene "click" chemistry for enhancing surface characteristics. *Journal of Biomaterials Applications* **32**, 446-462, doi:10.1177/0885328217733443 (2017).

50 Weeks, A., Luensmann, D., Boone, A., Jones, L. & Sheardown, H. Hyaluronic acid as an internal wetting agent in model DMAA/TRIS contact lenses. *Journal of Biomaterials applications* **27**, 423-432 (2012).

51 Weeks, A. *et al.* Photocrosslinkable hyaluronic acid as an internal wetting agent in model conventional and silicone hydrogel contact lenses. *Journal of Biomedical Materials Research Part A* **100**, 1972-1982 (2012).

52 Singh, A., Li, P., Beachley, V., McDonnell, P. & Elisseeff, J. H. A hyaluronic acid-binding contact lens with enhanced water retention. *Contact Lens and Anterior Eye* **38**, 79-84 (2015).

53 Desai, A. R. *et al.* Co-delivery of timolol and hyaluronic acid from semi-circular ring-implanted contact lenses for the treatment of glaucoma: in vitro and in vivo evaluation. *Biomaterials science* **6**, 1580-1591, doi:10.1039/c8bm00212f (2018).

54 Ali, M. & Byrne, M. E. Controlled release of high molecular weight hyaluronic Acid from molecularly imprinted hydrogel contact lenses. *Pharm Res* **26**, 714-726, doi:10.1007/s11095-008-9818-6 (2009).

55 Zhong, J. *et al.* Hyaluronate Acid-Dependent Protection and Enhanced Corneal Wound Healing against Oxidative Damage in Corneal Epithelial Cells. *Journal of Ophthalmology* **2016**, 6538051, doi:10.1155/2016/6538051 (2016).

56 Gupta, R. C., Lall, R., Srivastava, A. & Sinha, A. Hyaluronic Acid: Molecular Mechanisms and Therapeutic Trajectory. *Frontiers in Veterinary Science* **6**, doi:10.3389/fvets.2019.00192 (2019).

57 Ho, W. T. *et al.* Enhanced corneal wound healing with hyaluronic acid and high-potassium artificial tears. *Clinical and Experimental Optometry* **96**, 536-541, doi: 10.1111/cxo.12073 (2013).

58 Gomes, J. A. P., Amankwah, R., Powell-Richards, A. & Dua, H. S. Sodium hyaluronate (hyaluronic acid) promotes migration of human corneal epithelial cells in vitro. *The British journal of ophthalmology* **88**, 821-825, doi:10.1136/bjo.2003.027573 (2004).

59 Misra, S., Hascall, V. C., Markwald, R. R. & Ghatak, S. Interactions between Hyaluronan and Its Receptors (CD44, RHAMM) Regulate the Activities of Inflammation and Cancer. *Front Immunol* **6**, doi:10.3389/fimmu.2015.00201 (2015).

60 Naor, D. Editorial: Interaction Between Hyaluronic Acid and Its Receptors (CD44, RHAMM) Regulates the Activity of Inflammation and Cancer. *Front Immunol* **7**, 39-39, doi:10.3389/fimmu.2016.00039 (2016).

61 Chen, W. Y. & Abatangelo, G. Functions of hyaluronan in wound repair. *Wound Repair Regen* **7**, 79-89, doi:10.1046/j.1524-475x.1999.00079.x (1999).

62 Ho, W. T. *et al.* Enhanced corneal wound healing with hyaluronic acid and high-potassium artificial tears. *Clin Exp Optom* **96**, 536-541, doi:10.1111/cxo.12073 (2013).

63 Jordan, A. R., Racine, R. R., Hennig, M. J. P. & Lokeshwar, V. B. The Role of CD44 in Disease Pathophysiology and Targeted Treatment. *Front Immunol* **6**, doi:10.3389/fimmu.2015.00182 (2015).

64 Tolg, C., McCarthy, J. B., Yazdani, A. & Turley, E. A. Hyaluronan and RHAMM in wound repair and the "cancerization" of stromal tissues. *Biomed Res Int* **2014**, 103923-103923, doi:10.1155/2014/103923 (2014).

65 Giannaccare, G. *et al.* Blood derived eye drops for the treatment of cornea and ocular surface diseases. *Transfus Apher Sci* **56**, 595-604, doi:10.1016/j.transci.2017.07.023 (2017).

66 Geerling, G., Maclennan, S. & Hartwig, D. Autologous serum eye drops for ocular surface disorders. *Br J Ophthalmol* **88**, 1467-1474, doi:10.1136/bjo.2004.044347 (2004).

67 Rauz, S. & Saw, V. P. Serum eye drops, amniotic membrane and limbal epithelial stem cells--tools in the treatment of ocular surface disease. *Cell Tissue Bank* **11**, 13-27, doi:10.1007/s10561-009-9128-1 (2010).

68 Sorsby, A. & Symons, H. Amniotic membrane grafts in caustic burns of the eye:(Burns of the second degree). *The British journal of ophthalmology* **30**, 337 (1946).

69 Kim, J. C. & Tseng, S. Transplantation of preserved human amniotic membrane for surface reconstruction in severely damaged rabbit corneas. *Cornea* **14**, 473-484 (1995).

70 Zidan, G., Rupenthal, I. D., Greene, C. & Seyfoddin, A. Medicated ocular bandages and corneal health: potential excipients and active pharmaceutical ingredients. *Pharm Dev Technol* **23**, 255-260, doi:10.1080/10837450.2017.1377232 (2018).

71 Choi, J. A. *et al.* Effects of amniotic membrane suspension in human corneal wound healing in vitro. *Mol Vis* **15**, 2230-2238 (2009).

72 Mobaraki, M. *et al.* Corneal Repair and Regeneration: Current Concepts and Future Directions. *Frontiers in Bioengineering and Biotechnology* **7**, doi:10.3389/fbioe.2019.00135 (2019).

73 Aramwit, P. in *Wound Healing Biomaterials* (ed Magnus S. Ågren) 3-38 (Woodhead Publishing, 2016).

74 Willoughby, C. E., Batterbury, M. & Kaye, S. B. Collagen corneal shields. *Surv Ophthalmol* **47**, 174-182, doi:10.1016/s0039-6257(01)00304-6 (2002).

75 Yazdanpanah, G. *et al.* Corneal Wound Healing Effects of Solubilized Porcine Cornea Extracellular-Matrix. *Investigative Ophthalmology & Visual Science* **60**, 4116-4116 (2019).

76 Musgrave, C. S. A. & Fang, F. Contact Lens Materials: A Materials Science Perspective. *Materials* **12**, 261 (2019).

77 McMahon, T. T. & Zadnik, K. Twenty-five Years of Contact Lenses: The Impact on the Cornea and Ophthalmic Practice. *Cornea* **19**, doi: 10.1097/00003226-200009000-00018 (2000).
78 Tighe, B. J. in *Biomaterials and Regenerative Medicine in Ophthalmology* (ed Traian Chirila) 496-523 (Woodhead Publishing, 2010).
79 Edward S Bennett, O. M. F. & Henry, V. A. *Clinical Manual of Contact Lenses*. (Wolters Kluwer, 2015).
80 Tighe, B. J. A decade of silicone hydrogel development: surface properties, mechanical properties, and ocular compatibility. *Eye Contact Lens* **39**, 4-12, doi:10.1097/ICL.0b013e318275452b (2013).
81 Shah, C., Raj, C. V. & Foulks, G. N. The evolution in therapeutic contact lenses. *Ophthalmol Clin North Am* **16**, 95-101, vii, doi:10.1016/s0896-1549(02)00066-4 (2003).
82 Mann, A. & Tighe, B. J. in *Advanced Wound Repair Therapies* (ed David Farrar) 284-320 (Woodhead Publishing, 2011).
83 Tromans, C. in *Contact Lenses (Sixth Edition)* (eds Anthony J. Phillips & Lynne Speedwell) 477-485 (2019).
84 McDermott, M. L. & Chandler, J. W. Therapeutic uses of contact lenses. *Survey of Ophthalmology* **33**, 381-394, doi:10.1016/0039-6257(89)90015-5 (1989).
85 Markoulli, M. & Kolanu, S. Contact lens wear and dry eyes: challenges and solutions. *Clin Optom (Auckl)* **9**, 41-48, doi:10.2147/OPTO.S111130 (2017).
86 Alipour, F., Khaheshi, S., Soleimanzadeh, M., Heidarzadeh, S. & Heydarzadeh, S. Contact Lens-related Complications: A Review. *J Ophthalmic Vis Res* **12**, 193-204, doi:10.4103/jovr.jovr_159_16 (2017).
87 Mero, A. & Campisi, M. Hyaluronic Acid Bioconjugates for the Delivery of Bioactive Molecules. *Polymers* **6**, 346-369, doi:10.3390/polym6020346 (2014).
88 A, S. *et al.* A facile one-pot synthesis of acrylated hyaluronic acid. *Chem Commun (Camb)* **54**, 1081-1084, doi:10.1039/c7cc08648b (2018).
89 Saha, G. B., Fundamentals of Nuclear Pharmacy (Springer, 1998).
90 Brash, J. L. *Protein Surface Interactions and Biocompatibility: A Forty Year Perspective*. (2012).
91 Hermanson, G. T. *Bioconjugate Techniques*.(1996).
92 Liu, L. & Sheardown, H. Development of Phenylboronic Acid Containing Mucoadhesive Hydrogel Materials for Ophthalmic Drug delivery applications. *Investigative Ophthalmology & Visual Science* **55**, 455-455 (2014).
93 Northrop, B. H. & Coffey, R. N. Thiol-ene click chemistry: computational and kinetic analysis of the influence of alkene functionality. *J Am Chem Soc* **134**, 13804-13817, doi:10.1021/ja305441d (2012).
94 Heide, P. *X-Ray Photoelectron Spectroscopy*. (John Wiley & Sons,Inc., 2011).

95 Maulvi, F. A., Soni, T. G. & Shah, D. O. Extended release of hyaluronic acid from hydrogel contact lenses for dry eye syndrome. *J Biomater Sci Polym Ed* **26**, 1035-1050, doi:10.1080/09205063.2015.1072902 (2015).

96 Maulvi, F. A., Soni, T. G. & Shah, D. O. Extended release of hyaluronic acid from hydrogel contact lenses for dry eye syndrome. *Journal of Biomaterials Science, Polymer Edition* **26**, 1035-1050, doi:10.1080/09205063.2015.1072902 (2015).

97 Maulvi, F. A. *et al.* Design and optimization of a novel implantation technology in contact lenses for the treatment of dry eye syndrome: In vitro and in vivo evaluation. *Acta Biomater* **53**, 211-221, doi:10.1016/j.actbio.2017.01.063 (2017).

98 Korogiannaki, M., Guidi, G., Jones, L. & Sheardown, H. Timolol maleate release from hyaluronic acid-containing model silicone hydrogel contact lens materials. *Journal of Biomaterials Applications* **30**, 361-376, doi:10.1177/0885328215581507 (2015).

99 Korogiannaki, M., Jones, L. & Sheardown, H. Impact of a Hyaluronic Acid-Grafted Layer on the Surface Properties of Model Silicone Hydrogel Contact Lenses. *Langmuir* **35**, 950-961, doi:10.1021/acs.langmuir.8b01693 (2019).

100 Jones, L., May, C., Nazar, L. & Simpson, T. In vitro evaluation of the dehydration characteristics of silicone hydrogel and conventional hydrogel contact lens materials. *Cont Lens Anterior Eye* **25**, 147-156, doi:10.1016/s1367-0484(02)00033-4 (2002).

101 Horst, C. R., Brodland, B., Jones, L. W. & Brodland, G. W. Measuring the modulus of silicone hydrogel contact lenses. *Optom Vis Sci* **89**, 1468-1476, doi:10.1097/OPX.0b013e3182691454 (2012).

102 Boisjoly, H. M. *et al.* Effects of EGF, IL-1 and their combination on in vitro corneal epithelial wound closure and cell chemotaxis. *Exp Eye Res* **57**, 293-300, doi:10.1006/exer.1993.1127 (1993).

Appendix A: Characterization

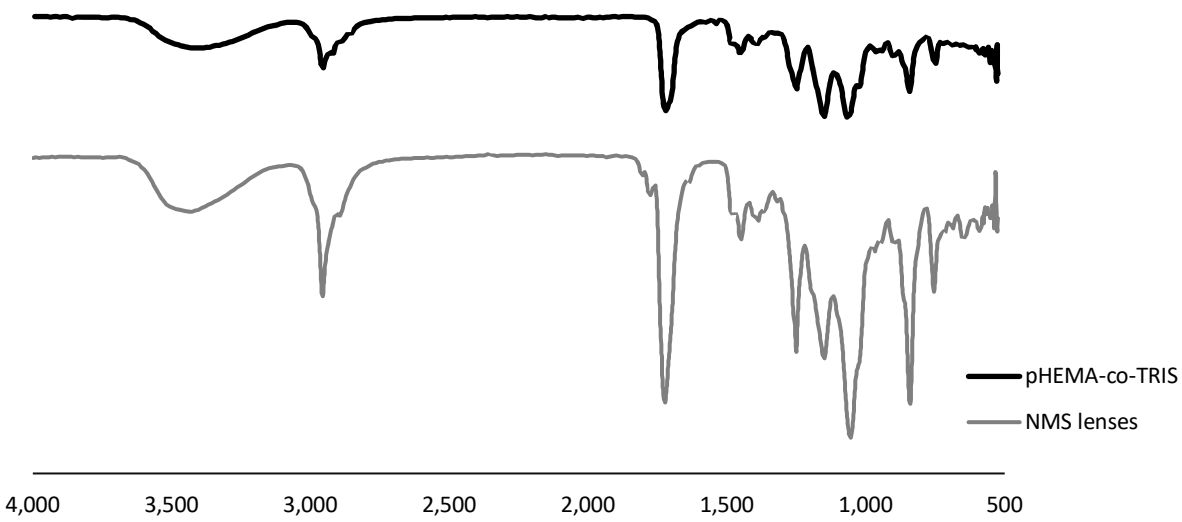

Figure A1:ATR-FTIR of NMS lenses compared to model pHEMA-co-TRIS lenses

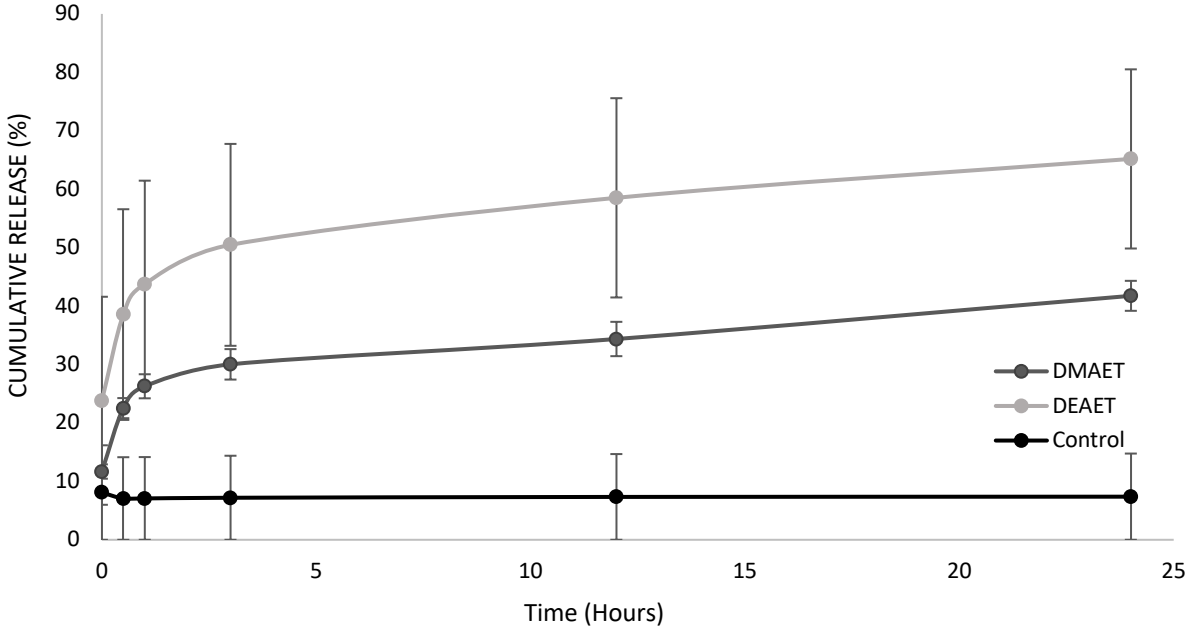

Figure A2: Cumulative release curve of DMAET, DEAET, and model pHEMA-co-TIRS modified lenses after an 8 hr soak in 1 mg/ml HA over 24 hours. Results showing standard deviation. (n=5)

To avoid using cracked lenses, all lenses after modifications were checked using a microscope and supplemented with contact angle.

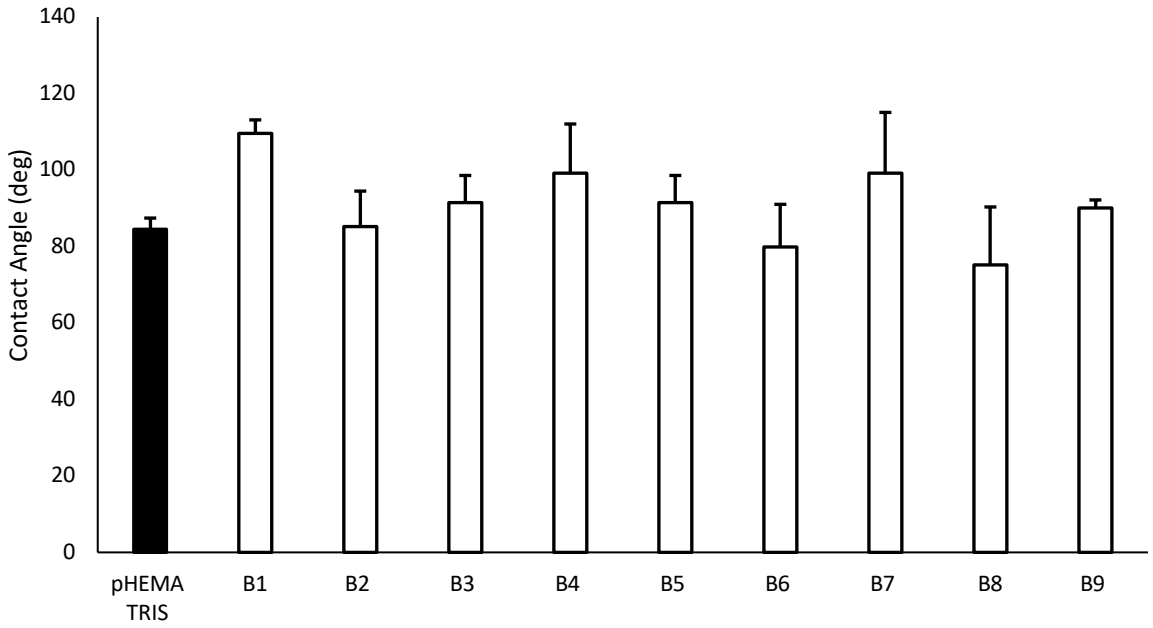

Figure A3:Contact angle of acrylated lenses between batches compared to pHEMA-co-TRIS. (n=3).

Appendix B: Cell Studies

Appendix B.1: Methods for Geisma and Hematoxylin Staining

The Boyden chamber method follows the same protocol as the method used previously up to the staining section. The inserts were placed in 4% formaldehyde (pH=6.9) for 7 mins, methanol for 2.5 min, and filtered hematoxylin stain for 5 mins with a PBS rinse in between each step. The cells were then imaged at 10x magnification using the Zeiss Axiovert 200 Inverted microscope using the AxioVision software.

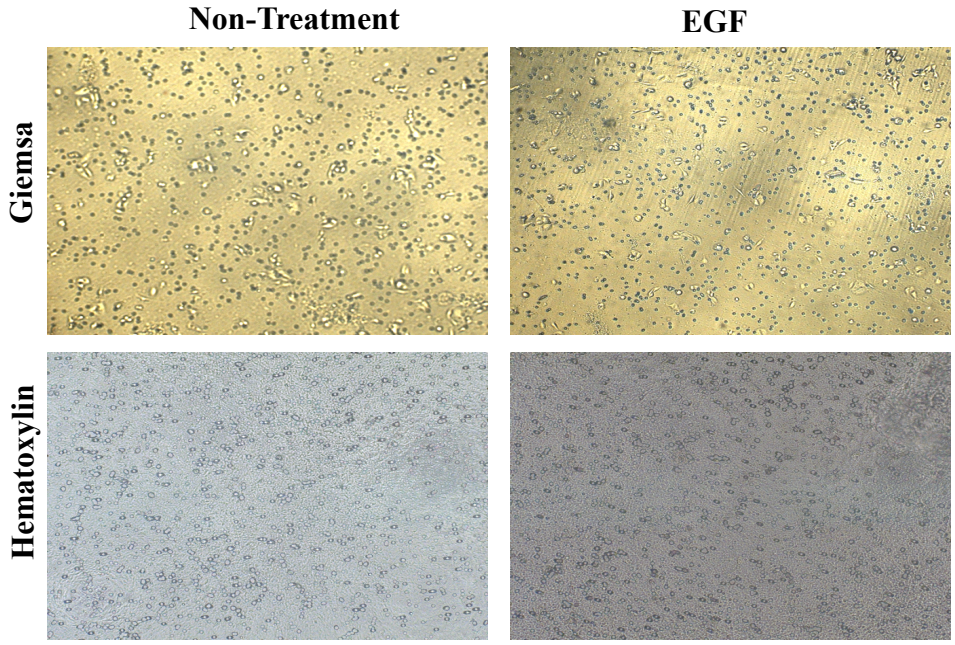

Figure B1:HCECs through 12 µm pore using Giemsa and Hematoxylin stains

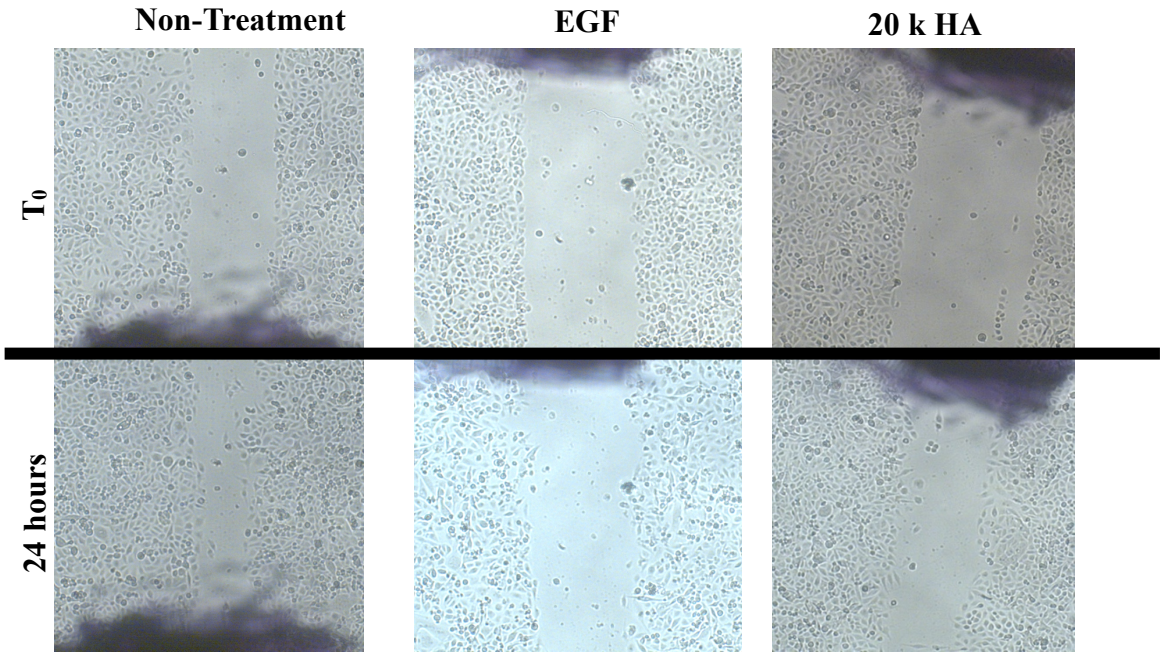

Figure B2: Wound closure model using HCECs measured at 0 and 24 hours. Cells are scraped using a p10 pipette and incubated for 24 hours. Images are taken at 10x magnification

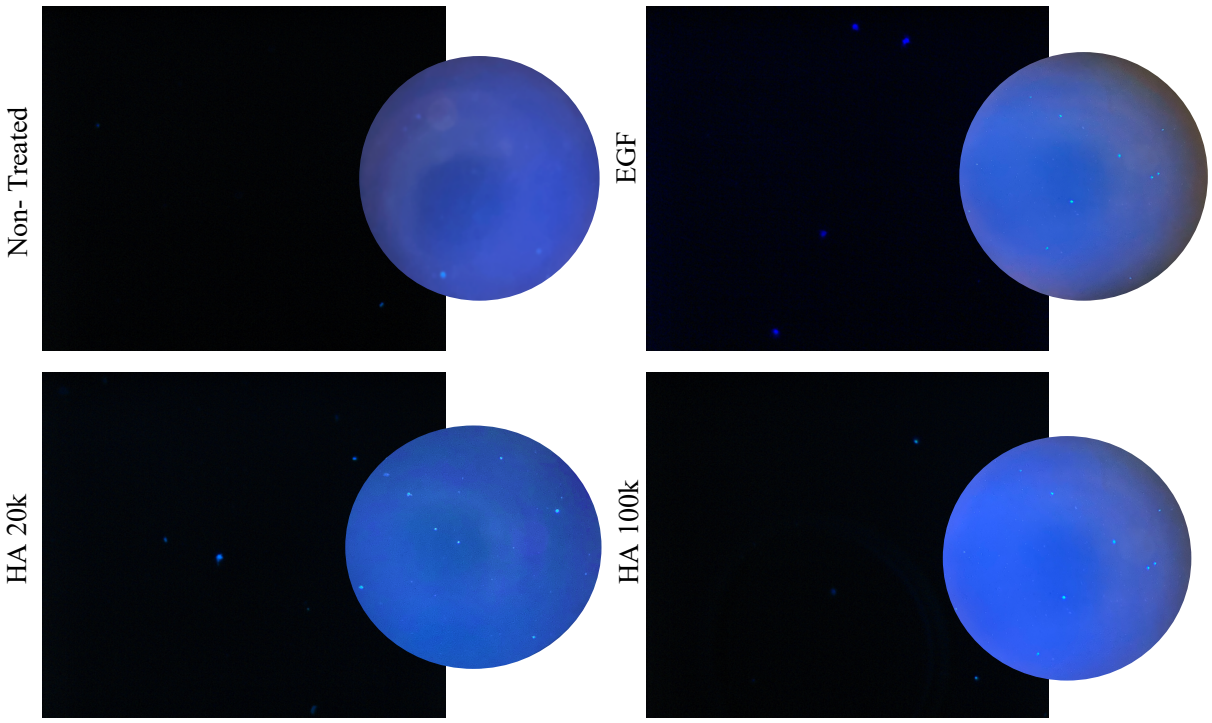

Figure B3: Boyden chamber images of HCECs (x10 magnification) stained with Hoesct stain through an 8 µm membrane filter. Images taken at 24 hours of cells which have migrated to the bottom chamber. Cells in the top chamber removed using a cotton swab.

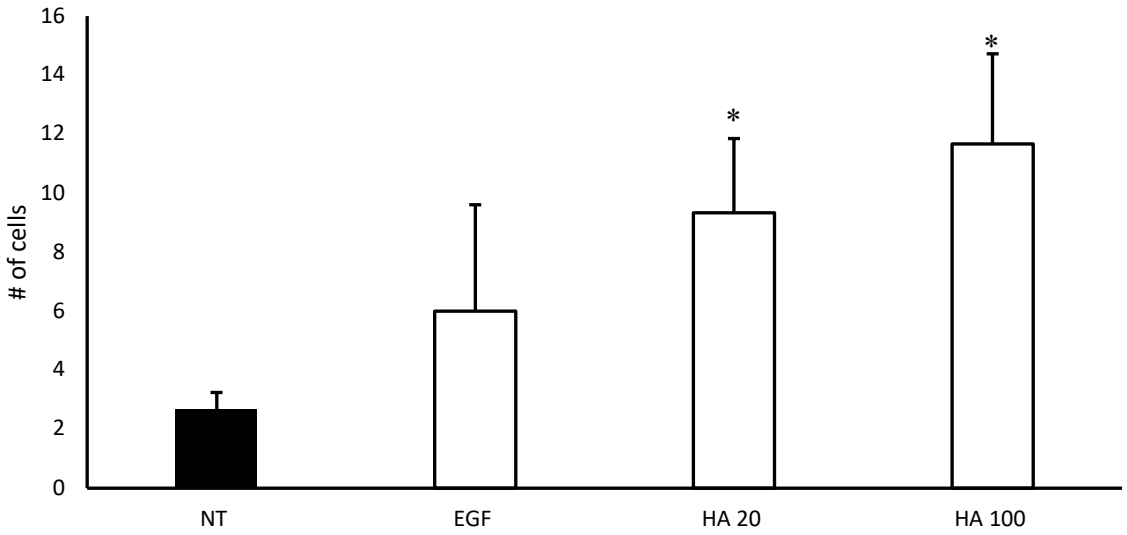

Figure B4:Number of HCEC cells counted at the bottom of the chamber through 8 µm pores. Results reported in standard deviation with no statistically significant difference amongst groups. (n=4)

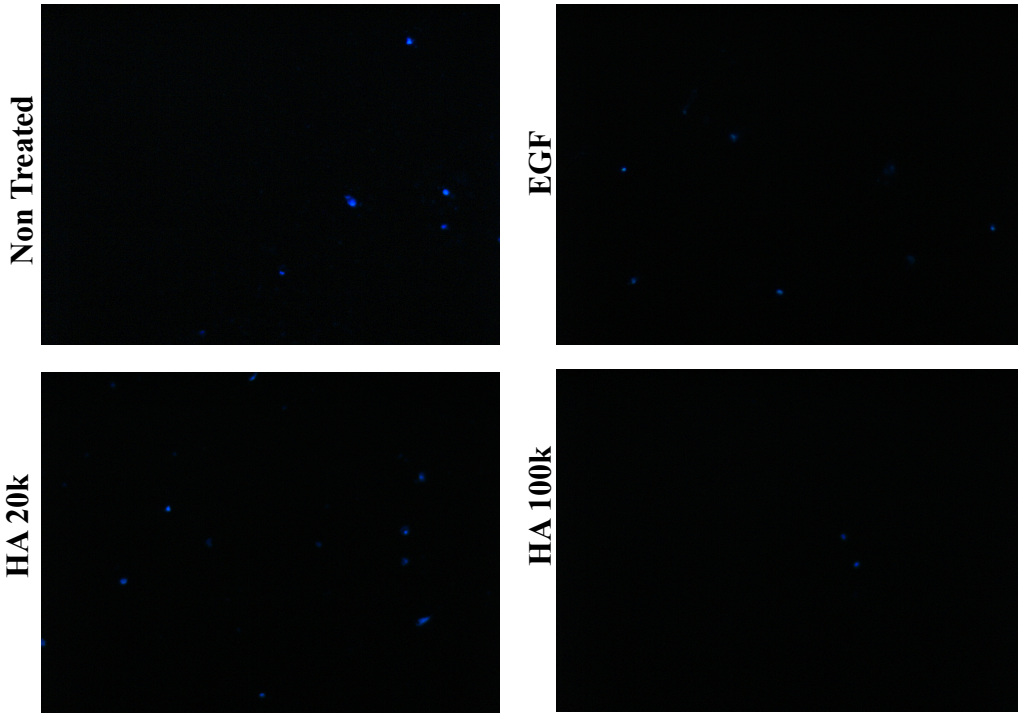

Figure B5:Boyden chamber images of HCECs (x10 magnification) stained with Hoesct stain through an 12 µm membrane filter. Images taken at 24 hours of cells which have migrated to the bottom chamber. Cells in the top chamber removed using a cotton swab.

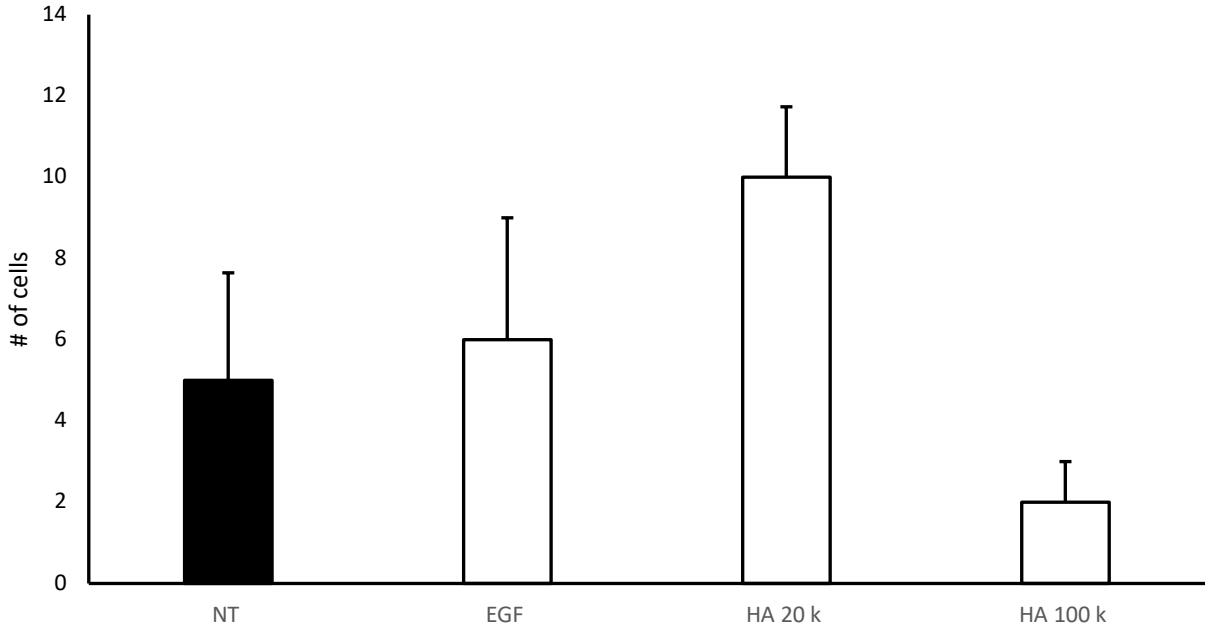

Figure B6:Number of HCEC cells counted at the bottom of the chamber through 12 µm pores. Results reported in standard deviation with no statistically significant difference amongst groups. (n=4)